AD

AD621515

USAAVLABS TECHNICAL REPORT 65-26

HEAVE STABILITY AND HEAVE DAMPING OF GROUND EFFECT MACHINES - THICK ANNULAR JET AND PLENUM TYPES

FINAL REPORT

By

Norman K. Walker
David A. Shaffer

DDC

July 1965

U. S. ARMY AVIATION MATERIEL LABORATORIES
FORT EUSTIS, VIRGINIA

CONTRACT DA 44-177-AMC-19(T)
NORMAN K. WALKER ASSOCIATES, INC.

CLEARINGHOUSE
FOR FEDERAL SCIENTIFIC AND
TECHNICAL INFORMATION

Hardcopy	Microfiche	
$4.00	$0.75	122 pp as

ARCHIVE COPY

DDC Availability Notice

Qualified requesters may obtain copies of this report from DDC.

This report has been furnished to the Department of Commerce for sale to the public.

Disclaimer

The findings in this report are not to be construed as an official Department of the Army position, unless so designated by other authorized documents.

When Government drawings, specifications, or other data are used for any purpose other than in connection with a definitely related Government procurement operation, the United States Government thereby incurs no responsibility nor any obligation whatsoever; and the fact that the Government may have formulated, furnished, or in any way supplied the said drawings, specifications, or other data is not to be regarded by implication or otherwise as in any manner licensing the holder or any other person or corporation, or conveying any rights or permission, to manufacture, use or sell any patented invention that may in any way be related thereto.

Disposition Instructions

Destroy this report when it is no longer needed. Do not return it to the originator.

DISCLAIMER NOTICE

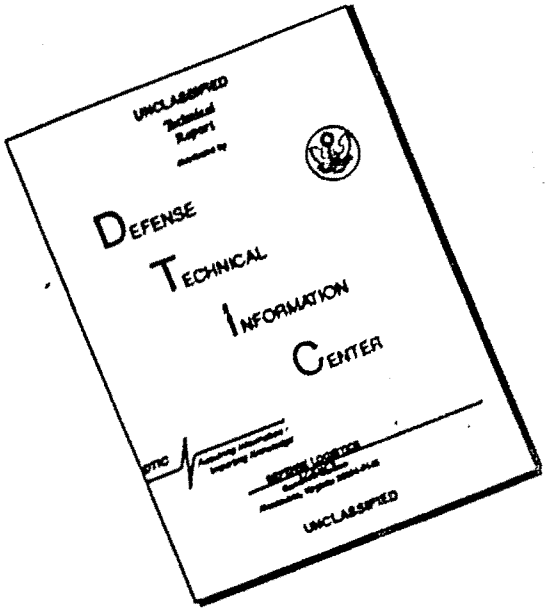

THIS DOCUMENT IS BEST QUALITY AVAILABLE. THE COPY FURNISHED TO DTIC CONTAINED A SIGNIFICANT NUMBER OF PAGES WHICH DO NOT REPRODUCE LEGIBLY.

HEADQUARTERS
U S ARMY TRANSPORTATION RESEARCH COMMAND
FORT EUSTIS, VIRGINIA 23604

The present study was undertaken to define the heave stability and damping characteristics of an air cushion vehicle in hovering flight. It is one of two reports concerned with air cushion vehicle stability and dynamics prepared under contract DA-44-177-AMC-19(T).

The report has been reviewed by the U.S. Army Transportation Research Command, and the data contained in it are considered to be valid. The report is published for the dissemination of information.

NOTE

On 1 March 1965, *after this report had been prepared,* the name of this command was changed from U.S. Army Transportation Research Command to:

U.S. ARMY AVIATION MATERIEL LABORATORIES

Task 1D021701A04802
Contract DA 44-177-AMC-19(T)
USAAVLABS Technical Report 65-26
July 1965

HEAVE STABILITY AND HEAVE DAMPING OF GROUND EFFECT MACHINES - THICK ANNULAR JET AND PLENUM TYPES

FINAL REPORT

by

Norman K. Walker
David A. Shaffer

Prepared by

Norman K. Walker Associates, Inc.
Bethesda, Maryland

for

U. S. ARMY AVIATION MATERIEL LABORATORIES
FORT EUSTIS, VIRGINIA

SUMMARY

This report describes an experimental investigation of the heave stability and heave damping characteristics in hovering flight of an electrically powered model Ground Effect Machine, arranged firstly with a thick annular jet and, secondly, as a simple plenum chamber.

The lift, rise height and power relationship were determined and the fan characteristics of the thick annular jet were measured. Air was bled from and fed into the air cushion to evaluate the GEM's change in lift. Finally, the machine was allowed to hover at a specific height and then forced to oscillate. From this the heave stiffness and damping ratio were determined.

The results show that the physical basis of the theory is correct and that good estimates may be made of the heave characteristics ω_0 and $2\zeta/\omega_0$ from which, of course, ζ can be determined.

However, it is suspected that other derivatives may be present, especially in the case of the plenum chamber, where unstable oscillations in a narrow attitude band were observed, and in any case the measured value of $2\zeta/\omega_0$ was much less than theory would predict.

It is considered that the latter result was not due to an unstable fan characteristic, but rather to an instability of flow in the plenum chamber itself.

PREFACE

This report presents the results of an experimental investigation of the heave stability and heave damping characteristics of thick annular jet and plenum chamber type model ground effect machines (GEM). The work was sponsored by the U. S. Army Transportation Research Command under Contract DA-44-177-AMC-19(T) and was performed by the members of the staff of Norman K. Walker Associates, Incorporated, at the firm's office and laboratory at Bethesda, Maryland, during the period from June 1963 to December 1964.

The model GEM was adapted from one which had been built by the hexicopter Model Research Company, Arvada, Colorado, and had been used in previous investigation.

Mr. Norman K. Walker and Mr. David A. Shaffer were the principal investigators on this study and were assisted by Messrs. Richard Brooks and Peter Ford. Mr. Peter Payne of Peter Payne Associates, Inc., contributed to the analysis in Appendix I and some selected sections in this report.

CONTENTS

SUMMARY..... iii

PREFACE..... v

LIST OF ILLUSTRATIONS..... ix

LIST OF TABLES..... xiii

LIST OF SYMBOLS..... xv

INTRODUCTION..... 1

CONCLUSIONS..... 3

THE EQUATION OF HEAVE MOTION..... 4

HEAVE STABILITY AS AN INDEX OF PERFORMANCE OVER ROUGH TERRAIN..... 8

HISTORICAL SURVEY..... 11

TULIN..... 11

EAMES..... 13

THE INFLUENCE OF FAN CHARACTERISTICS..... 13

CROSS, STRAND, AND WALKER..... 14

DESCRIPTION OF MODEL AND THE EXPERIMENTAL PROCEDURE..... 16

MEASUREMENT OF LIFT..... 16

FAN CALIBRATION TESTS..... 23

DETERMINATION OF $\partial L/\partial \dot{h}$ BY FEEDING AND BLEEDING THE AIR CUSHION..... 32

DETERMINATION OF $\partial L/\partial h$ AND $\partial L/\partial \dot{h}$ FROM OSCILLATION TESTS..... 36

COMPARISON OF MEASURED VALUES OF $\partial L/\partial h$ AND $\partial L/\partial \dot{h}$ WITH DETERMINATIONS FROM THE DIRECT LIFT MEASUREMENTS ALLOWING FOR FAN EFFECTS..... 44

COMPARISON OF THE RESULTS WITH SIMPLE THEORY (APPENDIX II) ALLOWING FOR FAN EFFECTS..... 52

FREQUENCY OF OSCILLATION, ω..... 52

RELATIVE DAMPING RATIO, ζ..... 58

THE DAMPING PARAMETER, $2\zeta/\omega$..... 60

TABLES..... 64

REFERENCES..... 82

DISTRIBUTION..... 85

APPENDIX I, DISCUSSION OF FAN AND DUCTING CHARACTERISTICS..... 87

APPENDIX II, THEORETICAL ESTIMATION OF THE HEAVE STABILITY OF A GEM, INCLUDING FAN CHARACTERISTICS..... 94

ILLUSTRATIONS

Figure		Page
1	Variation of Total Lift With Clearance Height	4
2	Simple Bellows Damper.....	6
3	The Idealization of Irregular Terrain.....	8
4	Linear Relationship Between x and h	10
5	Jet Flow Patterns for "Underfed," "Balanced," and "Overfed" Operations.....	12
6	Different Estimates of the Damping Ratio ζ	15
7	The Annular Gem Model (Sheets 1 and 2).....	17, 18
8	The Plenum Chamber GEM Model.....	19
9	Variation of Rise Height With RPM for Fixed Lifts - Thick Annular Jet GEM Model.....	20
10	Consolidated Lift Results - Thick Annular Jet GEM Model.....	21
11	Variation of Rise Height With RPM for Fixed Lifts - Plenum Chamber GEM Model.....	22
12	Consolidated Lift Results - Plenum Chamber GEM Model.....	24
13	Ducting System for GEM Fan Calibration.....	25
14	Duct System Calibration for Various Blockages....	26
15	Duct System Calibration for Various Blockages....	27
16	Duct System Calibration for Various Blockages....	28
17	Duct System Calibration for Various Blockages....	29
18	Comparison of Fan Pressure Coefficient C_p With Fan Flow Parameter λ for Thick Annular Jet GEM Model.....	30

Figure		Page
19	Fan Pressure Coefficient C_p Versus Fan Flow Parameter λ for Plenum Chamber GEM Model.....	33
20	Apparatus for Feeding and Bleeding Air Cushion	34
21	Variation of Lift Change $\Delta L/L_r$ With the Effective Heave Velocity $\dot{h}/h_r$ for the Thick Annular Jet GEM Model, Measured With Steady State Airflow.....	35
22	Variation of Lift Change $\Delta L/L_r$ With the Effective Heave Velocity $\dot{h}/h_r$ for the Plenum Chamber GEM Model, Measured With Steady State Airflow.....	37
23	Heave Rig and Model GEM System.....	38
24	Oscillatory Amplitudes Versus Cycles for Specific Hover Heights - Thick Annular Jet GEM Model	39
25	Oscillatory Amplitudes Versus Cycles for Specific Hover Heights - Thick Annular Jet GEM Model	40
26	Typical Oscillatory Profiles for Thick Annular Jet GEM Model.....	41
27	Oscillatory Amplitudes Versus Cycles for Specific Hover Heights - Plenum Chamber GEM Model	45
28	Oscillatory Amplitudes Versus Cycles for Specific Hover Heights - Plenum Chamber GEM Model	46
29	Typical Oscillatory Profiles for Plenum Chamber GEM Model - In Stable Region.....	47
30	Oscillatory Profile for Plenum Chamber Model Near Unstable Region.....	48
31	Oscillation Profile in the Unstable Region for the Plenum Chamber GEM Model.....	49
32	Comparison of Heave Stability Parameter $\partial L/N^2 \partial h$ as Determined From Oscillation Tests and Static Lift Measurements.....	51
33	Comparison of Heave Damping Parameter $\partial L/N \partial \dot{h}$ as Determined From Several Different Methods	53

Figure		Page
34	Variation of Air Supply Factor "F" With Fan Pressure Coefficient "C_p" - Thick Annular Jet GEM Model	55
35	Variation of Fan and Duct Stability Parameter $\mathcal{F}$ With Rise Height "h" - Thick Annular Jet GEM Model	55
36	Comparison of Free Flight Circular Frequency With Various Theoretical Estimates	57
37	Comparison of Experimental Results With Different Estimates of the Damping Ratio	59
38	Comparison of the Experimentally Determined Damping Ratio ζ With the Constant Mass Flow Theory	61
39	Comparison of Heave Damping Parameter $\frac{2\zeta/\omega}{S_b/C\ \sqrt{P/2p_{bo}}}$ as Determined from Oscillation Tests and Simple Theory	62
40	Characteristics of a High-Pitch Axial Fan (Globe VAX-2-MM)	88
41	Fan and Ducting Geometry	89
42	Fan Geometry	90

TABLES

Table		Page
1.	Variation of Rise Height With RPM for Fixed Lifts. Thick Annular Jet GEM Model	64
2.	Consolidated Lift Results Thick Annular Jet GEM Model	65
3.	Variations of Rise Height With RPM for Fixed Lifts Plenum Chamber GEM Model	66
4.	Consolidated Lift Results Plenum Chamber GEM Model	67
5a.	Pressure Coefficient C_p and Fan Flow Parameter λ as a Function of Duct Blockage - Thick Annular Jet Model	68
5b.	Pressure Coefficient C_p and Fan Flow Parameter λ as a Function of Rise Height "h" as Calculated From Static Lift Results - Thick Annular Jet Model	69
6.	Pressure Coefficient C_p vs. fan Flow Parameter λ as Calculated From Static Lift Results for the Plenum Chamber GEM Model	70
7.	Variation of Lift Change $\frac{\Delta L}{L_r}$ With the Heave Velocity $\frac{\dot{h}}{h_r}$	71
8.	Variation of Lift Change $\frac{\Delta L}{L_r}$ With Heave Velocity $\frac{\dot{h}}{h_r}$ for Plenum Chamber Model	72
9.	Thick Annular Jet Model Oscillation Tests	73
10.	Plenum Chamber Model Oscillation Tests	74
11.	Consolidated Lift Results Plenum Chamber Model - Thick Annular Jet Model	75
12.	Thick Annular Jet Model $\frac{2\,\zeta/\omega}{S_b/C\sqrt{P/2\rho_0}}$	76
13.	Plenum Chamber Model	77
14.	Heave Damping Parameter $\partial L/N\partial\dot{h}$ Calculated by Various Methods Thick Annular Jet GEM Model	78
15.	Heave Damping Parameter $\partial L/N\partial\dot{h}$ Calculated by Various Methods Plenum Chamber GEM Model	79

Table		Page
16.	Free Flight Circular Frequency as a Function of Rise Height - Thick Annular Jet GEM Model	80
17.	Damping Ratio " ζ " - Thick Annular Jet GEM Model	81

LIST OF SYMBOLS

b	length of base to inside edge of jets
C	perimeter of base
C_D	discharge coefficient of the plenum chamber
C_p	fan pressure coefficient = $\frac{\text{total head immediately behind fan}}{}$
D	fan diameter
F	air supply parameter for plenum chamber = $\frac{\partial P_t}{\partial Q} \frac{Q_o}{P_{t_o}} \Big/ \left[1 - \frac{1}{2} \frac{\partial P_t}{\partial Q} \frac{Q_o}{P_{t_o}}\right]$ (stabilizing if negative)
$\mathcal{H}$	fan and ducting stability parameter for annular jet GEM
g	acceleration due to gravity
G	thickness of jet at exit (Normal to flow)
h	height of jet exit above ground plane
h_o	height of jet exit above ground plane at equilibrium
h_b	height of base above ground plane at equilibrium
h_σ	effective equilibrium height of jet exits (includes Eames correction)
K	damping coefficient
K_s	damping coefficient - jet "overfed" (GEM sinking)
K_r	damping coefficient - jet "underfed" (GEM rising)
L	gross lift of machine $= P_{b_o} S_b$
m	mass of vehicle
p	static pressure of atmosphere
P_{b_o}	base pressure relative to atmosphere at equilibrium
P_t	total head at jet exit
P_b	base pressure relative to atmosphere

P_{t_o}	total head at jet exit at equilibrium
P_m	total head just behind fan
q_m	dynamic head just behind fan
q_t	dynamic head at the tip of the fan due to rotation
Q	volume flow through fan
Q_o	volume flow through fan at equilibrium
S_b	base area
S_j	jet area
V_{e_o}	velocity of jet when exhausted to atmospheric pressure
α	pitch angle from horizontal
β	Tulin's stability parameter (Stable if $\beta < 1.0$)
γ	ratio of specific heat for air ($\gamma = 1.4$)
ζ	damping ratio
ζ_o	damping ratio (Thin Jet)
η	diffuser efficiency (i.e., $\frac{\text{dynamic head recovery}}{\text{dynamic head at inlet}}$)
ρ	mass density of air
λ	jet angle from vertical (positive if directed inwards)
λ	fan airflow coefficient = $\frac{\text{average velocity through fan}}{\text{tip speed of fan}}$
ξ	a function of h, G, λ
ξ'	$\partial\xi/\partial h/\ h_o$
ω_o	undamped frequency in heave
ω	damped frequency in heave
ω_1	free flight angular frequency $=\sqrt{g/h_o}$
ω_r	angular frequency of heaving rig
ψ	P_{b_o}/P_t
ψ'	$\partial\psi/\partial h/\ h_o$

INTRODUCTION

Although the steady-state performance of a GEM is fairly well understood, at least qualitatively, the picture is by no means as clear as far as performance under dynamic conditions is concerned. The difference between the two states lies in the time dependent flows, of course. We might characterize the "steady-state" conditions as perfectly controlled hovering or flying with a forward velocity over a smooth and level surface, or by the operation of a GEM model in a wind tunnel. The flow is "steady state" because, at least so far as its gross details are concerned, the picture seen does not vary with time.

In contrast, dynamic effects are experienced in flight over irregular terrain, or over waves at sea, where the height and angle of the vehicle is constantly varying with respect to the local ground plane. Also, even over a plane surface, dynamic effects govern the vehicle's response to a control movement by its operator, the accuracy with which he can control it, and the vehicle's response to an external disturbance.

The simplest dynamic case is that of vertical or "heave" motion. Until recently, relatively little attention has been devoted to this case because most GEMs are both statically and dynamically stable in heave, and usually possess adequate damping.

Recent developments have emphasized the need for a better understanding of the mechanism of vertical motion, however.[1] Briefly these may be summarized as follows:

(a) The trend towards increased base loading in small size GEMs will result in lower damping values, possibly below an acceptable level, at large clearance heights.

(b) The use of skirts and trunks at low aerodynamic clearance heights can result in a large increase in heave damping and frequency when the skirt is essentially inextensible. Even on the very small Bell Carabao, for example, it was found[2]". . . that over small steep waves the ride was similar to a Jeep over cobble stones and most unlike the soft wallowing ride expected from GEMs"

(c) Heave damping, expressed as a ratio of critical damping, increases linearly with vehicle size, for constant clearance height and base loading.

For example, Reference 3 indicates that if the fan characteristics approximate to constant mass flow, a 300-foot plenum GEM with a base loading of 100 pounds per square foot would be critically damped. For this case, the accelerations caused by operation over waves could well be intolerable, from a physiological point of view. Most practical fans are less "stiff" than the limit case of constant mass flow, but on the other hand most future GEM's are likely to have less than a three-foot edge clearance because of developments in skirt and trunk technology, coupled with the ever-present need to reduce power requirements to a minimum. Thus we are in the position of being concerned over both too much and too little damping in heave. It is evidently necessary, therefore, that we should be able to estimate the damping accurately at the design stage, and that we should find ways of "tuning" the damping to the optimum value for each particular vehicle. This present report is concerned with developing the predictive ability which is essential to the accomplishment of both aims.

CONCLUSIONS

(1) Neither the "constant momentum flux" (constant mass flow constant volume flow for incompressible conditions) nor the alternative "constant total head" theories agree at all well with experimental measurements of heave frequency.

(2) If the theoretical formulation is extended to allow for the measured variation of total head with mass flow, then the theoretical results for heave frequency agree quite well with measured values for both annular jet and plenum chamber GEM's.

(3) However an equally good result can be obtained by assuming that the heave frequency is calculated directly from the measured slope of the curve of lift against altitude.

(4) In each case there is a small residual discrepancy, possibly due to an additional stability derivative--perhaps associated with the base vortex system.

(5) No simple theory gives a good estimate of the damping ratio ζ per se, unless corrected for fan characteristics.

(6) However, a much better description of heave dynamics can be obtained by separately estimating ω_0, the natural frequency (for 2 or 3), and also $2\zeta/\omega_0$, which theory shows is independent of fan characteristics and only dependent on the geometry and loading of the GEM.

(7) The calculated values of $2\zeta/\omega_0$ are in good agreement with the measured results for the annular jet GEM, showing that the physical basis for the damping theory is in this case essentially correct.

(8) The results for oscillation tests are not in such good agreement for the plenum chamber, although the direct measurements derived from feeding and bleeding the air cushion are. Apparently in this case there is a large additional destabilizing damping derivative present, and it is believed this is caused by instability of the flow in the plenum chamber itself.

(9) Undamped limit-cycle oscillations, apparently due to the same cause, were observed in the case of the plenum chamber. No instability could be found in the case of the annular jet machine, although several fan combinations were tried.

(Apparently an unstable fan characteristic can only be obtained from a high pitch fan of much greater solidity.) Fan instability will, in any case, show itself as an unstable variation of lift with altitude, without making oscillation tests.

THE EQUATION OF HEAVE MOTION

Most dynamic motions can be described, at least for small oscillations about an equilibrium position, by the equation

$$\ddot{x} + 2\zeta w\dot{x} + w^2 x = f(t), \qquad (1)$$

where x is the disturbance from the equilibrium position

$\dot{x}$ is the velocity of the disturbance

$\ddot{x}$ is the acceleration

w is the undamped natural frequency of the system

ζ is the "damping ratio", or the ratio of the damping to the "critical value" for deadbeat motion.

For stable systems, if $\zeta < 1.0$ the motion is a damped oscillation, while for $\zeta > 1.0$, it is a simple convergence to the trim value.

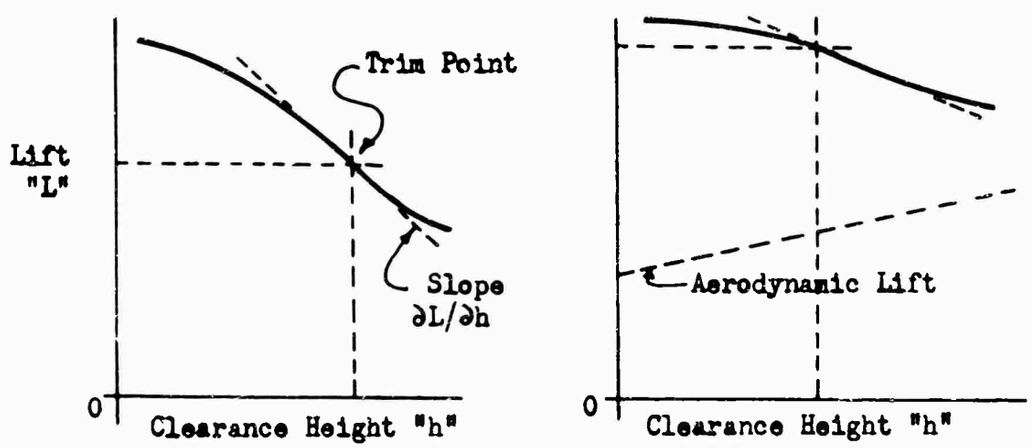

(a) Hovering (b) At Forward Speed

Figure 1. Variation of Total Lift With Clearance Height.

For an ACV the natural frequency is given by

$$w^2 = -\partial L/\partial h \;/\; m, \qquad (2)$$

where $\partial L/\partial h$ is the local slope of the <u>total</u> lift with respect to clearance height

and m is the total vehicle mass.

As indicated in Figure 1, since the cushion and jet momentum lift generally diminish with increasing clearance height in hover, an ACV is stable. In practice, the frequency is found[3] to be roughly

$$w = \frac{4}{\sqrt{h}} = \sqrt{-\partial L/\partial h \,/ m} \quad , \tag{3}$$

where h is the clearance.

When the vehicle has an appreciable forward speed we may generalize by saying that the cushion lift is reduced, but that this is more than made up for by the aerodynamic lift generated by the "mound flow" over the upper portions of the GEM. Payne[4] has shown that the lift coefficient of a GEM correlates well with

$$C_L = 4\eta_m (t/l), \tag{4}$$

where t is the maximum height of the body surface above the ground plane

l is the body length

η_m is the mound flow efficiency, (for most GEMs = 0.5).

Since $t = t_o + h$ this gives the lift derivative

$$\partial L/\partial h = (\tfrac{1}{2}\rho V^2)(lb)(2/l)$$

$$= \rho b V^2. \tag{5}$$

Accepting the cushion contribution as that given by equation (3), the heave frequency in forward flight is therefore seen to be

$$w^2 = 16/h - \rho b V^2/m \tag{6}$$

$$w = 4/h \sqrt{1-(g/8)(h/l)(q/P_{bo})} \quad . \tag{7}$$

Obviously the frequency will fall to zero when the dynamic pressure q due to forward speed is

$$q/P_{bo} \cong \frac{1}{4}\left(\frac{\text{vehicle length}}{\text{clearance height}}\right) \qquad (8)$$

This will correspond to a divergence upward. In this simple criterion we have ignored the reduction of cushion lift with forward speed, of course, so that equation (8) is somewhat conservative.

Information on the variation of total lift with forward speed is given in References 5,6, and 8, where it is shown that the loss in base pressure due to forward speeds of the order of -q is due to suction around the periphery.

However, intake ram pressure recovery from the intake is at least $+\frac{1}{2}q$, so the net result is a reduction in base pressure of $\frac{1}{2}q$.

Equation 8 can then be modified to

$$\frac{q}{P_{bo} - \frac{1}{2}q} \cong \frac{1}{4}(l/h)$$

or

$$\frac{q}{P_{bo}} \cong \frac{(l/h)}{4 + \frac{1}{2}(l/h)} .$$

The damping term in equation (1) is a little less obvious than the frequency (or "stiffness") term. We can understand it by considering the simple bellows arrangement of Figure 2, however, where the collapsible bellows is assumed to be completely flexible. At any height (h), the internal (of "cushion") pressure is equal to the outside pressure ($P_b = 0$) if the orifice plate is stationary and if sufficient time has elapsed to permit "steady state" conditions to exist.

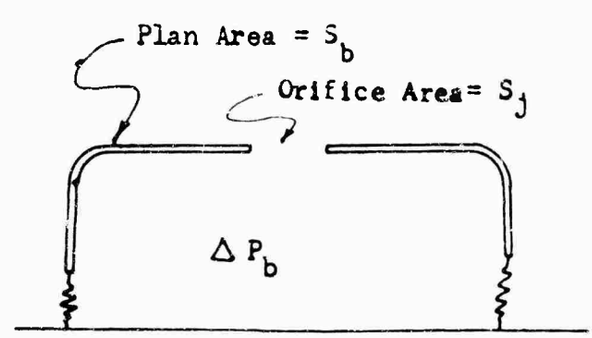

Figure 2.
Simple Bellows Damper.

Suppose we now move the orifice plate upwards from an initial position h_o. Air will flow into the cushion region via the orifice, and the total mass fow corresponding to a movement of Δh will be

$$m_j = \int \dot{m}_j \, dt = \rho S_b \cdot \Delta h.$$

Thus the mass flow rate will be

$$\dot{m}_j = \frac{\partial m_j}{\partial t} = \rho S_b \frac{\partial h}{\partial t} . \tag{9}$$

The effective (discharge) area of the orifice is $S_j C_D$, where C_D is the coefficient of discharge. The velocity of the airflow is obviously

$$V_j = \sqrt{(2/\rho)(\Delta P_b)},$$

from Bernoulli. Thus the air mass flow rate through the orifice is

$$\dot{m}_j = \rho S_j C_D V_j = S_j C_D \sqrt{(2/\rho)(\Delta P_b)} \tag{10}$$

Equating (9) and (10)

$$\rho S_b \frac{\partial h}{\partial t} = S_j C_D \sqrt{2 \rho \cdot \Delta P_b}$$

$$\therefore \Delta P_b = -\left(\frac{S_b}{S_j C_D}\right) \tfrac{1}{2} \rho \left(-\frac{\partial h}{\partial t}\right)^2 . \tag{11}$$

Thus the damping is not linear, for this example, but varies with the square of the displacement velocity; this is generally known as 'orifice damping.'

When the pressure inside the chamber is greater than ambient, due to air being pumped into it by some external means, such as a fan, we find that a linear damping term occurs also, and that equation (11) assumed the form

$$P_b = -K_1 \frac{\partial h}{\partial t} - K_2 \left(\frac{\partial h}{\partial t}\right)^2 . \tag{12}$$

For small perturbations the linear term is the most important and will generally be sufficient to define stability but the nonlinear terms will have an important influence upon the motion over waves or irregular terrain. In the present report we pay attention, generally, only to linearized theory, since we are primarily interested in stability. The importance of the nonlinear terms is such that they should be studied as soon as possible, however.

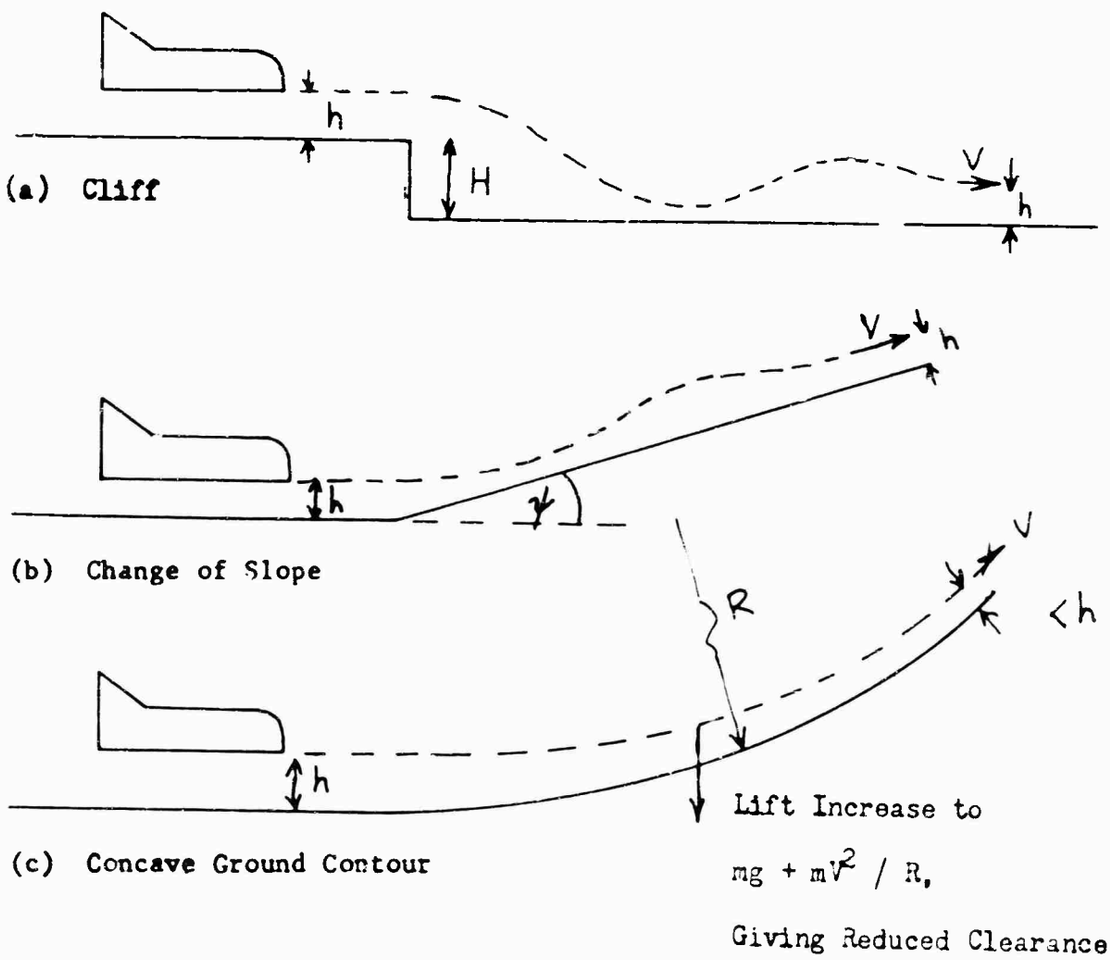

Figure 3. Three Idealizations of Irregular Terrain.

Three idealizations of typical terrain features are sketched in Figure 3. In each case the nature of the terrain change is such that the vehicle will approach closer to the ground during the transient phase of adjusting its flight path to the new terrain conditions. It is obvious that the greater the heave stiffness and damping, the greater the terrain discontinuity which the vehicle can cross without impacting its structure on the ground.

The importance of this aspect can be seen by considering the case of a change in slope, depicted in Figure 3(b). This is analogous to the sudden application of a downwards magnitude.

$$V \sin \chi$$

Using linear theory we can show[8] that the maximum excursion is given by

$$x_{max} = \frac{V \sin \chi}{\omega} e^{\xi/\eta(\phi - \theta)} \sqrt{\xi^2 + 2\zeta\xi + 1} , \qquad (13)$$

where $\sin \theta = \xi\eta / \sqrt{\xi^2 + 2\zeta\xi + 1}$ (first quadrant)

$\sin \phi = \eta$ (second quadrant)

$\xi = \omega x_0 / V \sin \chi , \quad \eta = \sqrt{1 + \zeta^2}$

x_0 = trim value

For the zero damping case this can be simplified to

$$x_{max} = \frac{V \sin \chi}{\omega} \sqrt{\left(\frac{\omega x}{V \sin \chi}\right)^2 + 1}$$

$$\frac{x_{max}}{x_0} = \sqrt{1 + \left(\frac{V \sin \chi}{\omega x_0}\right)^2} . \qquad (14)$$

Substituting equation (3) for ω, and since, from Figure 4

$$k x_0 = m g = (h^* - h_0) k ,$$

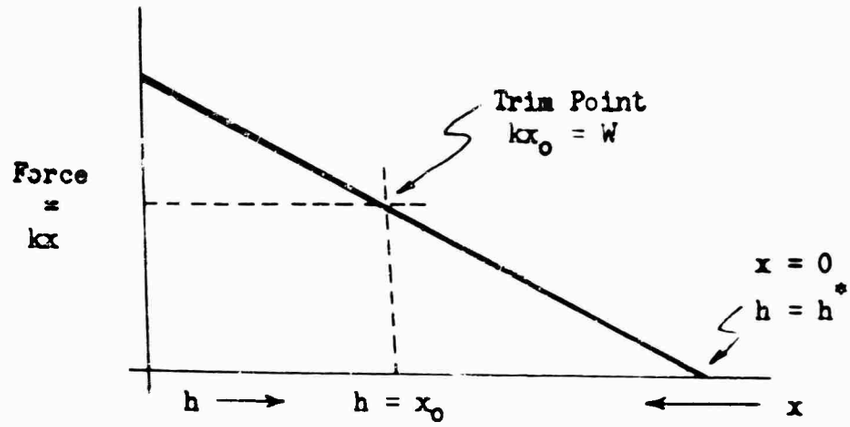

Figure 4. Linear Relationship Between x and h.

$$h^* - h_o = mg/k = g/w^2 \qquad \text{and} \qquad \frac{x_{max}}{x_o} = \frac{h^* - h_{min}}{h^* - h_o}$$

$$\therefore \frac{x_{max}}{x_o} = 1 + \frac{h_o w^2}{g} - \frac{w^2 h_{min}}{g}$$

$$\therefore \frac{h_{min}}{h_o} = 2\left\{\frac{3}{2} - \sqrt{1 + \frac{(V \sin \chi)^2}{2h_o}}\right\} . \tag{15}$$

An obvious limit is when the vehicle strikes the ground; that is, when $h_{min} = 0$. This is given by

$$V \sin \chi \Big]_{max} \cong \sqrt{\frac{5}{2} h_o} . \tag{16}$$

Thus a vehicle travelling at 50 knots, with a clearance height of 3 feet, would strike the ground if the slope change exceeded about 2^0. Although the inclusion of finite damping would increase this limiting angle, the smallness of the result justifies the crude linearizations used to obtain it.

A vehicle so limited would have little practical utility at high cruising speeds. Hence it is of the utmost importance, on this score alone, that we obtain a more comprehensive knowledge of heave stability, and a better predictive ability.

HISTORICAL SURVEY

TULIN [9]

The first published account of the dynamics of a GEM in heave is due to Tulin[9], who examined the case of a thin annular jet machine with compressible flow, and constant momentum flux.

Tulin showed that in addition to the ordinary "balanced" operation of the jet, two forms of "unbalanced" operation could occur; and he coined the terms "overfed" and "underfed" to describe these characteristics. In the "overfed" case the momentum flux of the jet is instantaneously greater than that required to support the base pressure. Hence the jet splits and part of the jet supplies additional air to the base region. Conversely, the "underfed" jet is too weak to support the base pressure and base cavity air is forced out below the jet. These flow regimes are depicted in Figure 5.

Obviously these conditions are transient, since the supply of air to the cavity will rapidly raise the base pressure in the case of the "overfed" jet, while the leakage of air from the base region with an "underfed" jet will rapidly reduce the base pressure until the pressure differential across the jet is balanced by the momentum flux.

Tulin's results showed that if overfeeding of the jet occurred when the GEM is rising, and underfeeding when it is sinking, then the motion is stable.

However, with very large base loadings or a large hollow below the base the converse could occur and the motion becomes unstable when the parameter β equals unity.

That is, for stability

$$\beta = \frac{h_o}{h_b} \gamma \frac{(P_b + P_a)}{P_b} > 1.0 \qquad (17)$$

where

γ = specific heat ratio = 1.4

h_b = height of base above ground

h_o = height of jet exit above ground at equilibrium

P_b = base pressure relative to atmosphere

P_a = static pressure of atmosphere

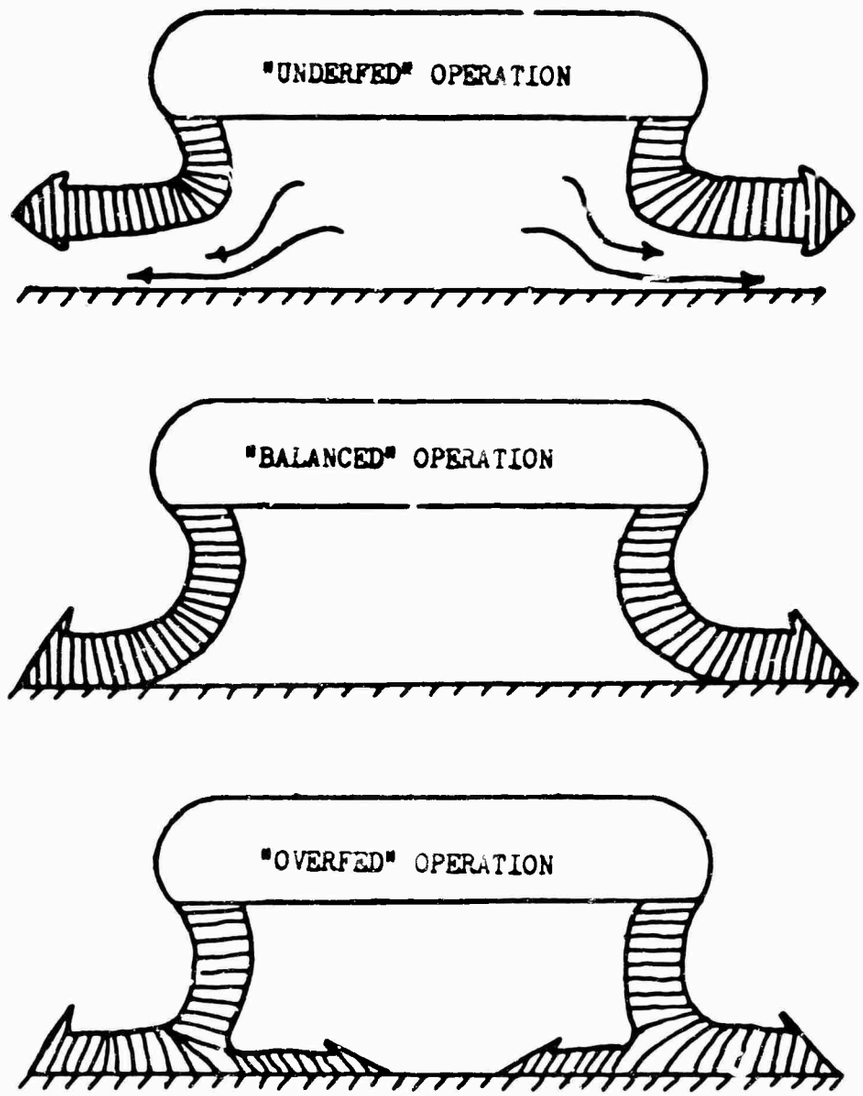

Figure 5. Jet Flow Patterns for "Underfed," "Balanced," and "Overfed" Operations.

Note that with a flat base ($h_b = h_o$) instability can never occur, but if $h_b = 14h_o$ then a base pressure of 220 pounds per square foot and more will cause instability.

Obviously, except in special cases, $\beta \gg 1$ and the heave motion will always be dynamically stable. Under these conditions "underfeeding" will always be associated with a sinking motion of the GEM, and "overfeeding" with a rising motion.

Tulin shows that the characteristic equation of motion is inhomogeneous and of third order, with two resonant frequencies, and that the coefficients differ in value depending on the condition of the jet (overfed or underfed). The natural frequencies of the heave motion are unaffected and are equal to

$$\omega_1 = \sqrt{g/h_o} \qquad \omega_2 = \sqrt{\beta \omega_1}\,.$$

EAMES [10,11]

A very detailed discussion of stability in heave and pitch was given by Eames in Reference 10 and summarized in Reference 11. In general, Eames agreed with Tulin's treatment and derived similar results, but showed that the time taken for the jets to adjust to changes in pressure distribution is very small and can be neglected.

Provided that β is large, the characteristic cubic equation in heave can be reduced to a subsidence of very short time constant (approximately $1/\beta - 1$) , and a quadratic. The frequency of the quadratic is as found by Tulin, and the damping ratio is bi-valued according to the condition of the jet. Eames recommended the use of the harmonic mean of the two damping values as being most accurate for a linear solution. Payne[12] subsequently showed that this was incorrect, and that the arithmetic mean should be used. Most of Eames work assumed that the fan supplied constant mass flow irrespective of the back pressure, but at the suggestion of the first author he later made a correction, which assumed the fan provided a constant total head. This latter is much more representative of the truth, and leads to reduced stability.

THE INFLUENCE OF FAN CHARACTERISTICS (NAY[13], WEBBER AND LIN[14], PAYNE[9])

Nay[13] investigated the heave stability of the Hughes Hydrostreak in 1960, and included terms to account for a linear variation

of fan pressure with flow. This is believed to be the first time that general fan characteristics were included in an investigation of GEM stability.

Webster and [illegible][14] and Payne[9] solved the problem of heave stability with general fan characteristics in 1962 and 1963 respectively, but the solutions are not readily applied to the standard type of fan characteristic curves, and Reference 14 continues to overemphasize the importance of β .

CROSS[15], STRAND[16] AND WALKER[17,18]

The assumption of "constant total head" was applied to the case of the GEM in heave by F. G. Cross, who took advantage of Eames' linearization to assume that he would be justified in calculating separately the "derivatives" or partial differentials of the heave motion, and specifically, the force due to rate of change of height through the equilibrium height, and the force due to change of height at zero rate of change of height; i.e.,

$$\left[\frac{\partial L}{\partial \dot{h}}\right]_{h = h_o}$$

and

$$\left[\frac{\partial L}{\partial h}\right]_{\dot{h} = 0,\ h = h_o}$$

Strand made a similar calculation for the "underfed" case only, and Walker attempted to correlate these theories with experiment. However, the results differed greatly (Figure 6) and did not agree well with experiment or with the theoretical values recalculated by Walker[17]; thus in 1962 he proposed to USATRECOM that an attempt should be made to solve the damping problem experimentally, suggesting:

1. that the derivative should be measured directly as $\partial L/\partial \dot{h}$ and $\partial L/\partial h$, in the former case using the artifice of sucking air out of the cushion or blowing it in to cause the "underfed" and "overfed" jet condition to appear as a steady phenomenon.

2. that the damping and frequency calculated from these measurements should be compared with the total damping coefficient and frequency derived from oscillation tests and various theories.

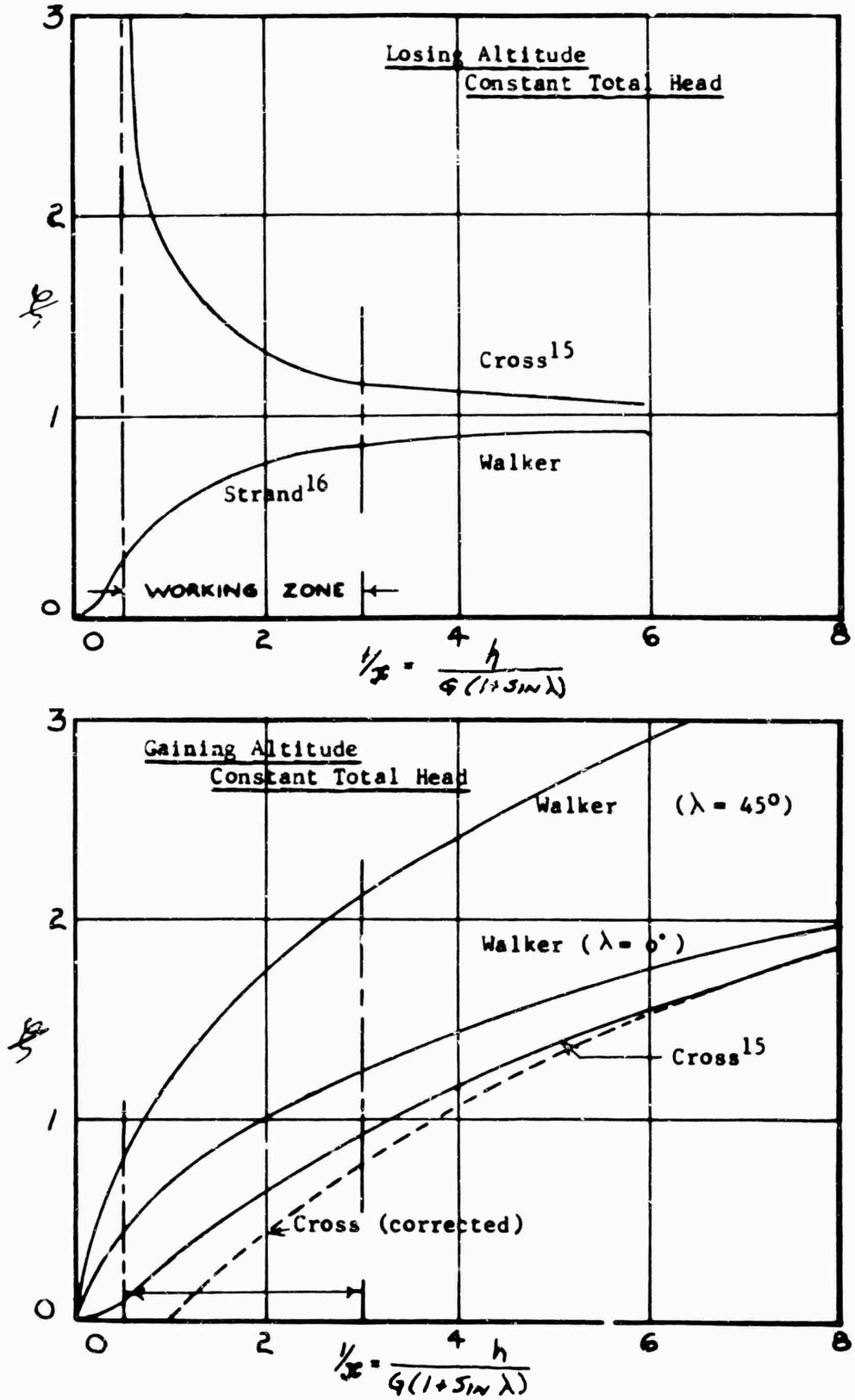

Figure 6. Different Estimates of the Damping Ratio " ζ " (Ref. 17).

3. that the fan characteristics of the model be determined and if possible the importance of these be demonstrated as we had suggested in Reference 1.

DESCRIPTION OF MODEL AND THE EXPERIMENTAL PROCEDURE

The model GEM had been built for a previous investigation[19] and required little modification for the present work. It is illustrated in Figures 7 and 8, in the forms used for this part of the report and also for the previous roll investigation - Part 1. Figure 7 shows the overall dimensions applicable to all versions and the base used on the thick jet model. The sectional view of Figure 8 shows the annular jet in greater detail and the removal of the base leaves the outer housing to act as a plenum chamber. The modified plenum chamber with ½ 'nozzle' type fairings used in Part I of this report was not used in the investigation of heave damping.

Further details of the model are given in Part 1 of this report.

MEASUREMENT OF LIFT

A. Thick Jet Model

The model was placed in the arms of a horizontal weight beam (Figure 23) where the axis of rotation of the machine was slightly above its CG to permit t ratural roll stability to hold the GEM parallel to the ground plane. The weight beam was pivoted to allow the machine to rise and fall vertically. The beam was also provided with a counterbalance so that the vertical force as seen by the GEM could be varied and measured.

The rise height of the machine - the clearance between the ground board and the GEM - was determined through an optical system attached to the weight beam and a fixed reference point. With the machine power off, the machine rested on the horizontal ground board. The lift of the machine was varied by adding weights to the GEM or to the weight beam. Data recorded were the rise height and RPM of the GEMs fan for a fixed lift. These results are shown in Figure 9 and in Table 1. Since the lift is proportioned to the square of the fan RPM, the results from Figure 9 can be replotted to show the variation of rise height with $RPM/1000^2/L = N^2/L$ in Figure 10 and in Table 2. From these plots the rise height can be determined from any given value of a fan RPM and lift.

B. Plenum Model

The same procedure used with the thick jet was followed in measuring the lift, fan RPM and rise height. Figure 11, the variation of rise height with fan RPM for fixed lifts, shows a region of in-

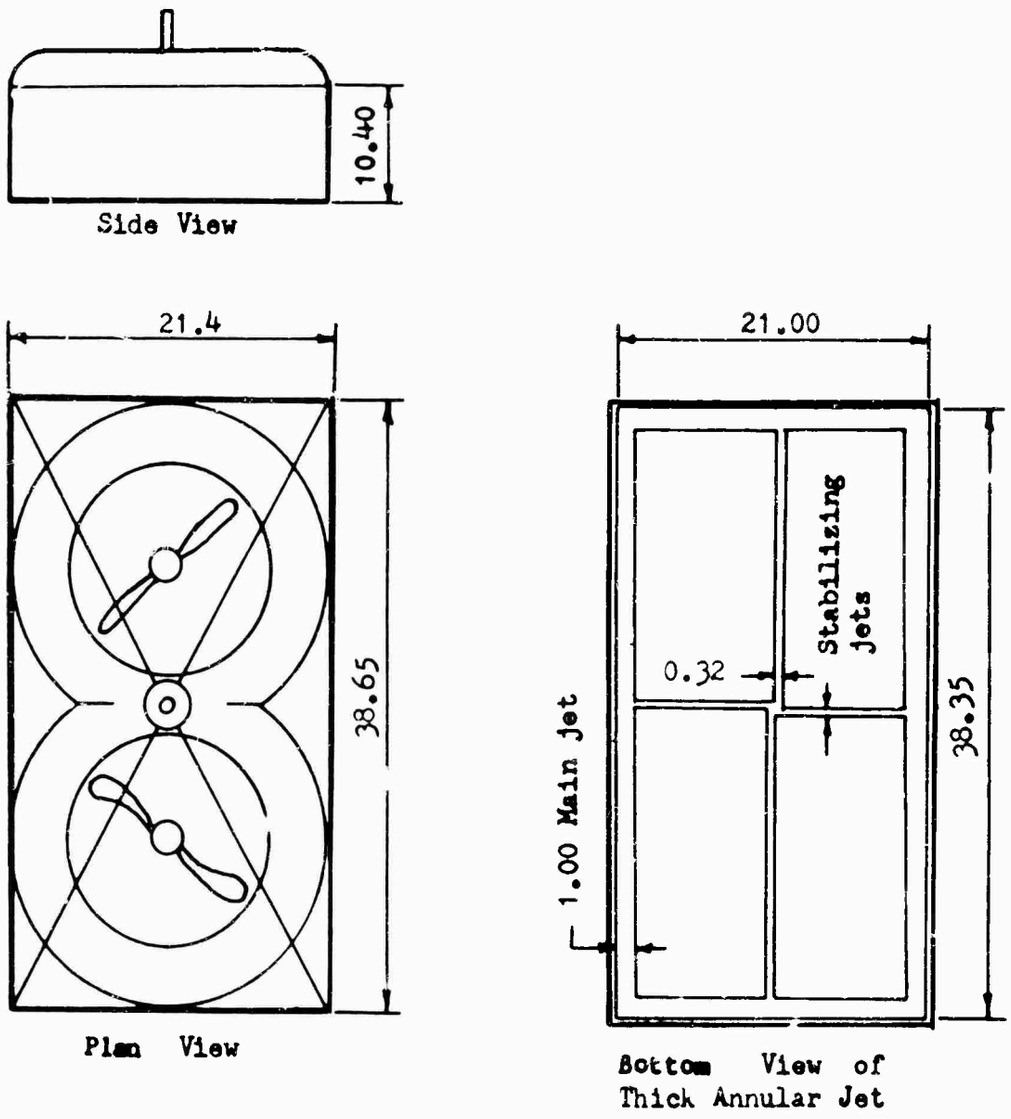

Figure 7. The Annular GEM Model Sheet 1.

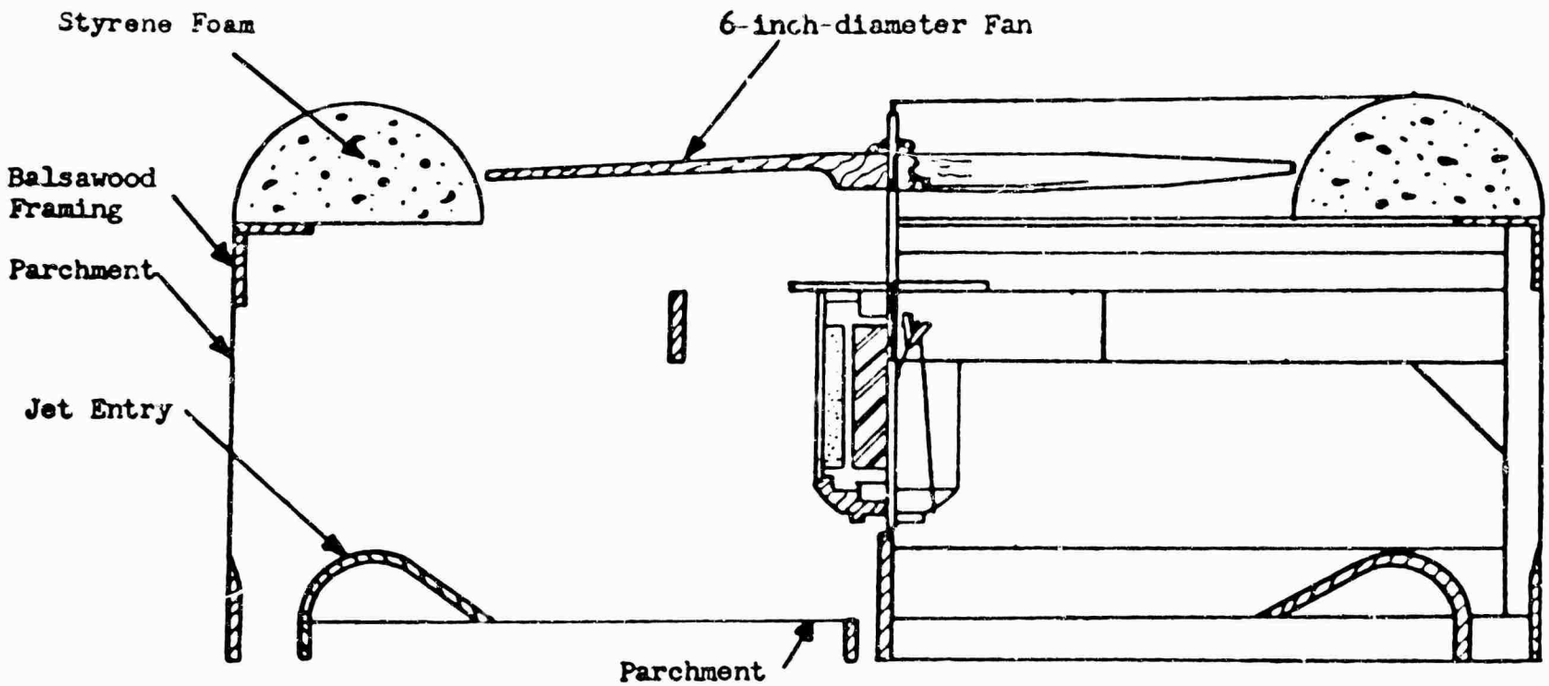

Transverse Half Section and Internal View of Motor Mounting

Figure 7. The Annular GEM Model Sheet 2.

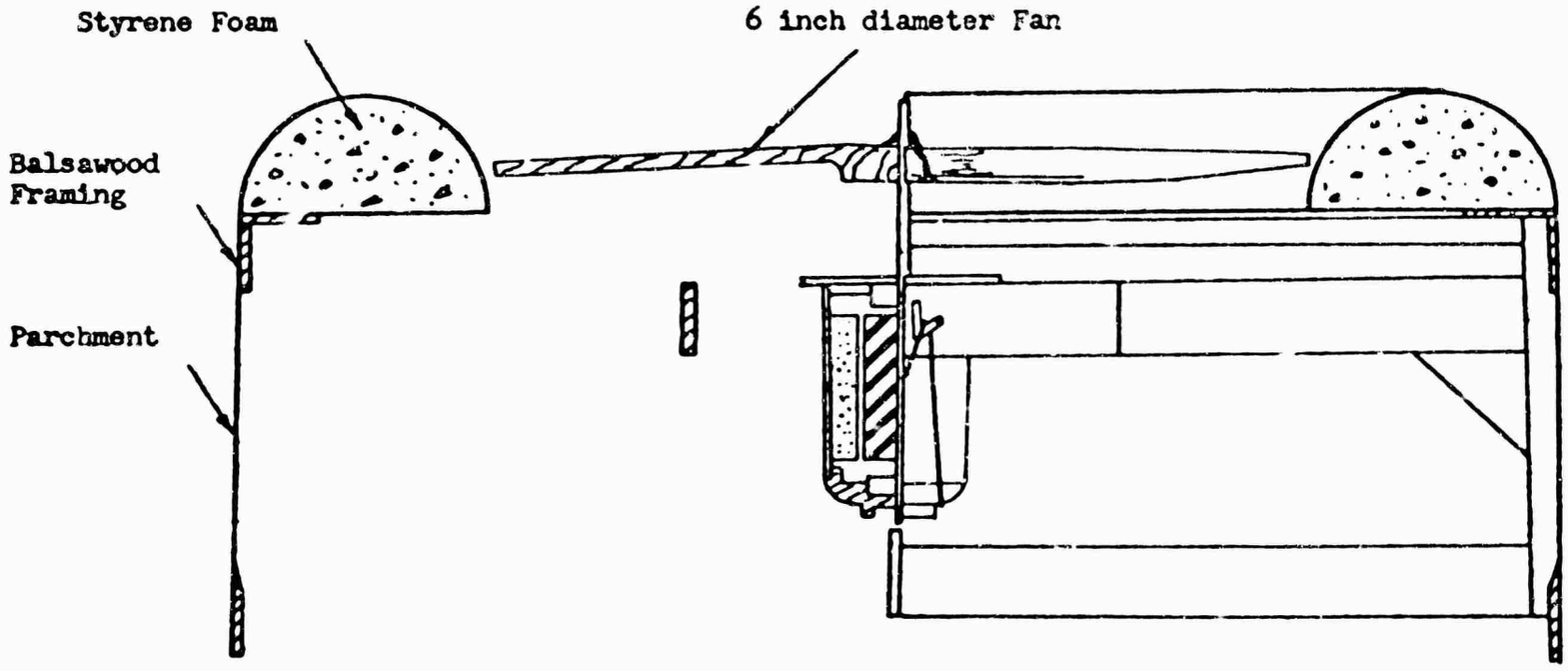

Tranverse Half Section and Interior View of Motor Mounting

Figure 8. The Plenum Chamber GEM Model.

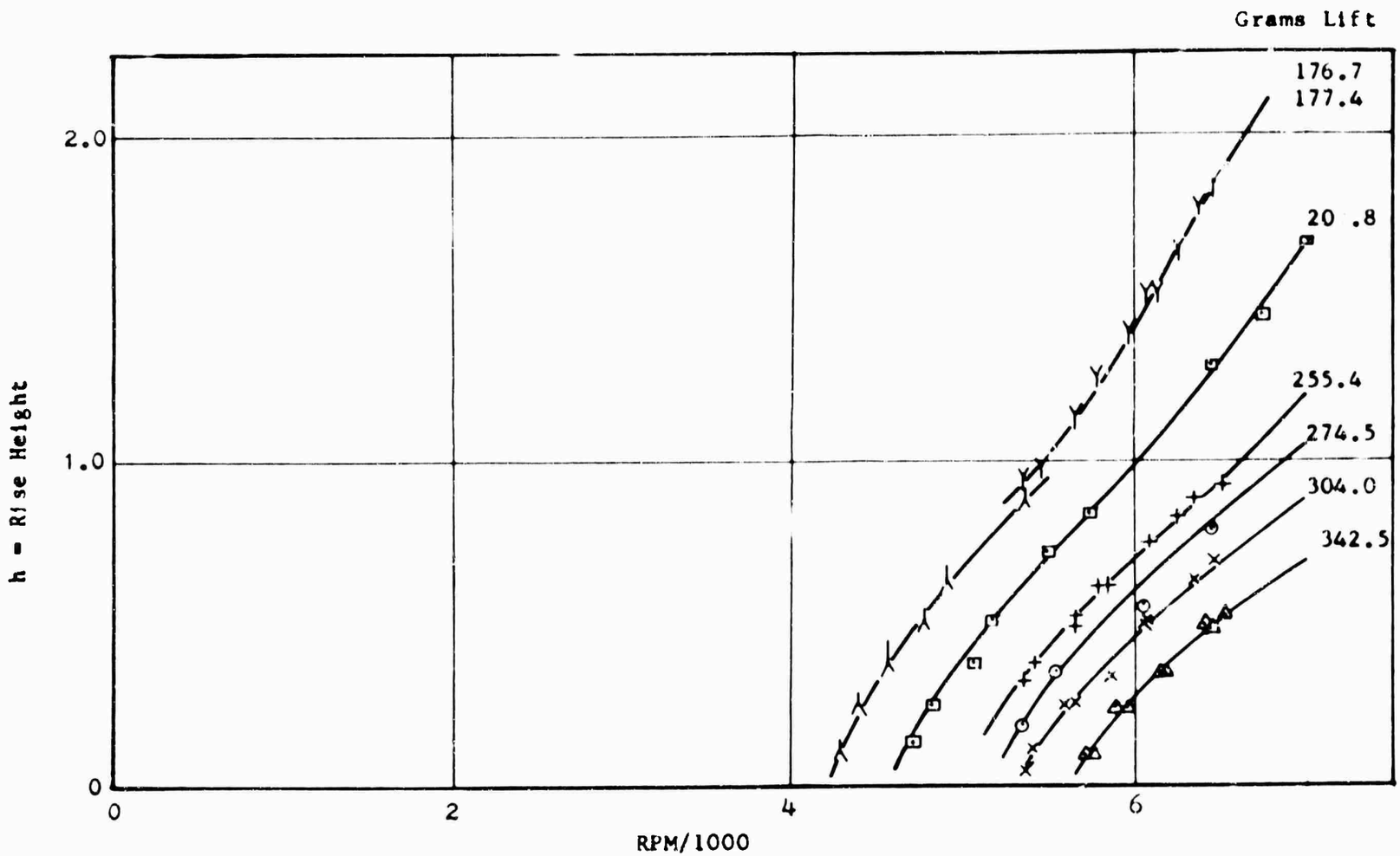

Figure 9. Variation of Rise Height With RPM for Fixed Lifts - Thick Annular Jet GEM Model.

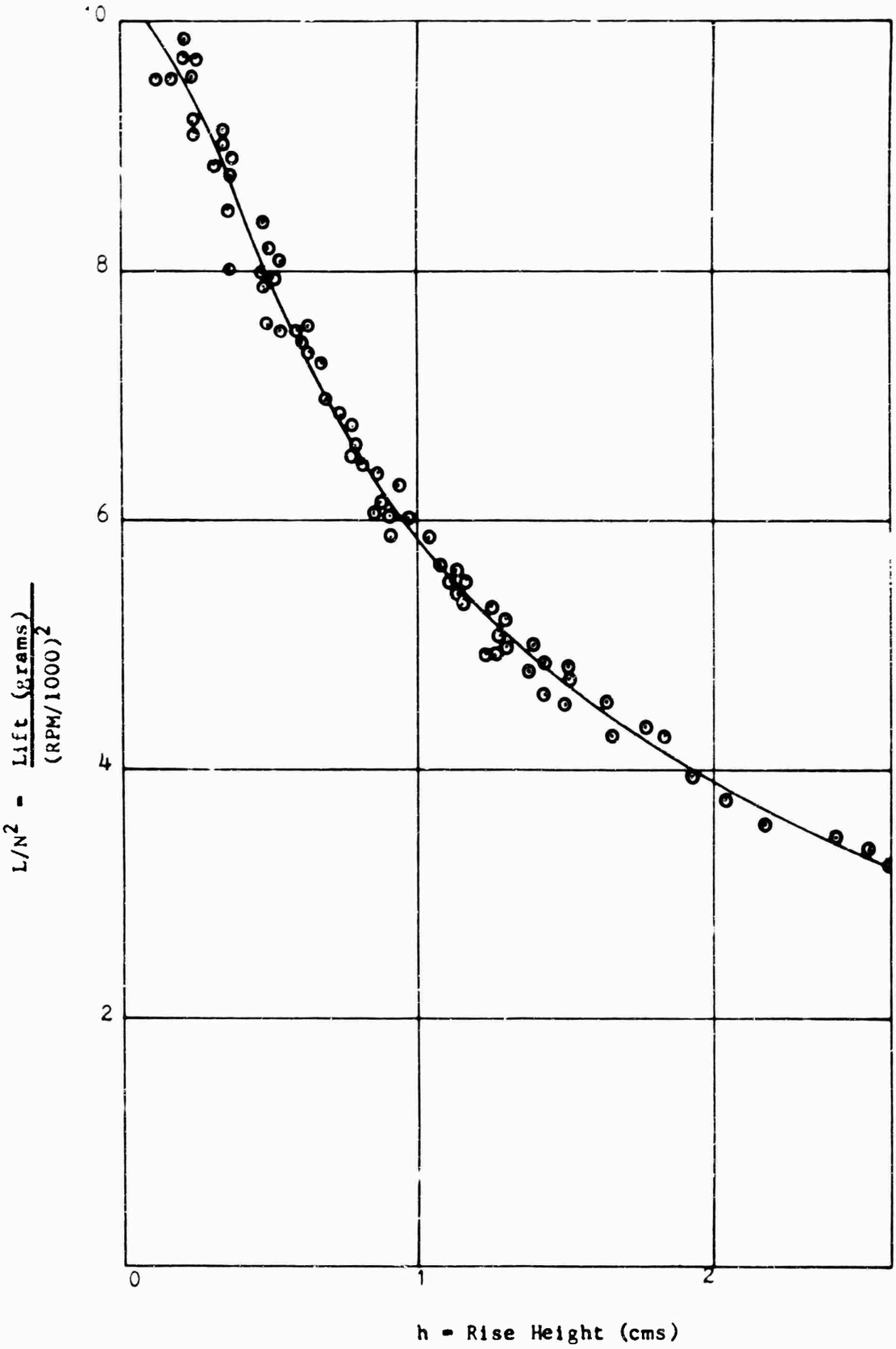

Figure 10. Consolidated Lift Results - Thick Annular Jet GEM Model.

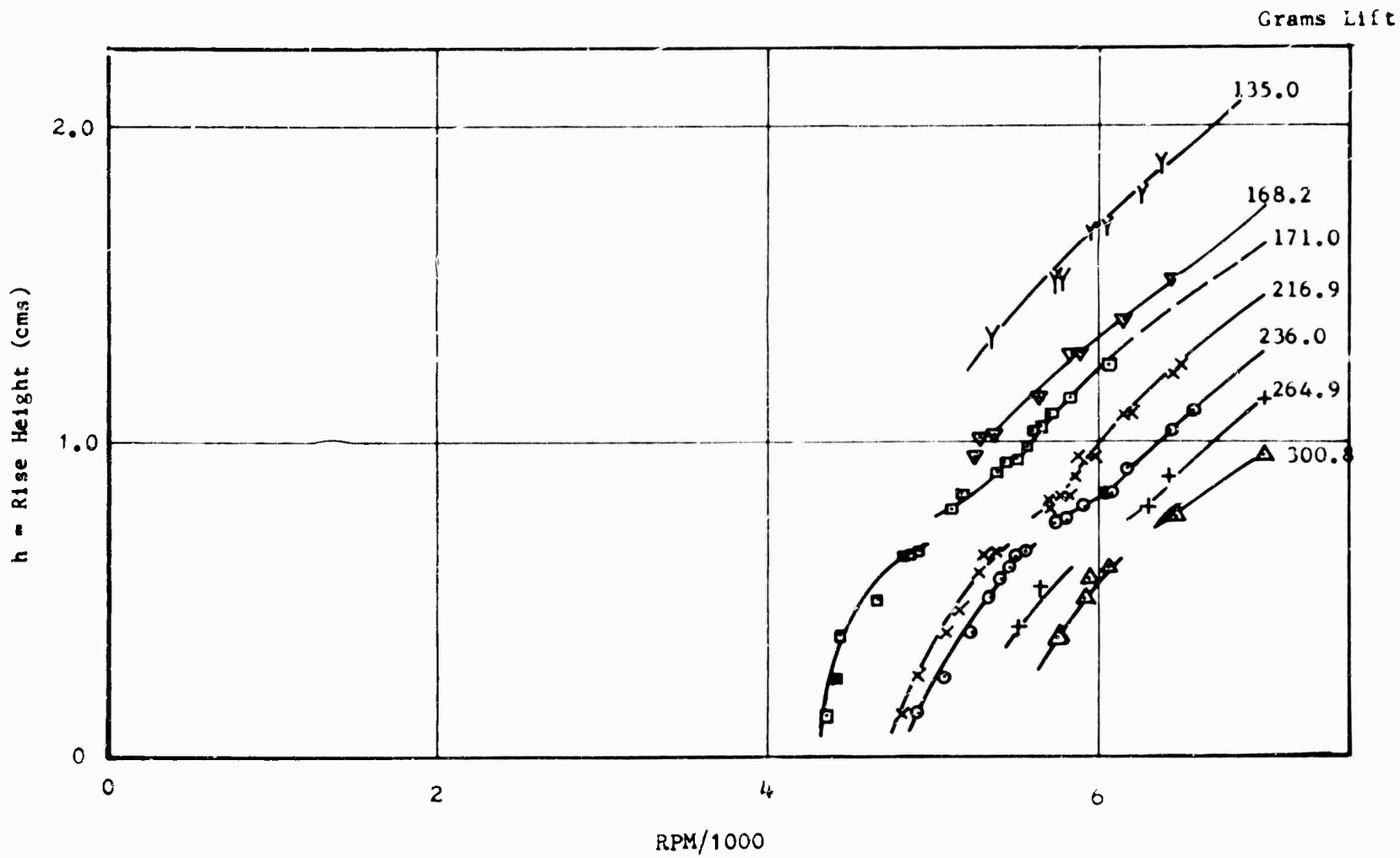

Figure 11. Variation of Rise Height With RPM for Fixed Lifts - Plenum Chamber GEM Model.

stability between .65cm and .75cm altitude, which was apparently due to the flow separation in the corners of the plenum model since the control altitude was not affected by change of weight or fan RPM. These results are substantiated in Table 3. As before, a consolidated plot of lift/(RPM/1,000)^2 versus rise height is given in Figure 12 and Table 4. (A wide range of groups were tested informally on the annular jet model but the instability could not be found in this case. It is therefore <u>not</u> due to the fan.)

FAN CALIBRATION TESTS

A. Thick Jet Model

A duct was constructed as shown in Figure 13, such that the total pressure in the jet of the GEM and the volume flow could be measured. Restrictions (blockages #0 to #10) were placed downstream from the wind-tunnel nozzle to vary the back pressure, so that different rates of flow were obtained while keeping the fan RPM and the exit conditions from the GEM nozzle constant.

A first test conducted was to check and see that there was a linear variation of pressure rise with (RPM)^2. Figures 14 through 17 show, for different blockages, a linear relationship of total pressure in the GEM nozzle (h_t) and duct exit dynamic head (h_v) with fan (RPM)^2.

From the slopes of these curves the fan characteristics C_p and λ were calculated (See Appendix I).

$$C_p = \frac{\text{Total pressure at exit of GEM jet}}{\text{Dynamic head at fan tip due to rotation}}$$

$$\text{or} \quad C_p = \frac{8\,P_t}{\rho\omega^2 D^2} = \frac{8.81\,h_o}{N^2} \quad \left(N = \frac{RPM}{1000}\right)$$

$$\lambda = \frac{\text{Average fan intake velocity}}{\text{Fan tip speed}}$$

$$= \frac{4Q}{\pi\,\omega\,D^3} = \frac{1.61\sqrt{h_v}}{N}$$

where Q = total volume flow through both fans.

The variation of C_p with λ for the thick jet model is plotted in Figure 18 and tabulated in Tables 5A and 5B.

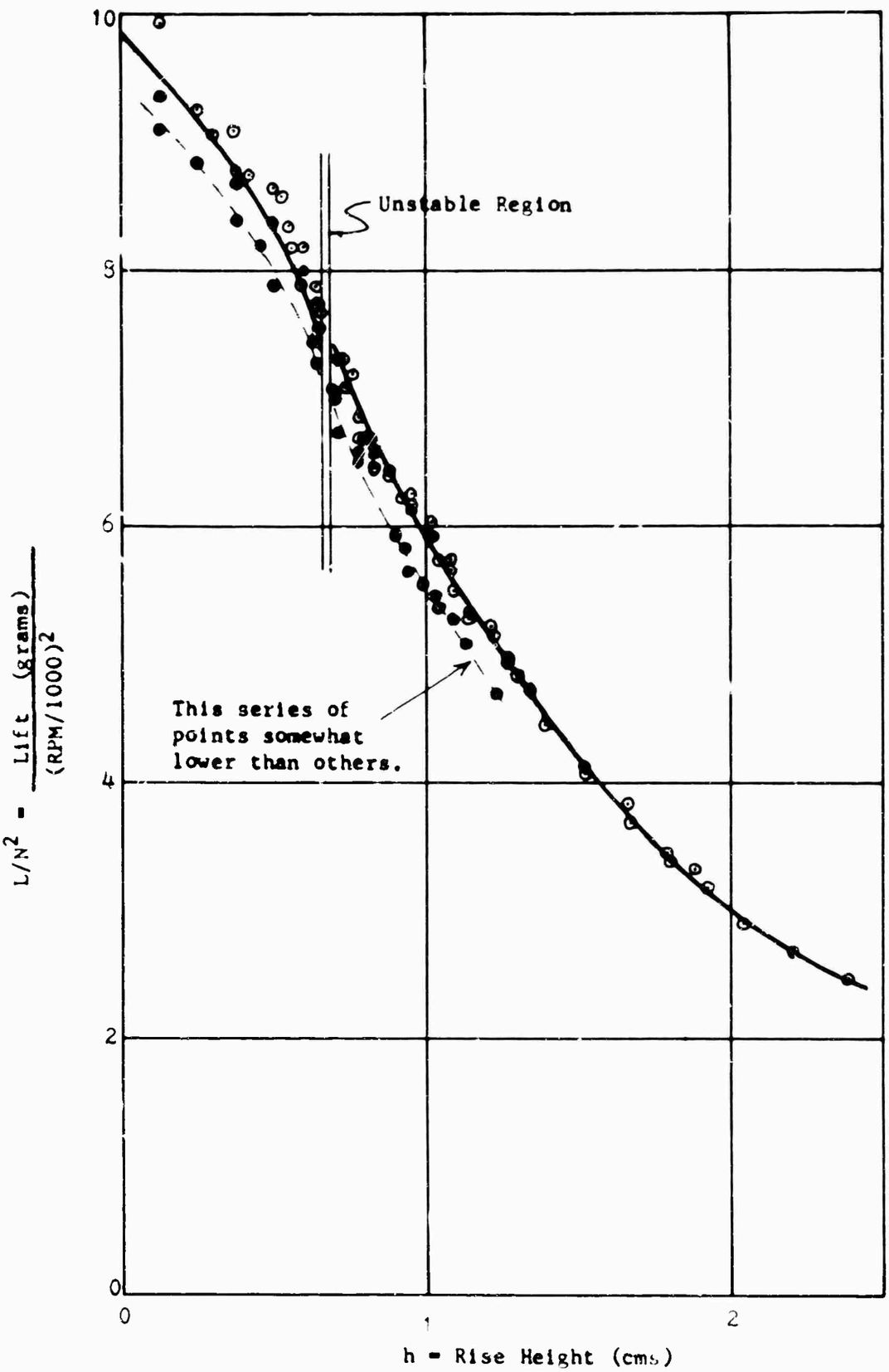

Figure 12. Consolidated Lift Results - Plenum Chamber GEM Model.

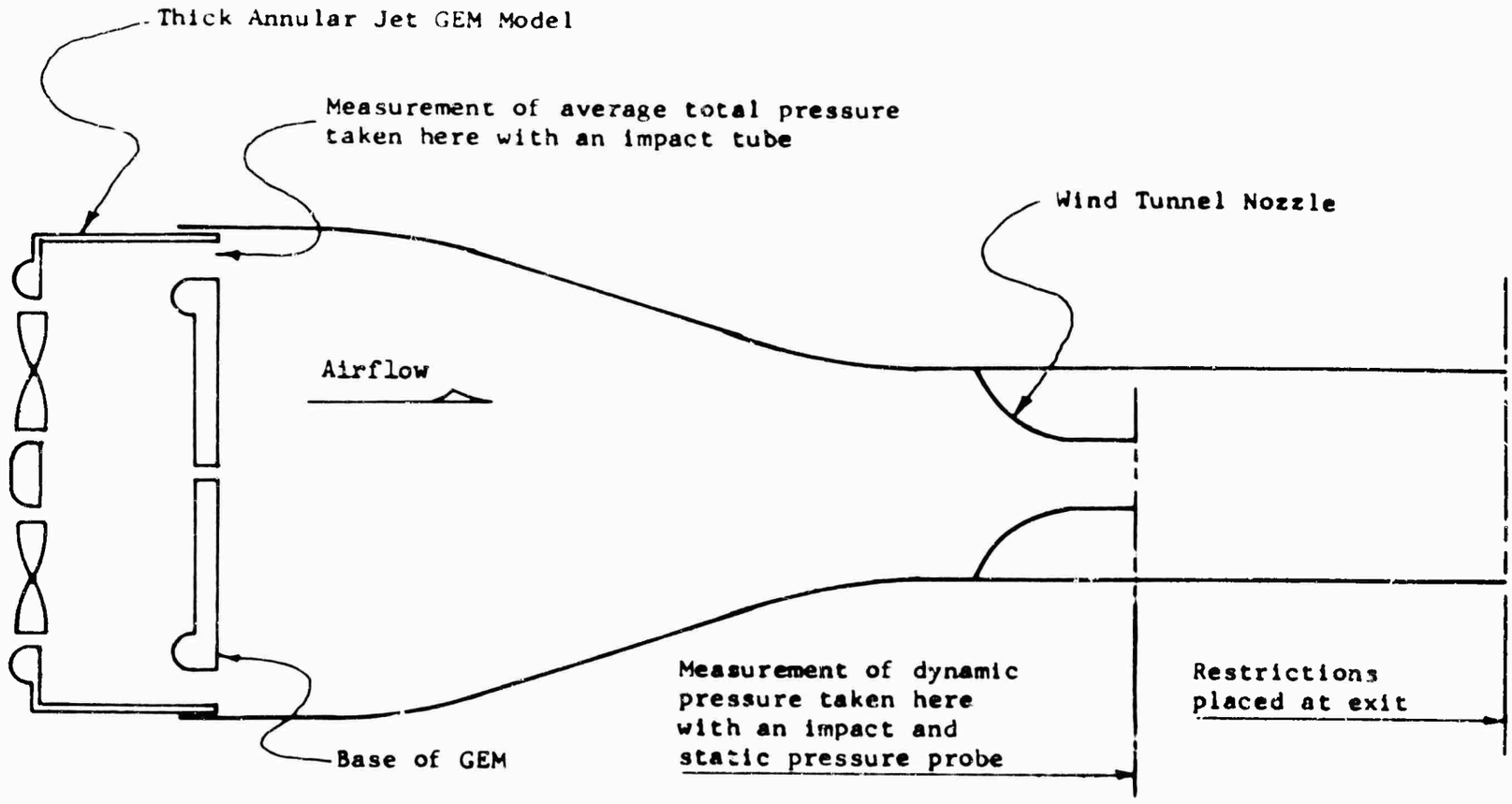

Figure 13. Ducting System for GEM Fan Calibration.

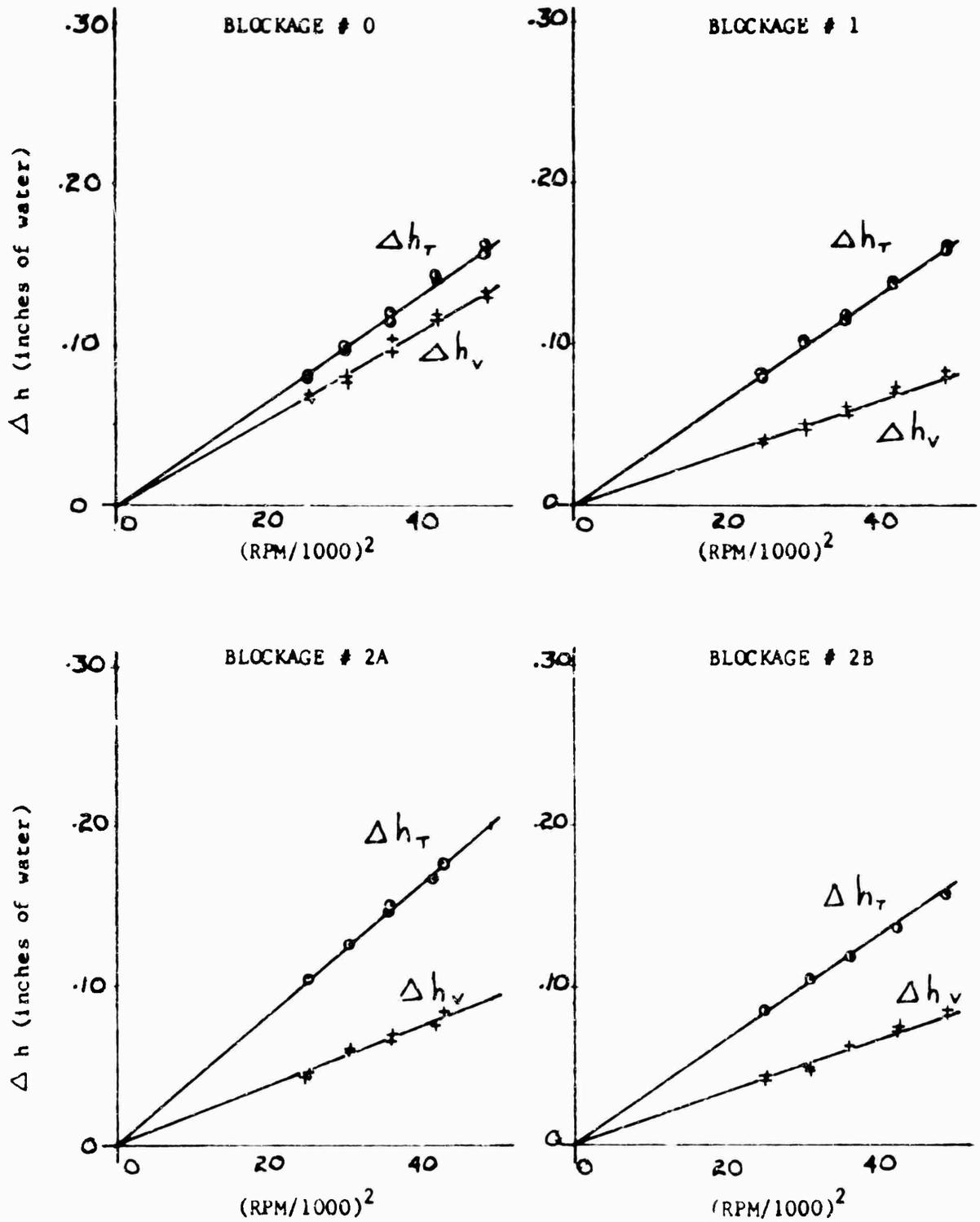

Figure 14. Duct System Calibration for Various Blockages.

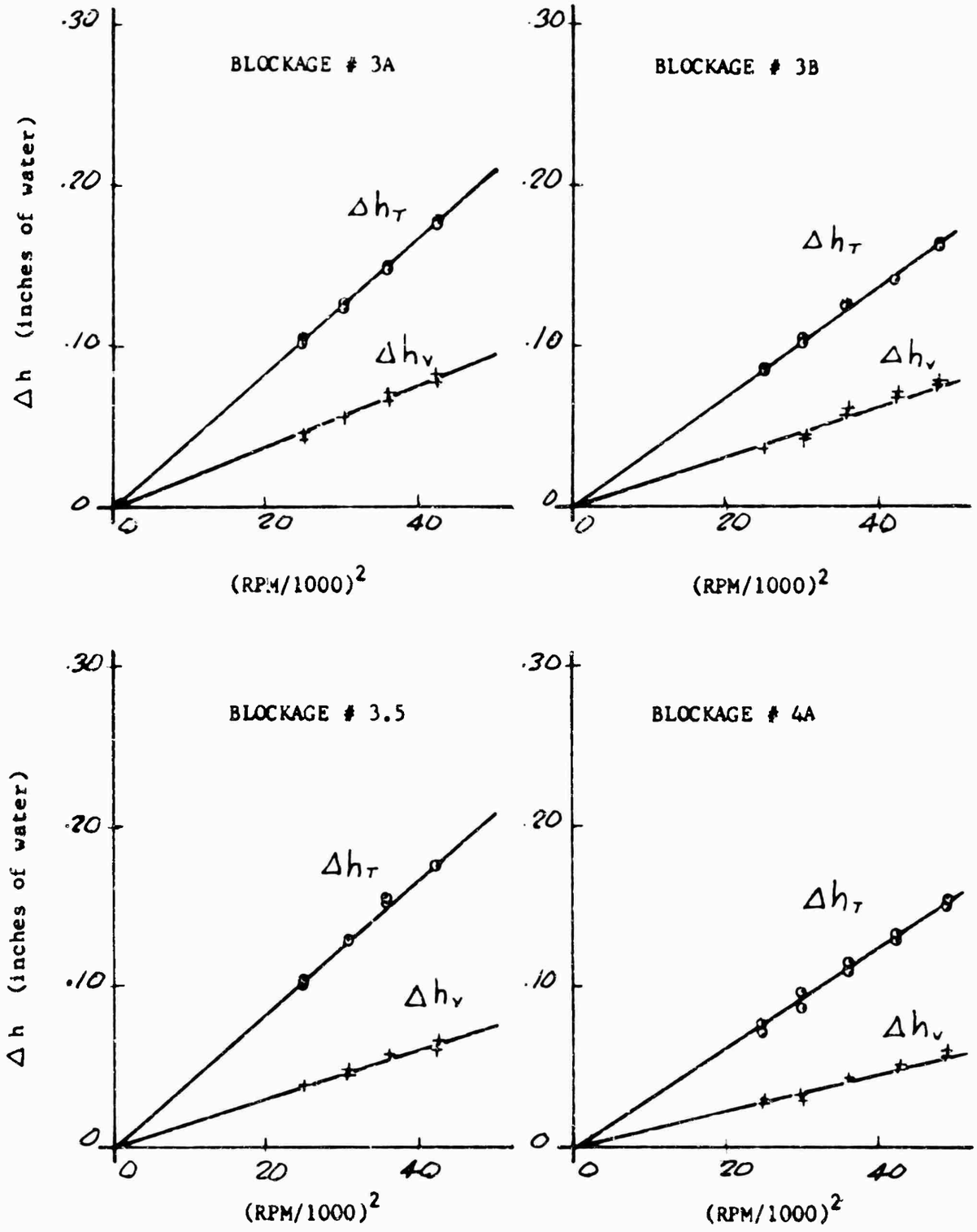

Figure 15. Duct System Calibration for Various Blockages.

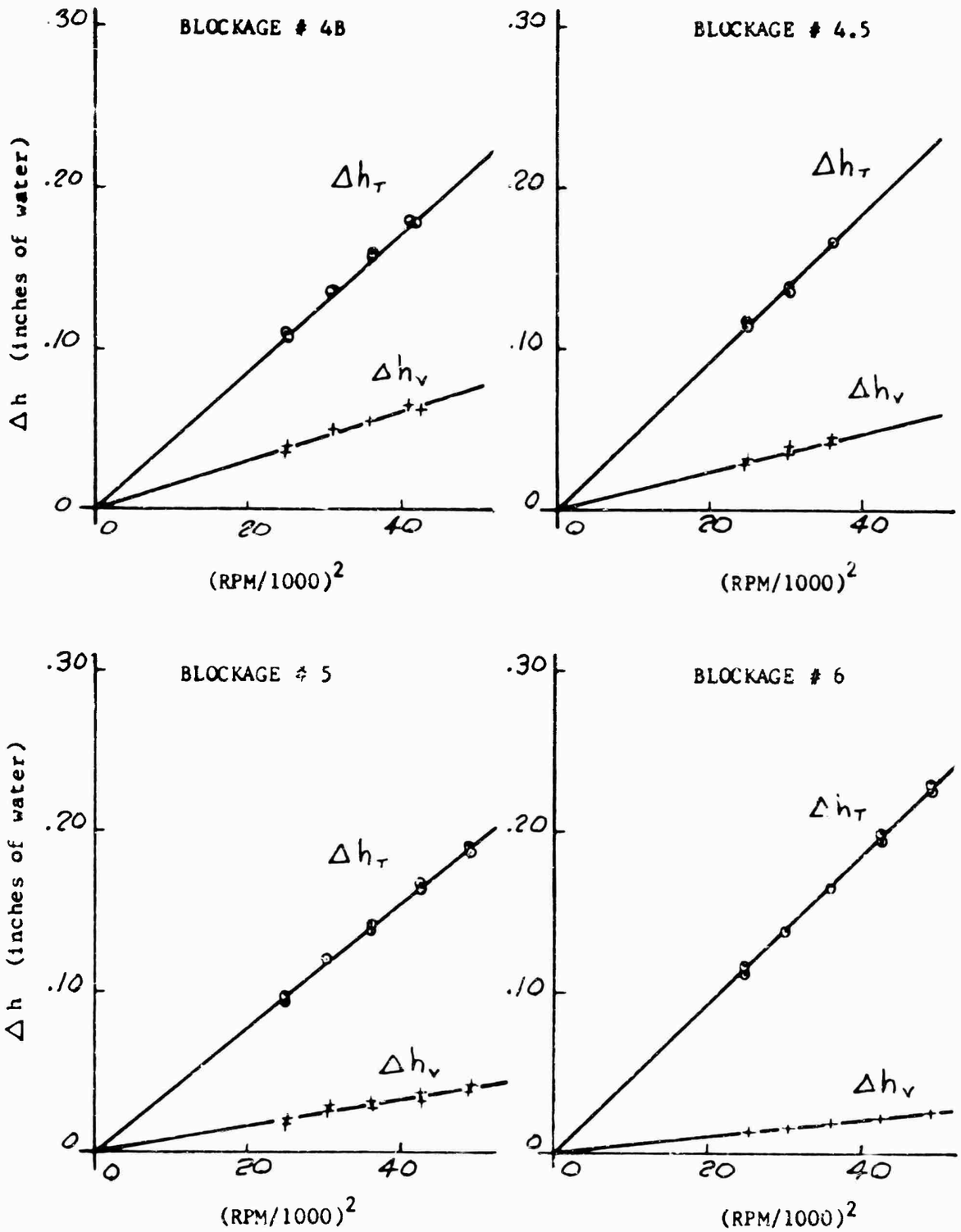

Figure 16. Duct System Calibration for Various Blockages.

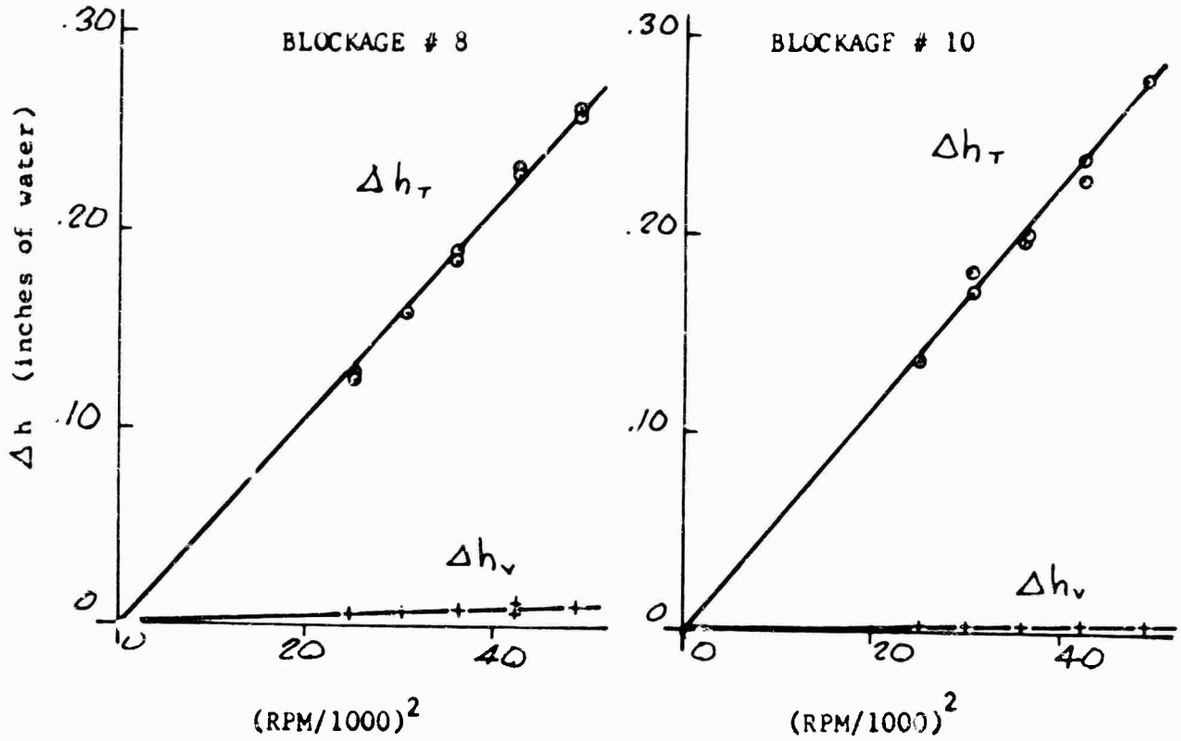

Figure 17. Duct System Calibration for Various Blockages

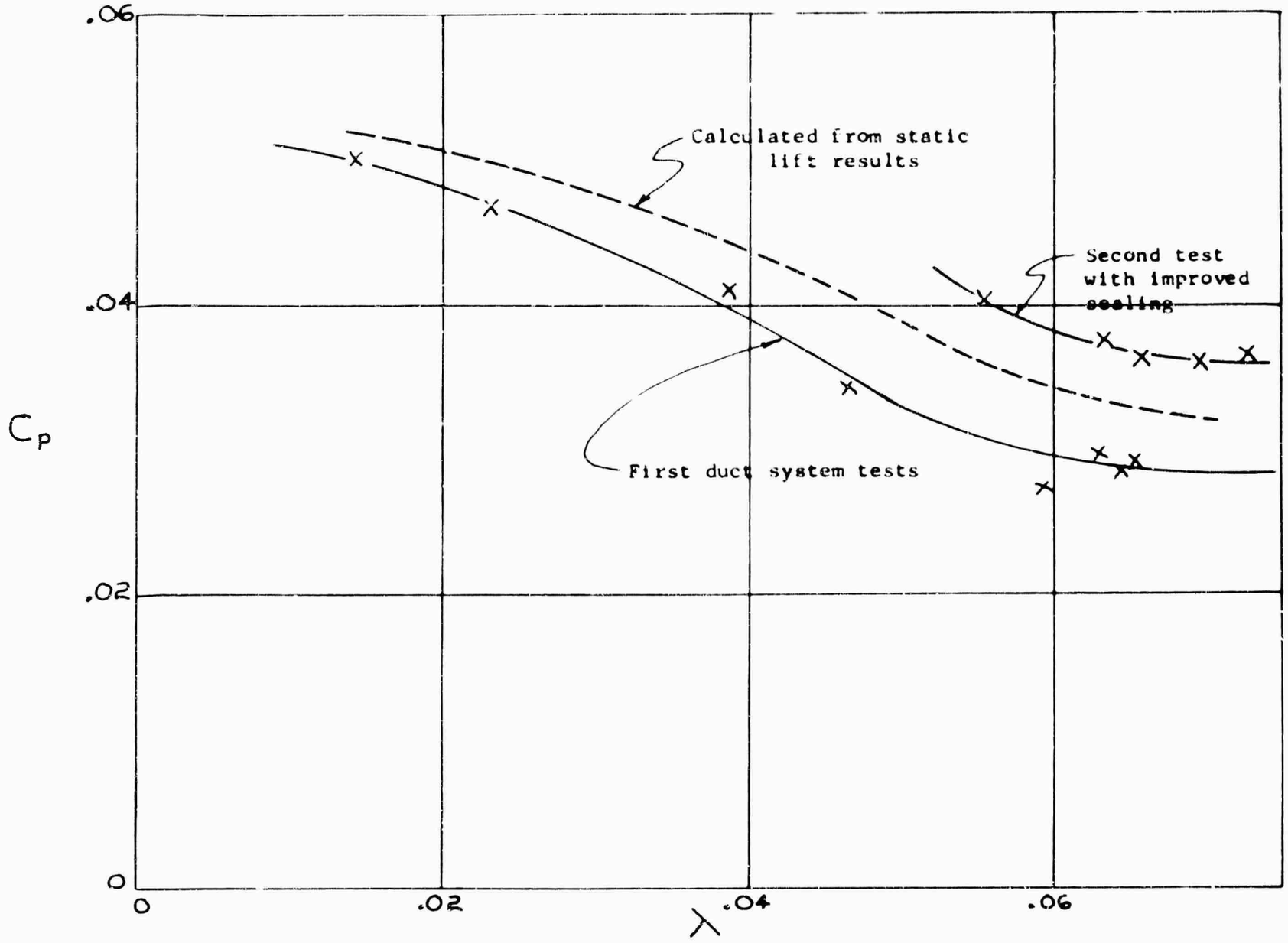

Figure 13. Comparison of Fan Pressure Coefficient C_p With Flow Parameter λ for Thick Annular Jet GEM Model.

B. Plenum Model

The equipment used to determine the fan characteristics for the thick jet model could not be used with the plenum model because the plenum would exhaust lengthwise into the duct instead of laterally on to a ground board and the flow conditions would not be duplicated. This could only be done by measuring the air-flow at the ake of the fans, and restricting the outlet with a ground board and contract funds did not permit this. However, the variation of C_p with λ can be determined from the lift curves for the plenum (assuming that the pressure in the plenum is uniform).

Assuming $L = SP_t$

then $$C_p = \frac{8\,P_t}{\rho w^2 D^2}$$

$$= \frac{8\,L}{\rho w^2 D^2\,S}\,. \qquad (18)$$

From the lift curves we can read of lift as a function of RPM^2 for each rise height.

Substituting into the above equation yields

C_p = for a particular rise height.

$$0.0045\,\frac{L}{N^2} = \frac{8.81}{N^2}\left[\frac{L/S}{1 - e^{-2/h}}\right]. \qquad (19)$$

Also $$\lambda = \frac{4\,Q}{\pi w D^3}\,. \qquad (20)$$

Where Q = the volume rate of flow out of the cushion

$$= C_D\,V_e h = C_D\,h\sqrt{\frac{2\,P_t}{\rho}}$$

Taking the discharge coefficient $C_D = 0.62$,

and by using $\frac{2P_t}{\rho} = C_p \; 2/8 \, . \, \omega^2 \; D^2 = V^2_e$,

then $\lambda = \frac{1.25}{\pi D^2} C \, h \sqrt{C_p}$

(21)

now $C = 118.7$cms

$D = 13.0$ cms

yielding $= 0.28 \, h \sqrt{C_p} = 0.0187 \, h \frac{\sqrt{L}}{N}$ (22)

Figure 19 and Table 6 show the relationship of C_p and for the plenum model, including the region of flow instability.

DETERMINATION OF $\partial L / \partial \dot{h}$ BY FEEDING AND BLEEDING THE AIR CUSHION

A. Thick Jet Model

The model was set up in the apparatus while the GEM was in the weight beam, as shown in Figure 20. A reference height was chosen, then the GEM power and the air pump were turned on. Weights were added to the GEM or weight beam to return the GEM to the reference height, which was monitored by an optical system. By changing the plumbing, the air pump could either draw air out of the air cushion or feed air into the cushion. Data recorded were the references rise height, (h_r = 0.95 and 0.35cm), the weights added, and the density and temperature of air bled or fed into the air cushion. The test for a particular rise height was conducted at a constant fan RPM.

The results of this test were plotted (Figure 21) in the form of $\Delta L / L_r$ versus $\dot{h}/h_r$ and tabulated in Table I.

Where ΔL = change in lift

L_r = lift of GEM when trimmed at reference altitude h_r

Now $\frac{\dot{h}}{h_r} = \frac{\Delta Q}{S h_r}$ ΔQ = flow rate into or out of cushion (23)

S = Base Area

h_r = reference rise height

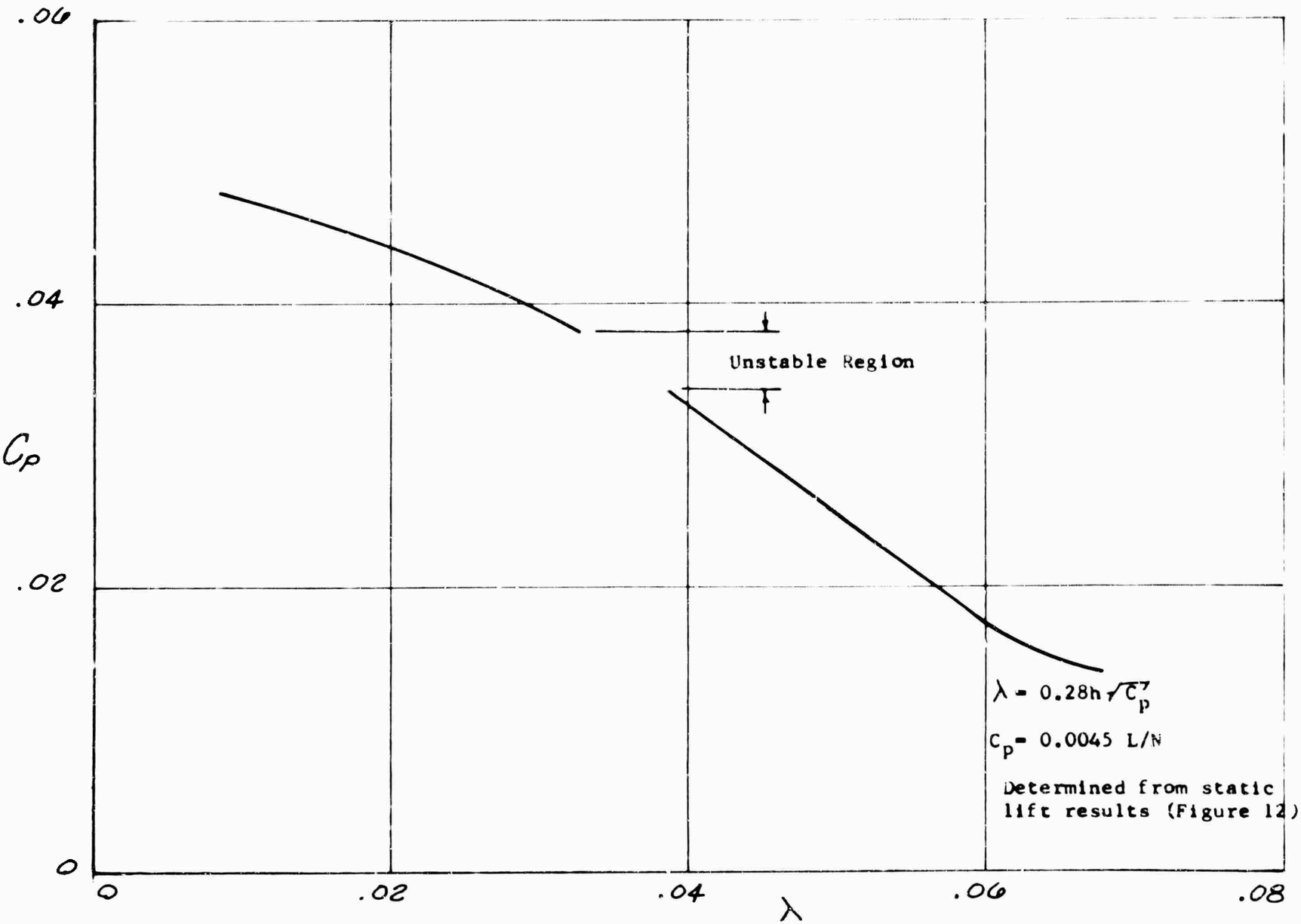

Figure 19. Fan Pressure Coefficient C_p Versus Fan Flow Parameter - Plenum Chamber GEM Model.

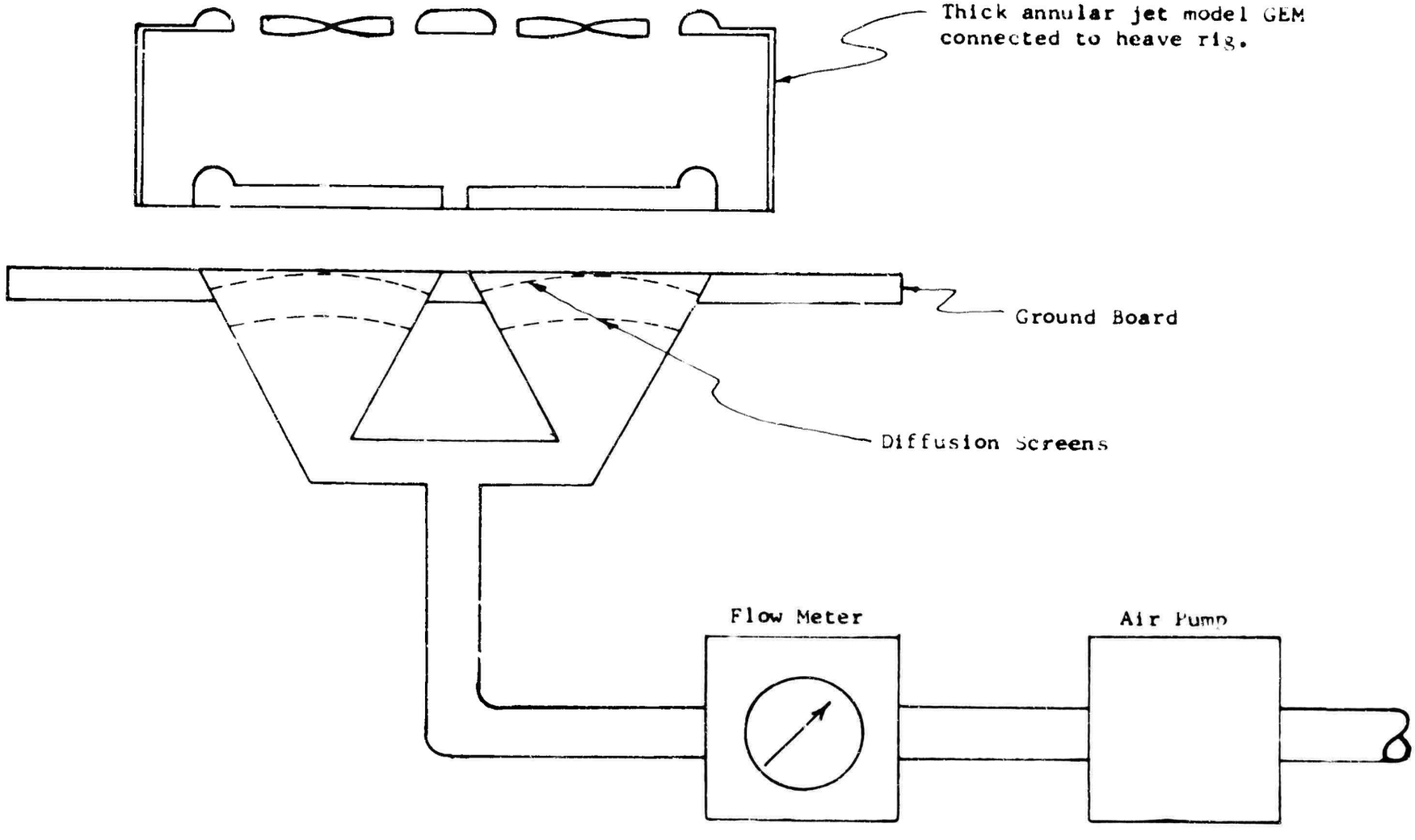

Figure 20. Apparatus for Feeding and Bleeding Air Cushion.

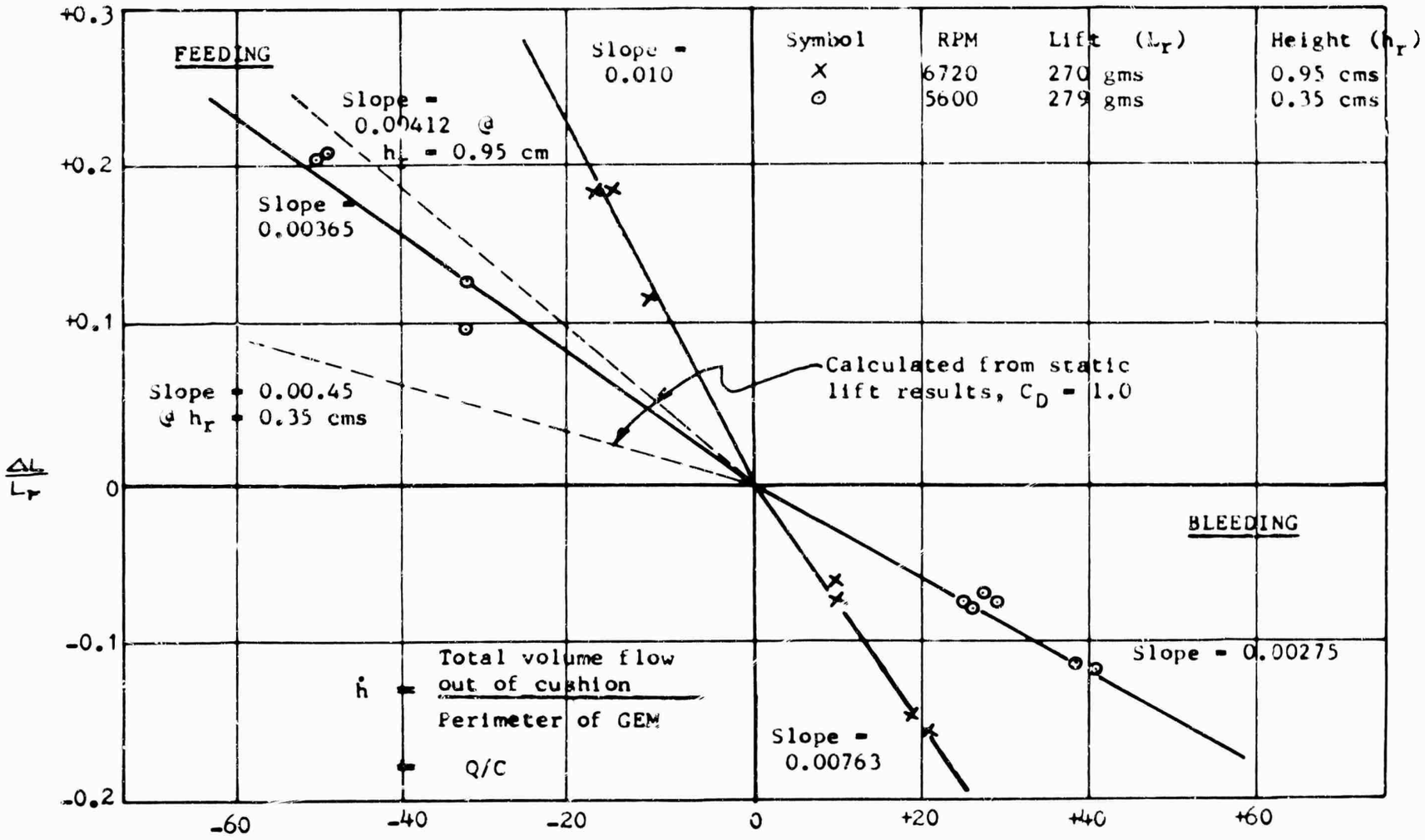

Figure 21. Variation of Lift Change $\Delta L/L_r$ With the Effective Heave Velocity $\dot{h}/h_r$ for the Thick Annular Jet GEM Model, Measured With Steady State Airflow.

and the value of the derivative $\partial L/\partial \dot{h}/\partial L/\partial h_r$ can be obtained for each rise height and for both feeding and bleeding condition. Note that as expected these two results are appreciably different.

Results are also given in Figure 33 for $\frac{\partial L}{N\,\partial \dot{h}}$, to faciliate the comparison with the lift results.

B. Plenum Chamber Model

The same procedure was followed here as with the thick annular jet model. The test was conducted at the same two rise heights, h_r = 0.35cm and 0.95cm. The parameter $\Delta L/L_r$ was again plotted against $\dot{h}/h_r$, as shown in Figure 22 and Table 8, and the slope measured for each condition.

Results are given for $\frac{\partial L}{N\,\partial \dot{h}}$ in Figure 3.

DETERMINATION OF $\partial L/\partial h$ AND $\partial L/\partial \dot{h}$ FROM OSCILLATION TESTS

A. Thick Jet Model

The purpose of oscillation tests in heave was to determine the natural frequency and damping of the GEM model and to relate these quantities to the derivatives $\partial L/\partial h$ and $\partial L/\partial \dot{h}$, as measured in other experiments and also calculated by various theories.

In practice, however, the GEM must be restrained in some way to obtain this data and a great simplification results from using the constrained data direct without conversion to the hypothetical results for a free flying model since the derivatives can be determined directly from the constrained tests.

The GEM model was suspended from pivot points above the CG in the same pivot frame which was used for the lift tests. Hence the model is free to lift, but can also rotate and roll so that the natural stability will hold the base parallel to the ground plane. Weights could be added to the rear of the frame thus reducing the lift force needed to maintain equilibrium, or to the model itself, thus increasing the necessary lift. In this way tests could be made at different hover heights with a fixed fan RPM. The fans were started and the model allowed to stabilize at the natural hover height which was recorded. The model was then disturbed in heave and the oscillations recorded with a friction-free electrolytic pickoff and Honeywell Visicorder. The oscillations were analyzed to give the damping ratio and natural frequency. At the greater hover heights and those at hover

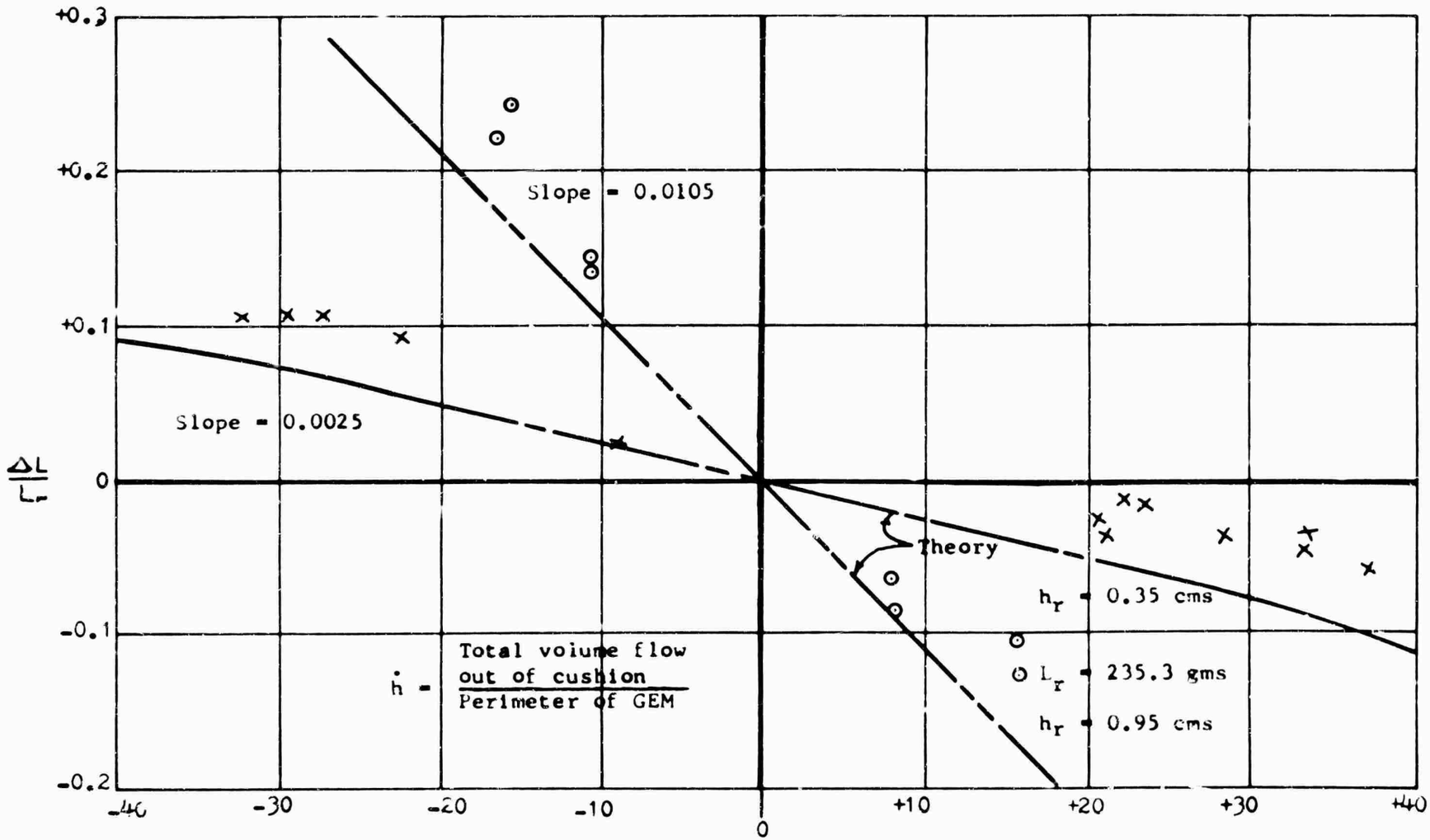

Figure 22. Variation of Lift Change $\Delta L/L_r$ With Effective Heave Velocity $\dot{h}/h_r$ for Plenum Chamber GEM Model, Measured With Steady State Airflow.

heights under 0.2 cm, a small undamped oscillation tended to persist and care was necessary to exclude the small amplitude oscillations in the determination of damping.**

In some cases the residual oscillation was so large that two determinations of damping were needed. In one case the decrement of the total amplitude was studied, and in the other case the decrement of the amplitude in excess of the residual amplitude was analyzed. This later data is denoted by * in the test figures and tables.

Tests were run at rise heights of 0.18, 0.30, 0.38, 0.62, 0.84, 0.97, 1.20, 1.33, 1.76 and 1.77 cms and at several RPM settings of the GEM fans.

Typical results are shown in Figures 24 and 25 and several oscillatory profiles are depicted and explained in Figure 26. They were analyzed as follows .

Consider the GEM mounted in the pivoted frame as below

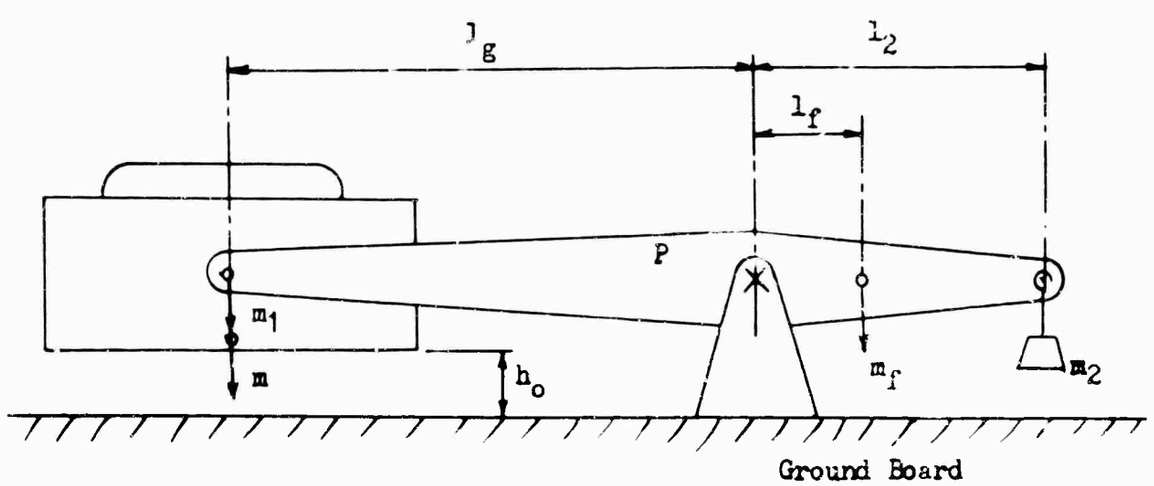

Figure 23. Heave Rig and Model GEM System.

**Note: Note that in most cases no weights were added to the GEM and the results are directly applicable to free flight, since the fan inertia was small. Results needed correction in free flight if the GEM weight is counterbalanced. See page 42 .

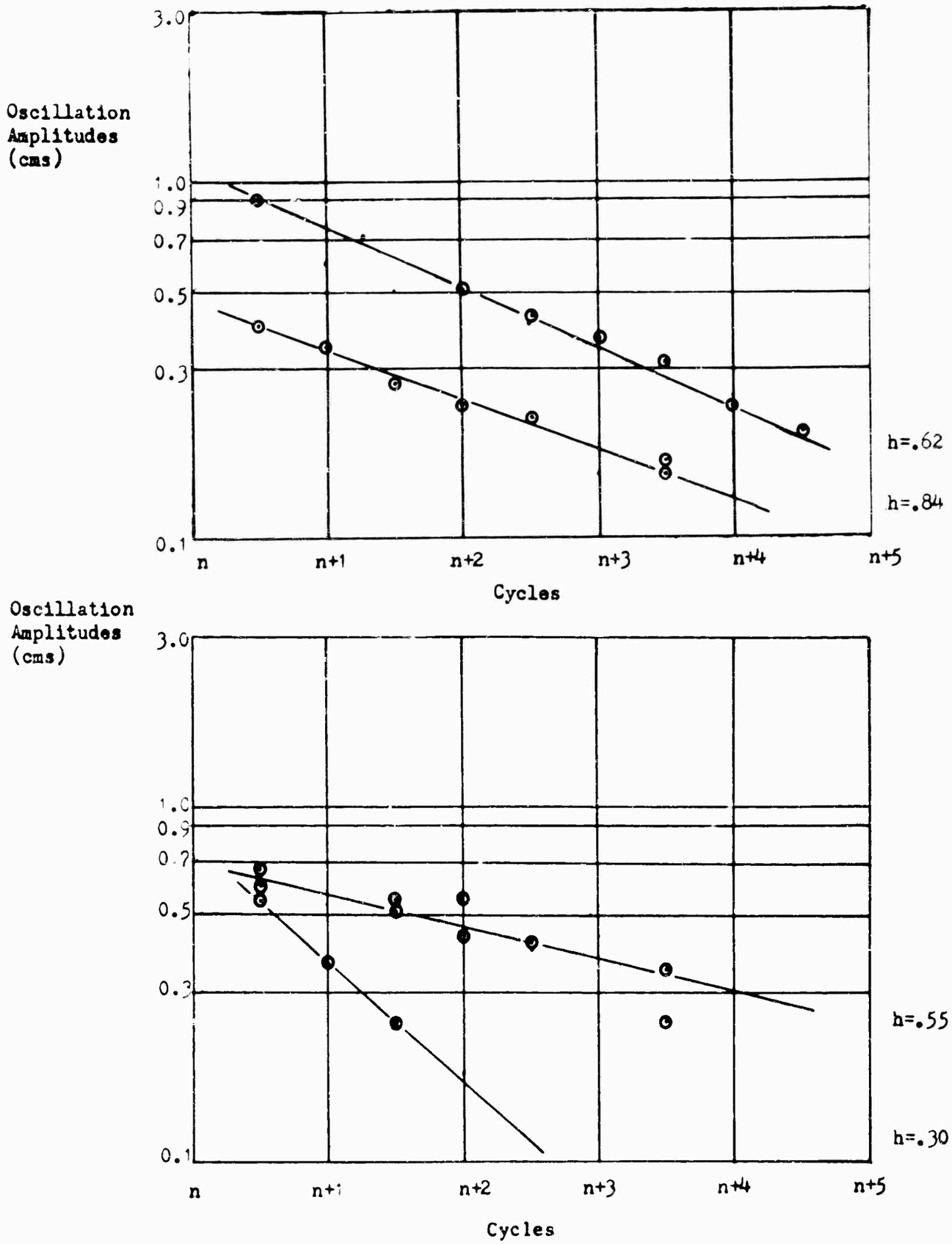

Figure 24. Oscillatory Amplitudes Versus Cycles for Specific Hover Heights - Thick Annular Jet GEM Model.

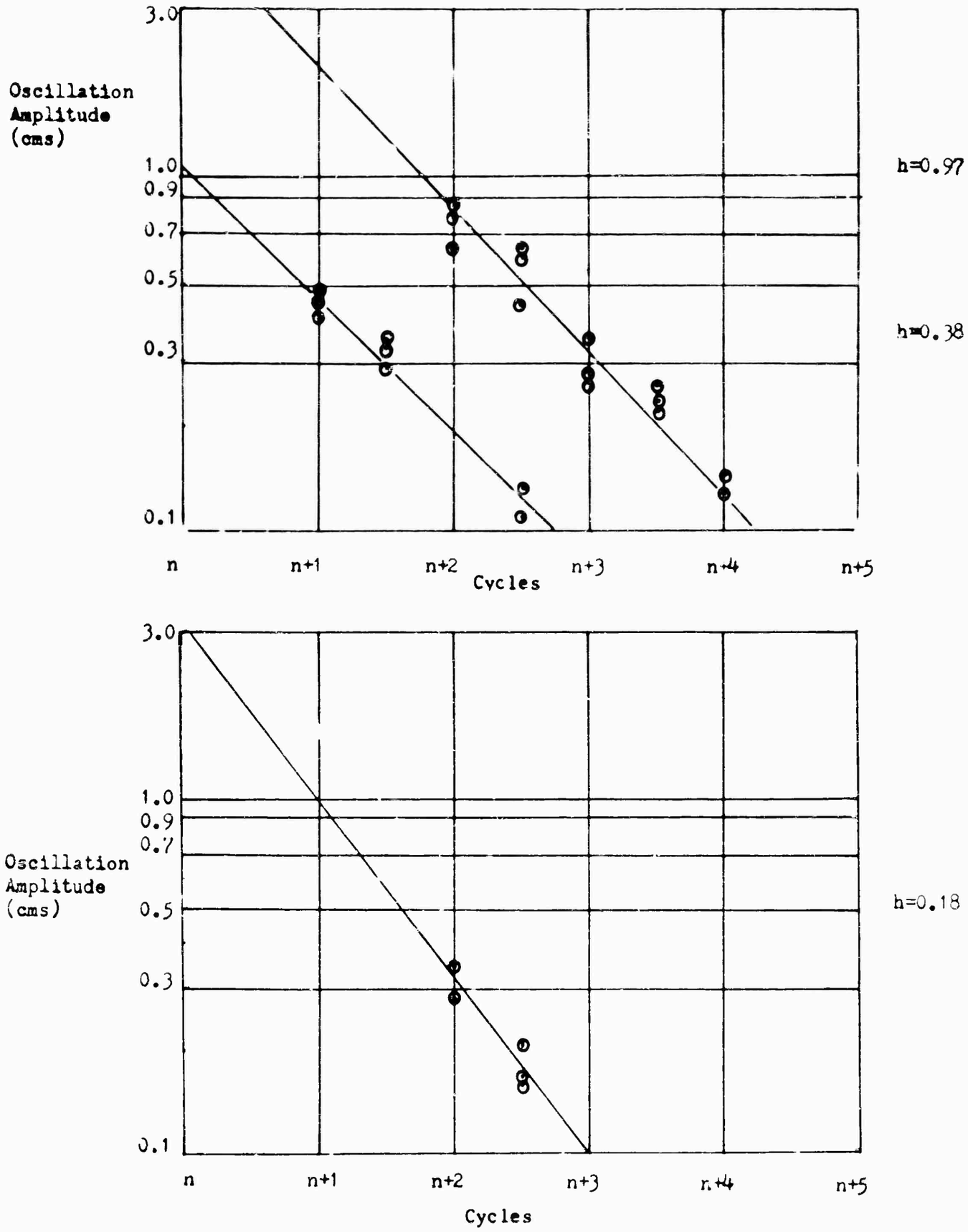

Figure 25. Oscillatory Amplitudes Versus Cycles for Specific Hover Heights - Thick Annular Jet GEM Models.

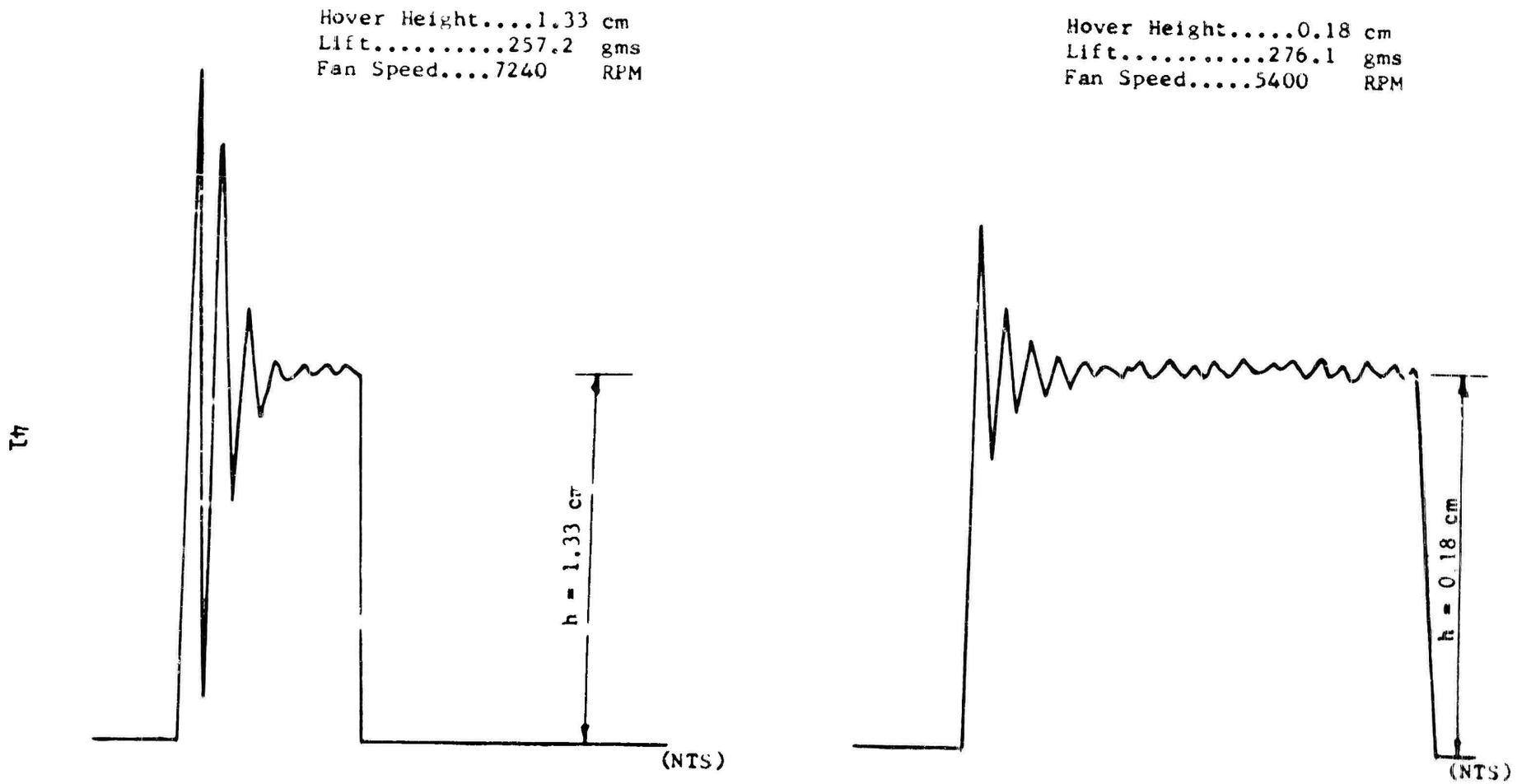

Figure 26. Typical Oscillation Profiles for Thick Annular Jet GEM Model.

The GEM has a mass m and is loaded with an additional mass m_1 both situated at a distance l_g from the pivot 'P' (or alternately the GEM is partly counterbalanced by a mass m_2, situated a distance l_2 on the other side of the pivot) to reduce the lift required for trim. The frame itself has a moment of intertia of I_f, a mass m_f, situated l_f from the pivot.

If the damping and stability are linear, then the equation of motion is:

$$I\ddot{\phi} + \dot{\phi}\cdot M\dot{\phi} + \phi\cdot M\phi = 0, \tag{24}$$

where ϕ is the angular displacement of the frame from equilibrium.

An angular displacement $\delta\phi$ corresponds to a change of height such that

$$\delta h = l_g \delta\phi$$

$$\therefore M_\phi = \partial M/\partial\phi = \partial L/\partial h\ (l_g)\ \partial h/\partial\phi$$

or $$M_\phi = \partial L/\partial h\ (l_g)^2. \tag{25}$$

Similarly, $$M_{\dot{\phi}} = \partial L/\partial \dot{h}\ (l_g)^2. \tag{26}$$

The equation may also be written

$$\ddot{\phi} + 2\zeta w\phi + w^2\phi = 0, \tag{27}$$

where $$w^2 \cong M_\phi/I \tag{28}$$

and $$2\zeta w = M_{\dot{\phi}}/I. \tag{29}$$

Hence, from the oscillation tests

$$\partial L/\partial h = \omega^2 I/(l_g)^2 \tag{30}$$

$$\partial L/\partial \dot{h} = 2\zeta\omega I/(l_g)^2 \tag{31}$$

and

$$\partial h/\partial \dot{h} = 2\zeta/\omega. \tag{32}$$

Since the values of the trimmed lift L_T varied with the fan $(RPM)^2$, this effect was eliminated by adopting as the final results for comparison with theory and the smoothed lift results

(a) $$\frac{\partial L}{N^2\ \partial h} \tag{33}$$

(b) $$\frac{\partial L}{N\ \partial \dot{h}} \tag{34}$$

(c) $$\frac{2\zeta}{\omega} = \frac{\partial h}{\partial \dot{h}}. \tag{35}$$

These revised parameters are also listed in Table 9.

OSCILLATION TESTS - PLENUM

The tests conducted on the plenum chamber followed closely the technique used for the thick jet model in the previous paragraph.

However, in this case serious instability in heave occurred around a trim altitude of 0.65-0.75 cms, as was noticed in the lift tests, and as a result no measurements with oscillations were possible in this region. The altitudes tested were 0.10, 0.15, 0.30, 0.55, 0.62, 0.84, 0.97, 1.08, 1.20, 1.42, and 1178 cms.

Results are shown in Figures 27 and 28 and the oscillatory profiles are shown in Figures 29, 30, and 31.

Table 10 lists the parameters $\partial L/N^2\partial h$, $\partial L/N\partial\dot{h}$, and $\partial h/\partial\dot{h}$ for the plenum chamber model as determined from the oscillation tests.

COMPARISON OF MEASURED VALUES OF $\partial L/\partial h$ AND $\partial L/\partial\dot{h}$ WITH DETERMINATIONS FROM THE DIRECT LIFT MEASUREMENTS ALLOWING FOR FAN EFFECTS

(A) $\partial L/\partial h$

If the theoretical structure assumed to date is correct, then certainly the circular frequency of the damped oscillations is given by

$$\omega^2 = -\frac{1}{M}\,\partial L/\partial h\ .$$

But we have calibrated lift versus altitude, and therefore we can determine

$$\partial L/\partial h$$

by simply measuring the slopes off the curve without making any further theoretical assumptions or requiring a knowledge of the fan characteristics.

The results for the thick jet model and for the plenum chamber are plotted in Figure 32 and tabulated in Table 11 in the form L/N^2 h versus hover height.

The general form of the curves is very similar, but in each case the "oscillation" result is appreciably and significantly lower than the "static" result. This is most interesting and surprising. If further investigation confirms this result there must be some other derivative present, as yet unsuspected which has a destabilizing influence in the dynamic case.

(B) $\partial L/\partial\dot{h}$

$\partial L/\partial\dot{h}$ can be determined in three different ways from the results. First, we may obtain $\partial L/\partial\dot{h}$ directly from the feeding and bleeding tests, dividing by N to eliminate the effect of fan speed.

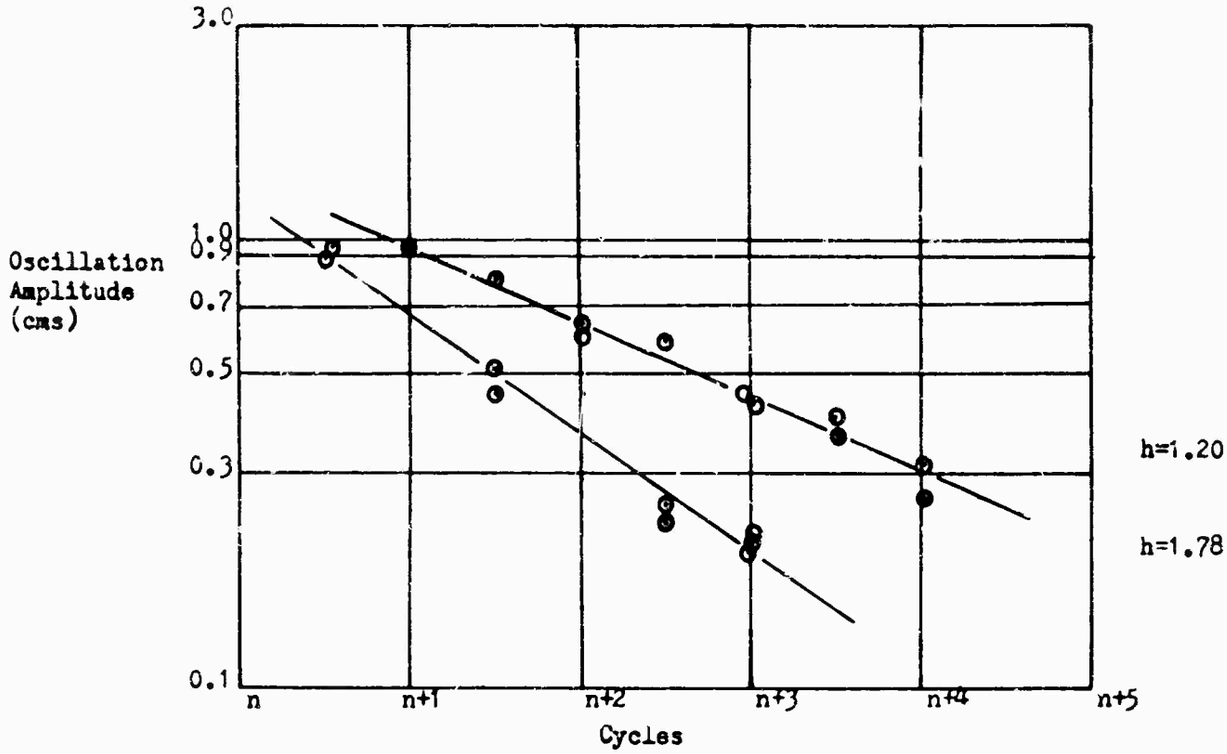

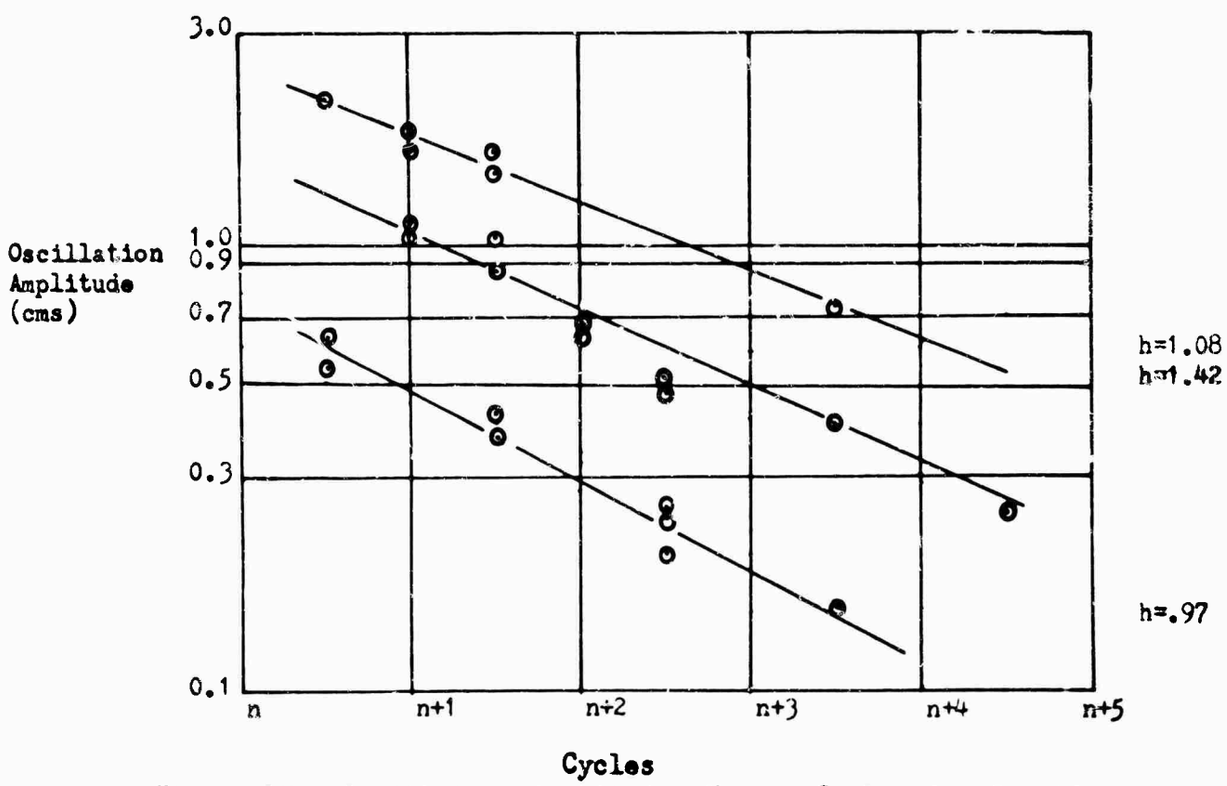

Figure 27. Oscillatory Amplitudes Versus Cycles for Specific Hover Heights - Plenum Chamber GEM Model.

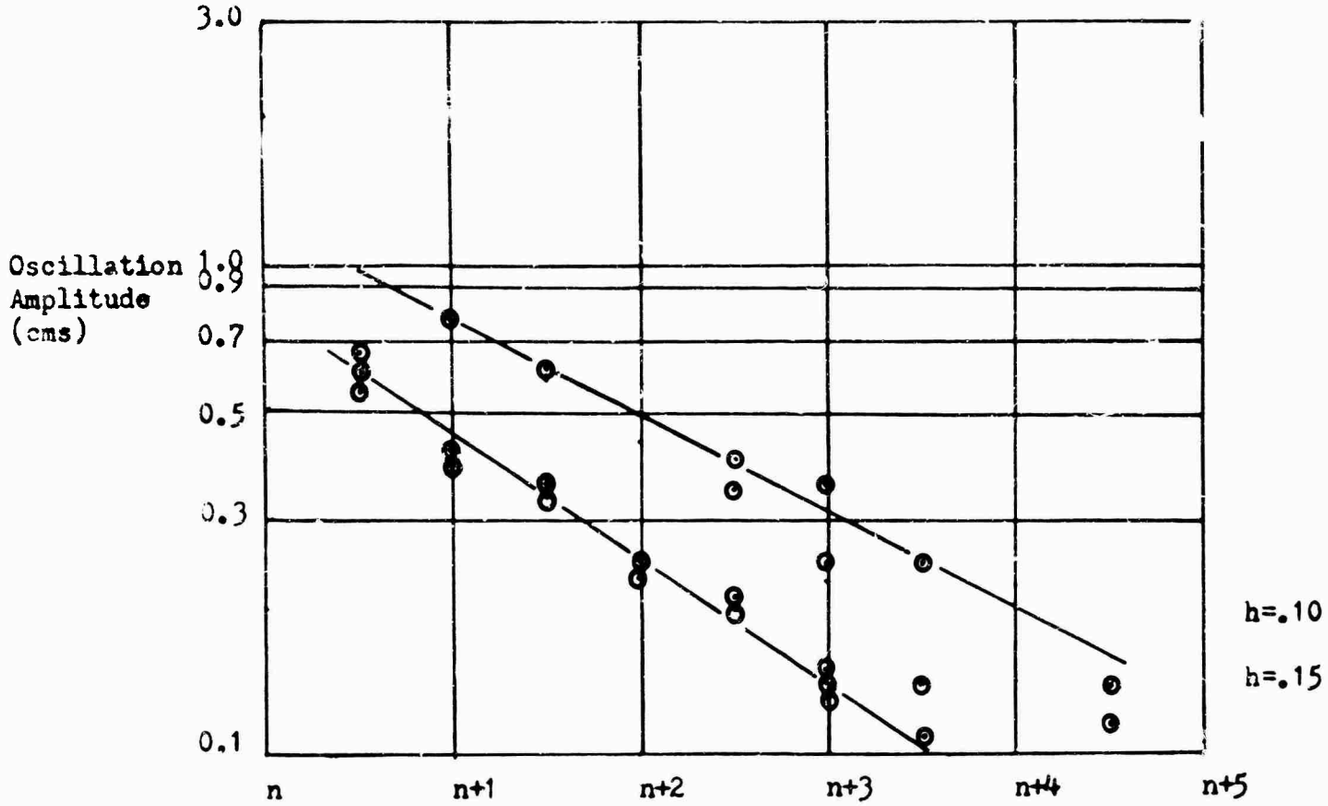

Figure 28. Oscillatory Amplitudes Versus Cycles for Specific Hover Heights - Plenum Chamber GEM Model.

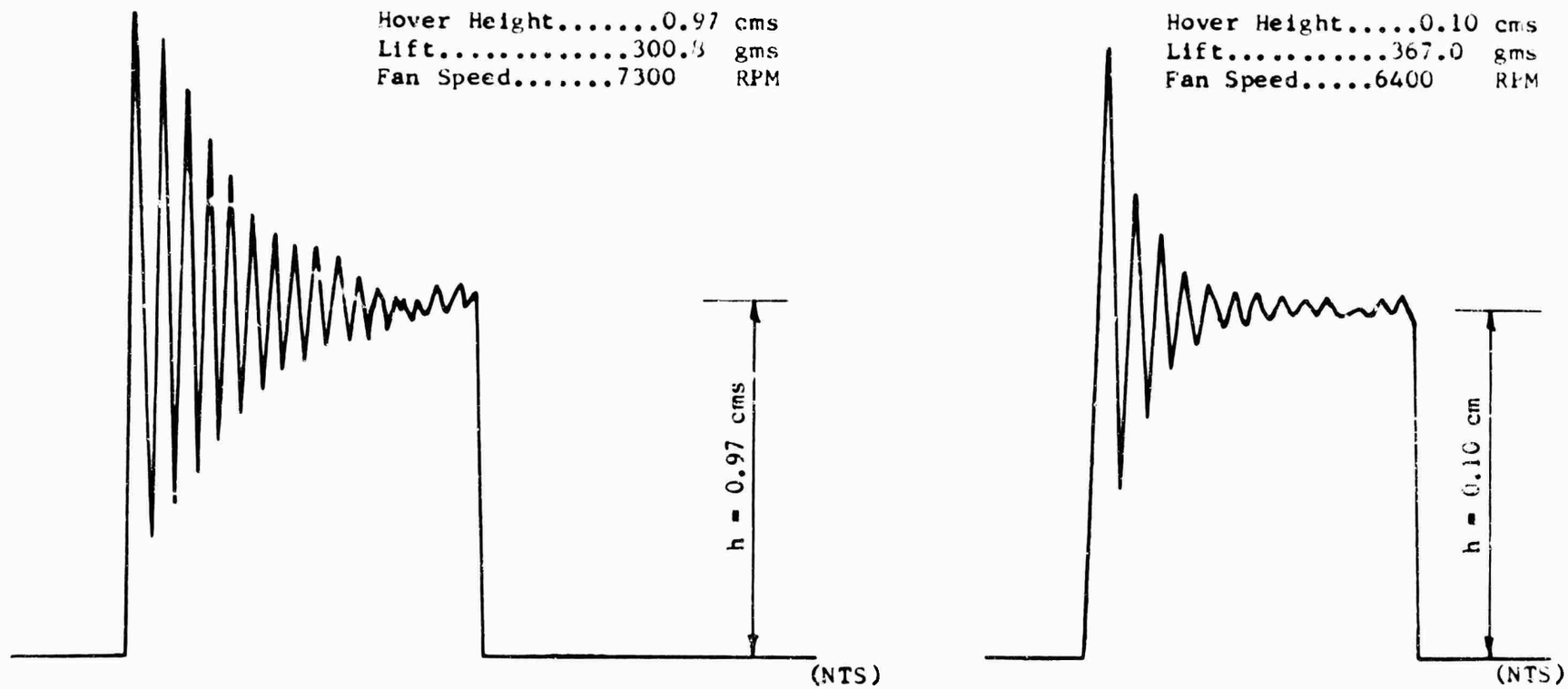

Figure 29. Typical Oscillatory Profiles for Plenum Chamber GEM Model - In Stable Region.

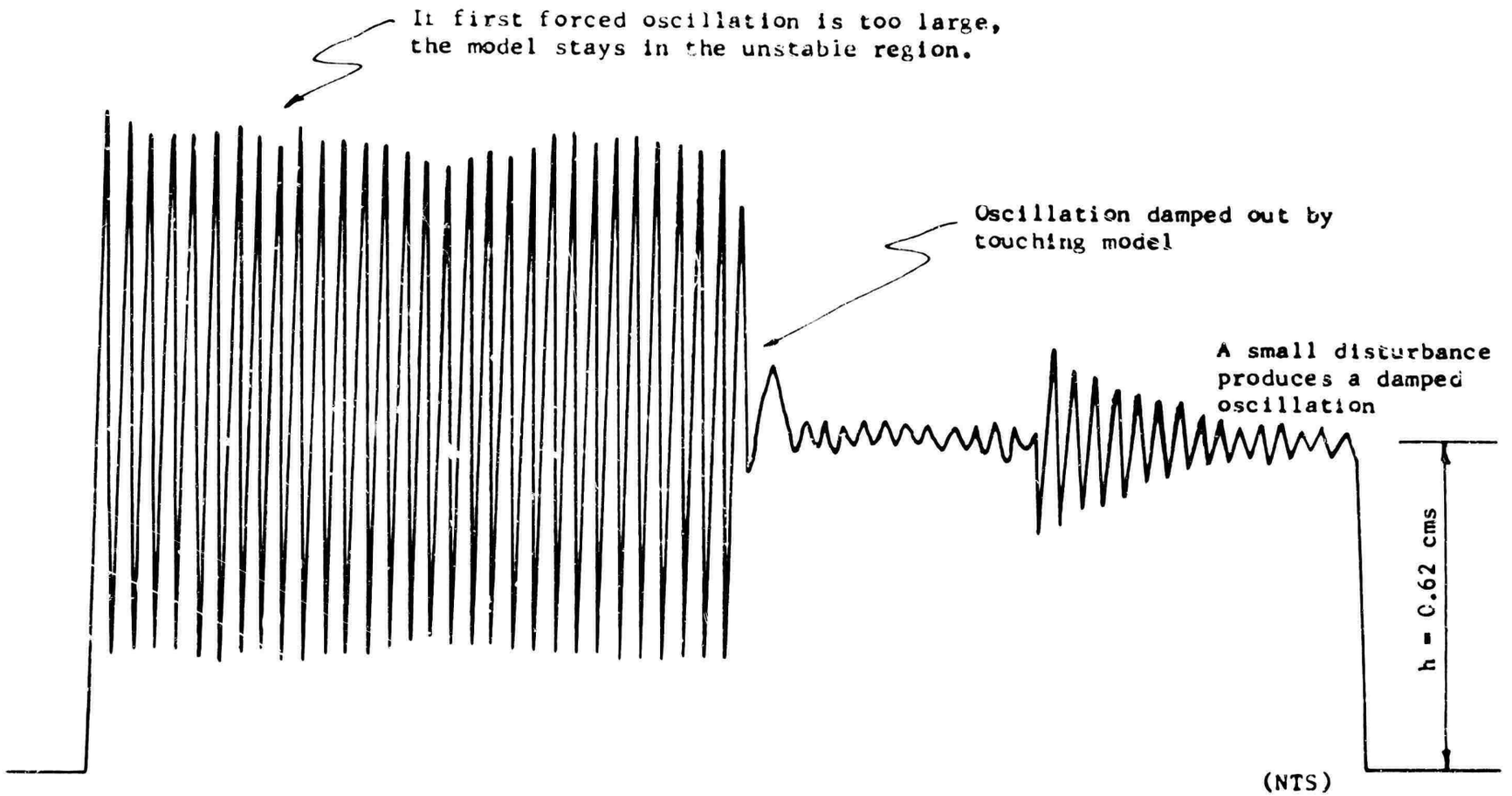

Figure 30. Oscillation Profile for Plenum Chamber Model Near Unstable Region.

Hover Height.....0.73 cm
Lift.....265.5 gms
Fan Speed.....6400 RPM

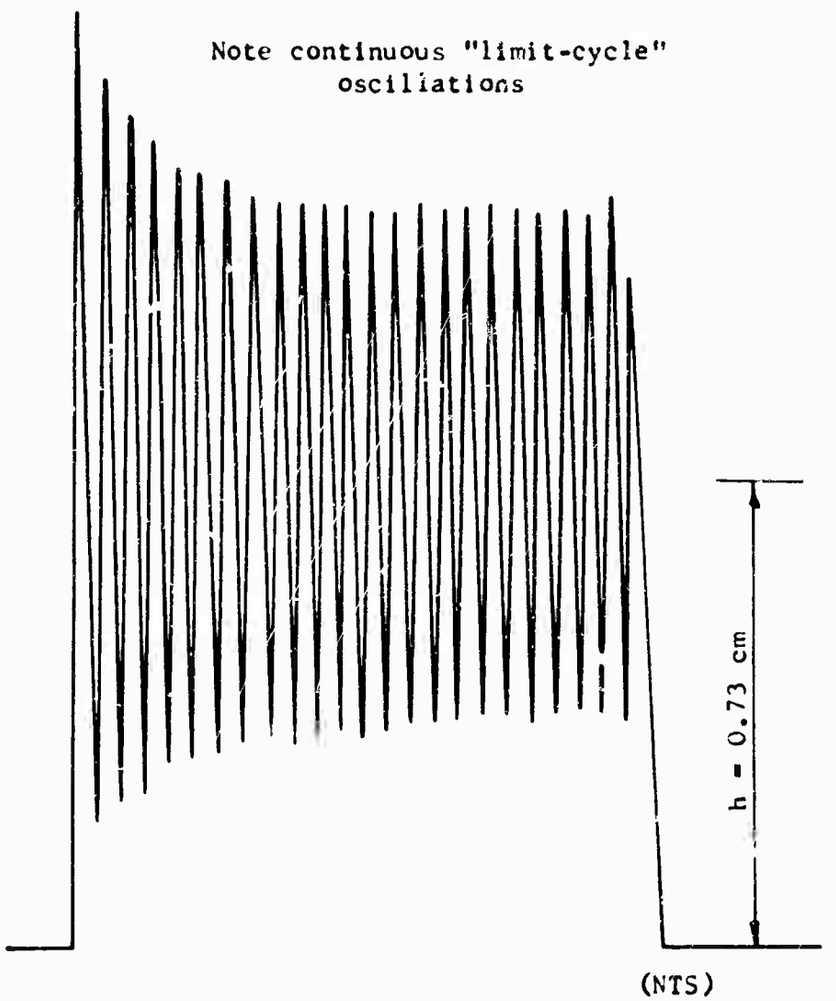

Figure 31. Oscillation Profile in the Unstable Region for the Plenum Chamber GEM Model.

Second, an estimate may be derived for the static lift results. In the case of the plenum chamber, we may simple assume that an increment in velocity, $-\dot{h}$, expresses a volume flow from the cushion, $\Delta Q = -\partial \dot{h} S$, and that this is equal to

$$\Delta Q = -V_e \, C \, C_D \Delta h,$$

$$\text{where} \quad V_e = \sqrt{2P_b/\rho} \tag{36}$$

$$\text{and} \quad P_b = \frac{\text{Lift}}{\text{Base Area}}$$

Hence Δh, the equivalent change in height of the GEM, is equal to

$$\Delta h = \Delta Q / V_e \, C \, C_D \, . \tag{37}$$

C_D = the discharge coefficient for a plenum = 0.62 and an equivalent change in height can be found for each of the measured flows, and the appropriate change in lift read off from the static lift curve, Figure 12.

Hence we may plot the variation of $\Delta L/L_r$ (the lift change expressed as a fraction of the reference lift - the lift with no base flow) with h/h_r, where h_r is the reference altitude. A comparison of the curve derived from the static lift measurement with the experimental feeding and bleeding results is given in Figure 22 and shows excellent agreement.

In the case of the thick annular jet GEM, a precisely similar calculation can be made for the case where air is blown out of the cushion (i.e., "underfed" jet) but not for the other case where the jet splits.

The comparison is shown in Figure 21 and it is apparent that the theoretical result using $C_D = 1$ is much too low, but is improved if $C_D = 0.61$, as for the plenum.

Third, we may obtain $\partial L/\partial \dot{h}$ from the values tabulated for ζ and ω from the oscillation tests using the methods described in the oscillation test section of this report.

These are listed in Tables 9, 10, 14, and 15 and again, to eliminate the effect of fan speed, they are divided by N.

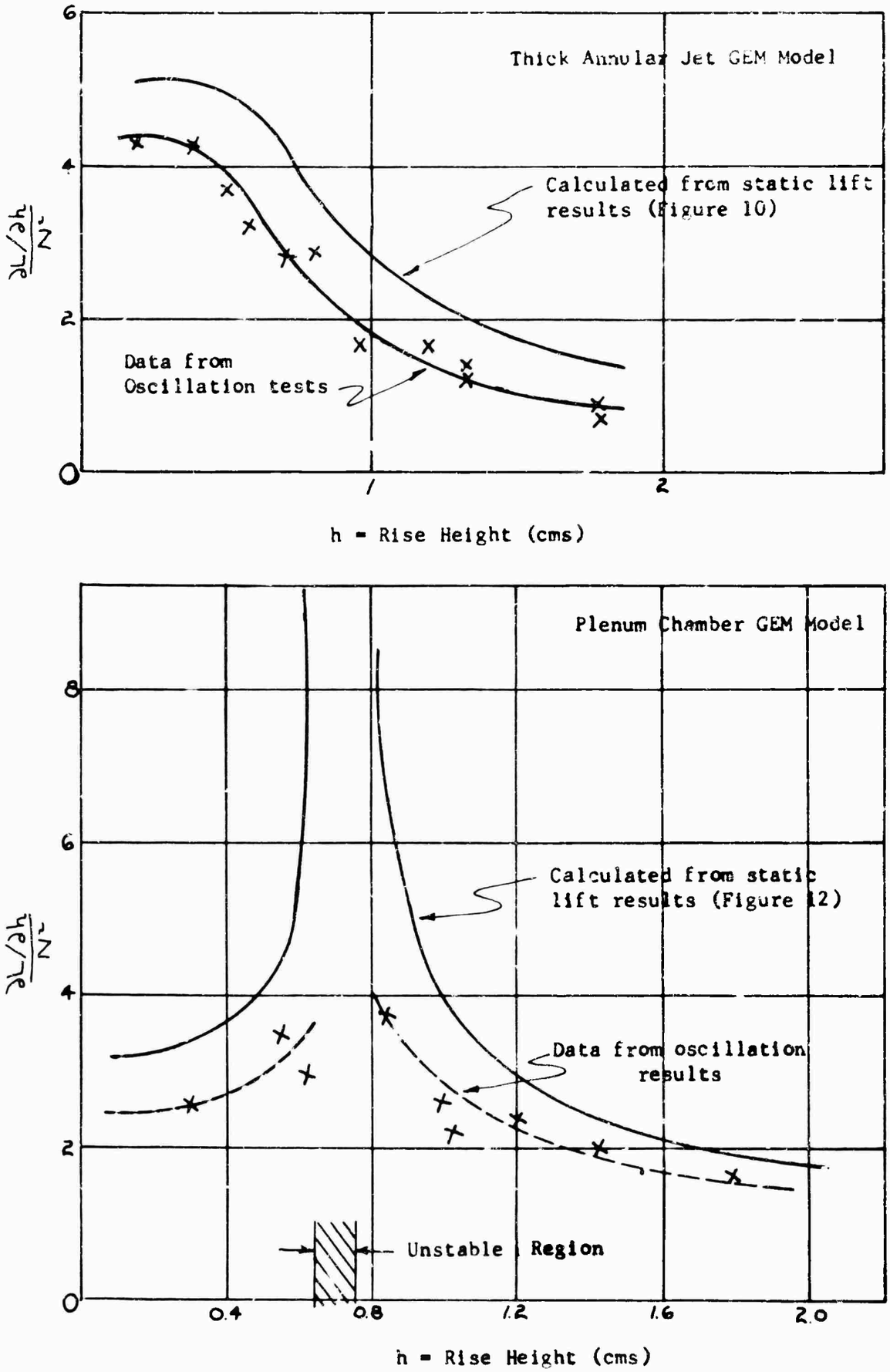

Figure 32. Comparison of Heave Stability Parameter $\partial L/N^2\partial h$ as Determined From Oscillation Tests and Static Lift Measurements.

These results are compared in Figure 33 with the results of the feeding and bleeding tests. The result, derived in Appendix II is that

$$\frac{\partial L}{N \partial \dot{h}} = \frac{S_b}{C_D C}\sqrt{\frac{\rho}{2P_b}} \; \frac{\partial L}{\partial h} \; \frac{1}{N} \qquad (38)$$

for the plenum chamber and the case of the GEM sinking ("underfed" jet).

The lower curve shows the results for the plenum chamber. As one would expect from the excellent agreement in Figure 22, the feeding and bleeding test results agree exceedingly well with those calculated from the static lift tests. However, the oscillation tests give an entirely different result, with a very much lower value for this damping parameter except when the altitude tends to zero. It is possible that these results could be due to a large difference in flow pattern in the plenum chamber on either side of the unstable region, as was postulated in Reference 18.

Two curves are given for the thick annular jet GEM, results, calculated f . the static lifts, as there is some doubt whether $C_D = 1$ (full line) or $C_D = 0.62$ (dotted line) would apply in this case. (This point is being examined further by Payne; also see Appendix II).

The oscillation results are scattered, but lie mostly in the region between the curves. However, the results from the feeding and bleeding tests are much higher than either of the two "static" curves or the oscillation results.

COMPARISON OF THE RESULTS WITH SIMPLE THEORY (APPENDIX II), ALLOWING FOR FAN EFFECTS

FREQUENCY OF OSCILLATION

The simple theory states that the equation of motion of the unrestrained GEM is:

$$\ddot{h} + \left(\frac{2\zeta}{\omega_0}\right)\omega_0^2 \, \dot{h} + \omega_0^2 \, (h - h_0) = 0, \qquad (39)$$

where $\frac{2\zeta}{\omega_0}$ is a parameter only, dependent on GEM geometry and loading, independent of the air supply characteristics,

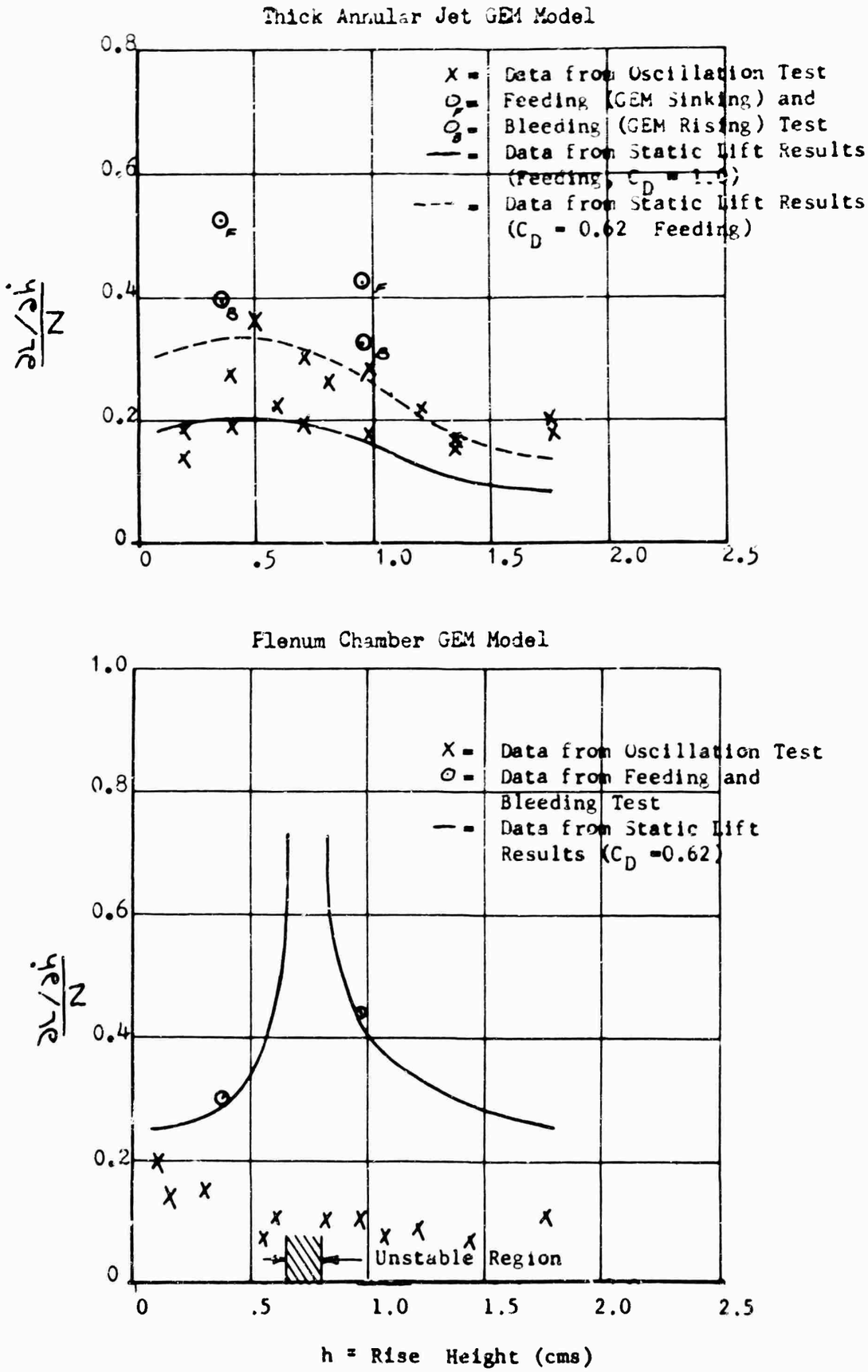

Figure 33. Comparison of Heave Damping Parameter as Determined From Several Different Methods.

and $\omega_o^2 = g/h_o(-\mathcal{F})$, where $(-\mathcal{F})$ is an (40)

air supply parameter dependent on the fan characteristics C_p and λ and also on the theoretical characteristics of the jet.

In the case of the Plenum Chamber we have no direct calibration of C_p versus λ, so no other comparison with theory is possible except the direct comparison of $\partial L/N^2\partial h$, derived for the static lift curve and oscillation tests described previously.

In the case of the thick jet machine, however, we have a separate calibration of C_p versus λ, so we can determine how closely the observed values of ω agree with $\sqrt{g/h_o\,(-\mathcal{F})}$, as calculated by theory.

The theory yields:

$$\mathcal{F} = F\,f'/f + \psi'/\psi \quad . \tag{41}$$

where
$$F = \frac{\lambda/C_p \;\; \partial C_p/\partial\lambda}{1 - \frac{1}{2}\,\lambda/C_p \;\; \partial C_p/\partial\lambda} \; . \tag{42}$$

f = a function of jet angle and hover height such that $Q = f(h, G, \lambda)(P_t)^{\frac{1}{2}}$ (43)

$f' = \partial f/\partial(h/h_o)$

ψ = a function of jet angle and hover height such that $P_b = \psi(h, G, \lambda)P_t$ (44)

$\psi' = \partial\psi/\partial(h/h_o)$

Using the exponential theory,

$$f'/f = 1 - \frac{x}{e^x - 1} \tag{45}$$

$$\psi'/\psi = \frac{-2x}{e^{2x} - 1} \tag{46}$$

whence,

$$\mathcal{F} = F\left(1 - \frac{x}{e^x - 1}\right) - \frac{2x}{e^{2x} - 1} \; . \tag{47}$$

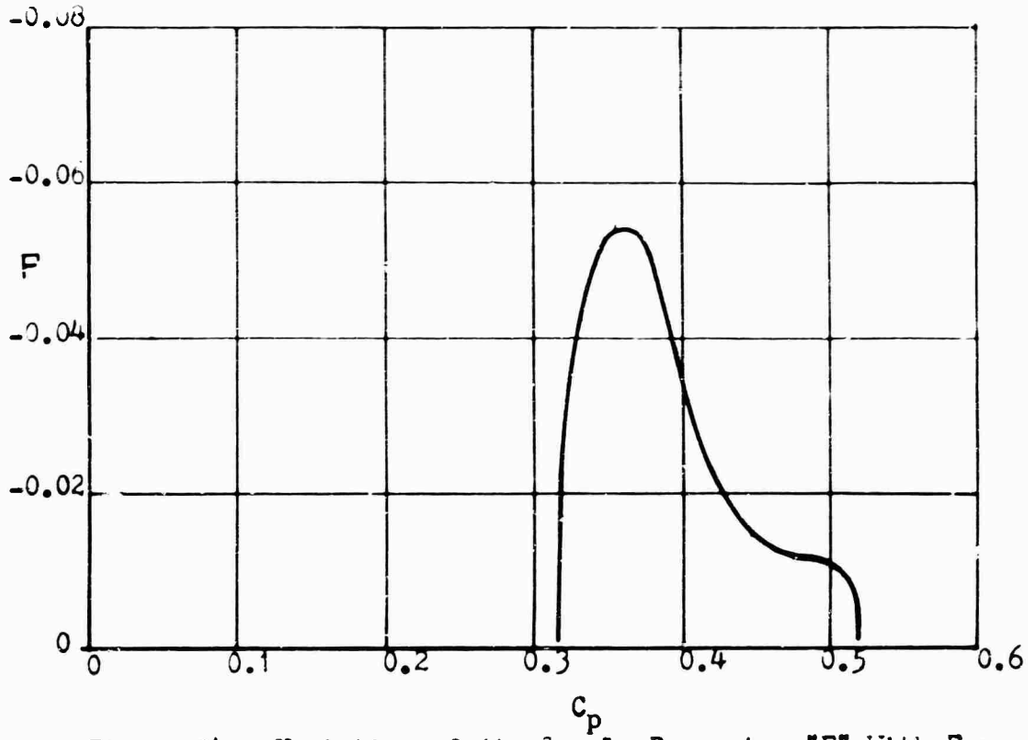

Figure 34. Variation of Air Supply Parameter "F" With Fan Pressure Coefficient "C_p" - Thick Annular Jet GEM Model.

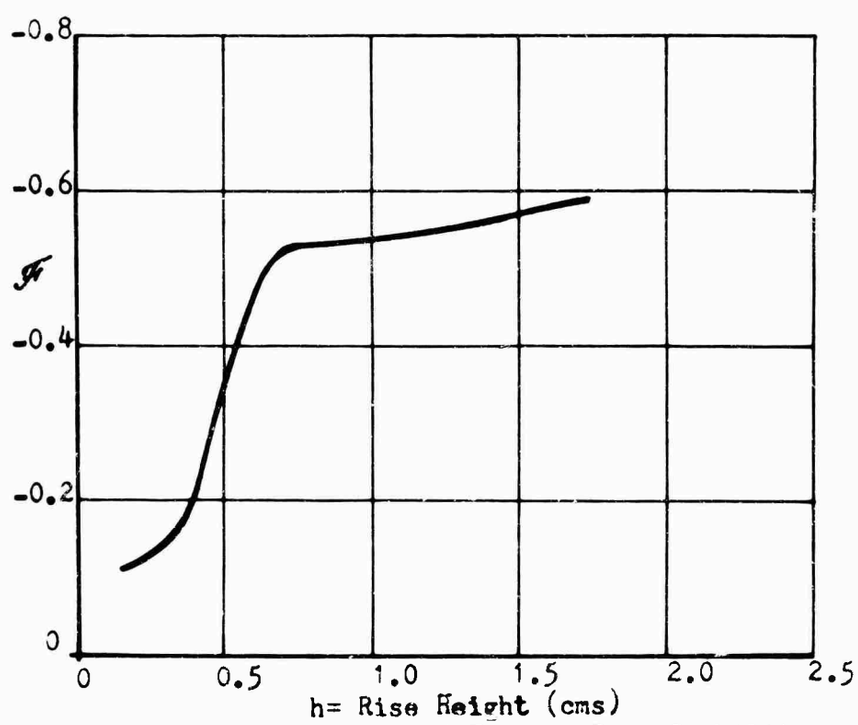

Figure 35. Variation of Fan and Duct Stability Parameter " $\mathcal{F}$ " with Rise Height "h" - Thick Annular Jet GEM Model.

For every value of 'h' there must be particular values of C_p and λ giving the correct lift and airflow. Assuming that the exponential theory applied (and this is known to give good correlation of base pressure against total head), we calculated the theoretical variation of C_p with λ, shown in Figure 18 for comparison with the test results. It is obvious that the curves are very similar and as the measured values of C_p were not averaged over the entire perimeter of the jet; the calculated values apply to particular values of 'h'. These calculated results have been used to correct the stability theory.

Hence, we can derive the value of F from equation (45) as plotted in Figure 34, and also assuming the exponential theory again, the variation of $\mathcal{F}$ with h, Figure 35.

From this we obtain

$$\omega_o = \sqrt{g/h\,(-\mathcal{F})}.$$

In the oscillation tests the GEM model exerted a lift m_1 g but had an effective mass of m_2.

Hence a free flying model having a mass in engineering units equal to the lift would have a much higher frequency such that

$$\omega_o^2 = \omega_r^2 \frac{\sum m}{\sum L} \qquad (48)$$

where $\sum m$ is the effective mass of the GEM and rig, located at the c.g. of the GEM

$\sum L$ is the lift exerted by the GEM

(This correction was only appreciable when the GEM weight was counterbalanced to give a greater hover height.)

The corrected values are given in Table 16 and are plotted in Figure 36 against the theory (note that results for a given hover height but different lifts and fan speed are quite consistent.)

It is clear that the two usual approximations of constant mass flow ($\partial\lambda / \partial C_p = 0$) and constant total head ($\partial C_p / \partial\lambda = 0$) do not agree at all well with the measured points.

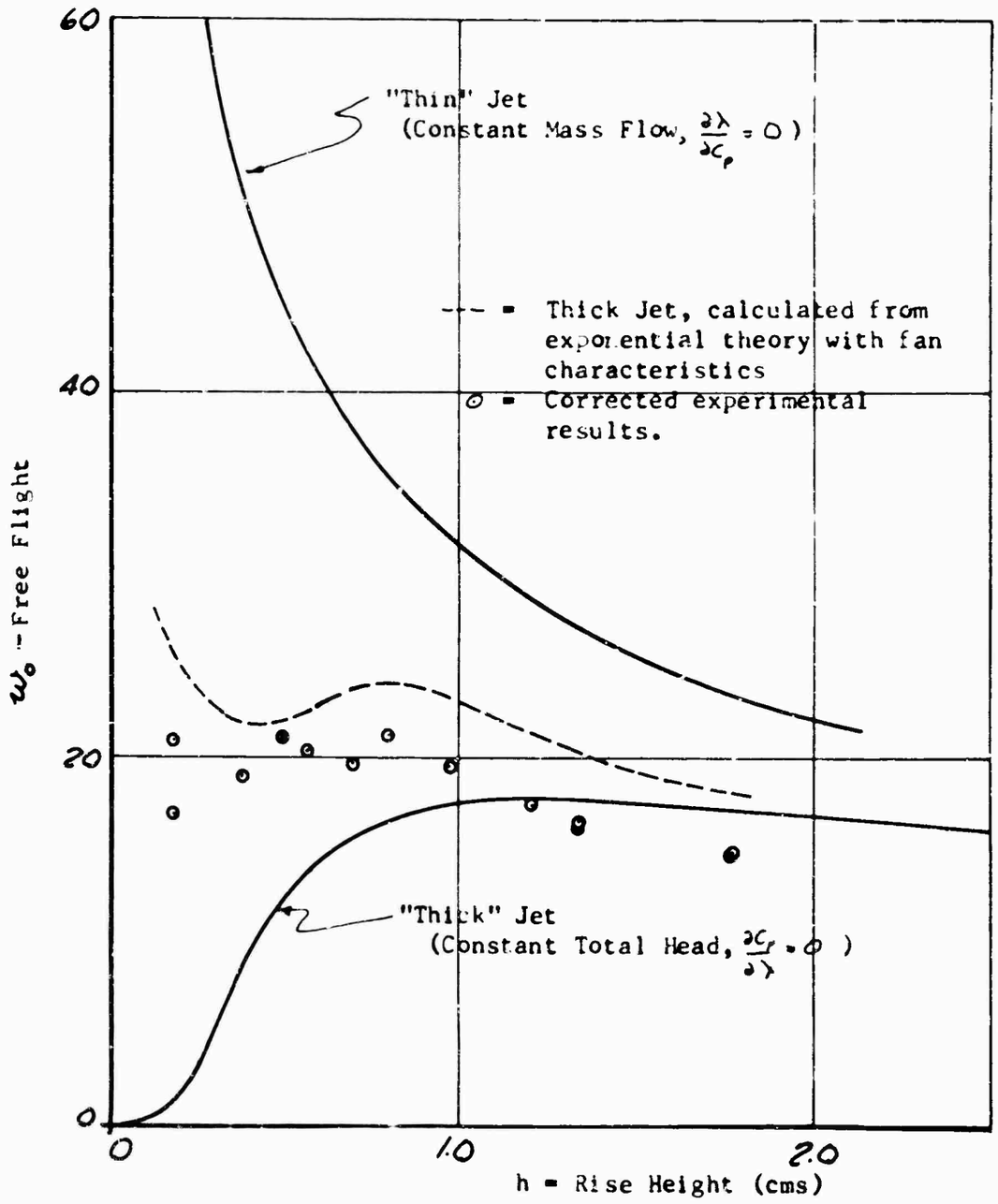

Figure 36. Comparison of Free Flight Circular Frequency With Various Theoretical Estimates.

The corrected exponential theory, using the fan characteristics from Figure 13, agrees extremely well with experiment, but the experimental values are rather lower, as would be expected from the comparison of $\partial L/\partial h\, N^2$ in Figure 32.

It is possible that an additional term is present which is as yet unknown, perhaps due to the base vortex system which produces the moderate discrepancy between the static stability as determined from the lift curve and the static stability derived from the dynamic tests.

However, as a first approximation, the static lift curve can be used to give ω_o .

RELATIVE DAMPING RATIO $\mathcal{G}$

The damping ratio of a GEM, ζ , varies with base loading, so in the proposal a new parameter $\mathcal{G}$ was described which is independent of the GEM size and loading, but which varies with "x" and the various theoretical deviations.

$$\mathcal{G} = \zeta/\zeta_o \qquad \text{where}$$

$$\zeta_o = \frac{1}{2}\,\frac{S_b}{C}\sqrt{\frac{1}{2}\frac{\rho}{P_{bo}}}\,\sqrt{g/h}\,.$$

This can be calculated from the experimental results or the product of

$$\frac{2\,\zeta/\omega}{\frac{S_b}{C}\sqrt{\frac{1}{2}\frac{\rho}{P_{bo}}}}$$ (which is independent of the rig balance weights)

and $$\frac{\omega_{cor}}{\omega_o}$$ (which is corrected for the rig balance weights)

where $\omega_o = \sqrt{g/h}$.

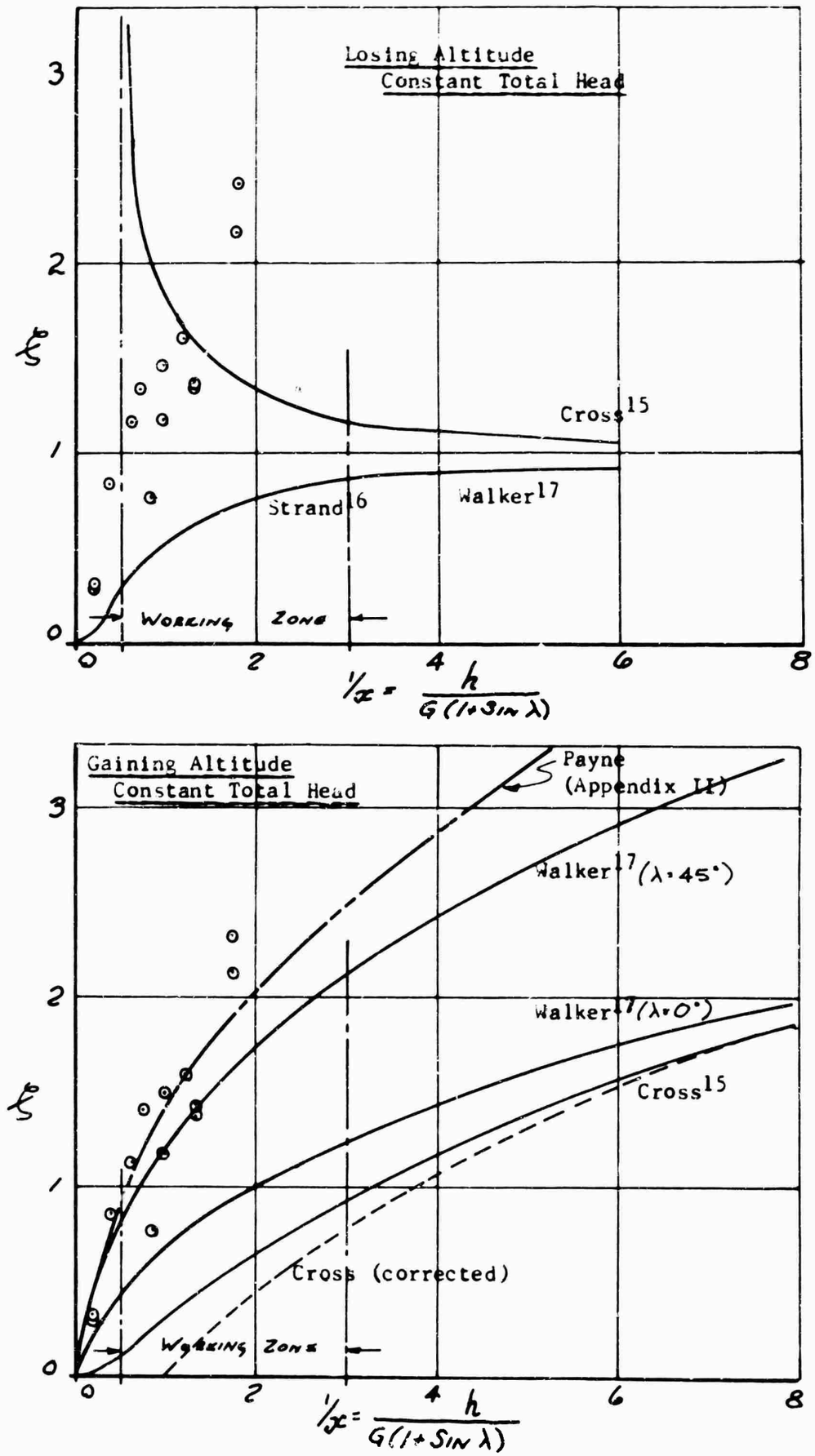

Figure 37. Comparison of Experimental Results with Different Estimates of the Damping Ratio " ξ ".

The results are tabulated in Table 17 and plotted in Figure 37 for comparison with the original curves given in Reference 27.

It is obvious that the experimental points do not agree at all well with the constant total head theory (Figure 37) which is not surprising in view of the results for the frequency comparison shown in Figure 36

Similarly, a comparison with the exponential theory for constant mass flow is given in Figure 38 and shows poor agreement.

This is to be expected since the fan did not operate either at constant total head or constant mass flow.

However, it is quite clear that the curve attributed to Cross in Figure 37 is unquestionably wrong and on examination a printing error was found in the original paper.

THE DAMPING PARAMETER, $2\zeta/\omega$

The "static" physical assumptions underlying the theory of Appendix II shows that $2\zeta/\omega$ is a parameter, dependent only on the geometry and loading of the GEM but not used on the fan characteristics; the same answers substantially are derived regardless of the theory used.

These are:

Plenum; $$\frac{2\zeta/\omega}{\frac{S_b}{C}\sqrt{\frac{\rho}{2P_{bo}}}} = \frac{1}{C_D}$$ which is independent of "h". (49)

For the Thick Jet the theory is;

(a) GEM Sinking (Feeding) $= \frac{1}{C_D}$, or 1 if $C_D = 1$ (50)

(b) GEM Rising (Bleeding) $= \frac{2}{\sqrt{2x}}\sqrt{\frac{e^{2x}-1}{2x}}$, (51)

following Walker as amended by Payne (Appendix II) in assuming the exponential theory as formulated by Eames applies and extending it unwarrantably into the thick jet region without allowing for the effect of jet thrust. (A simple allowance for jet thrust was, in fact, made

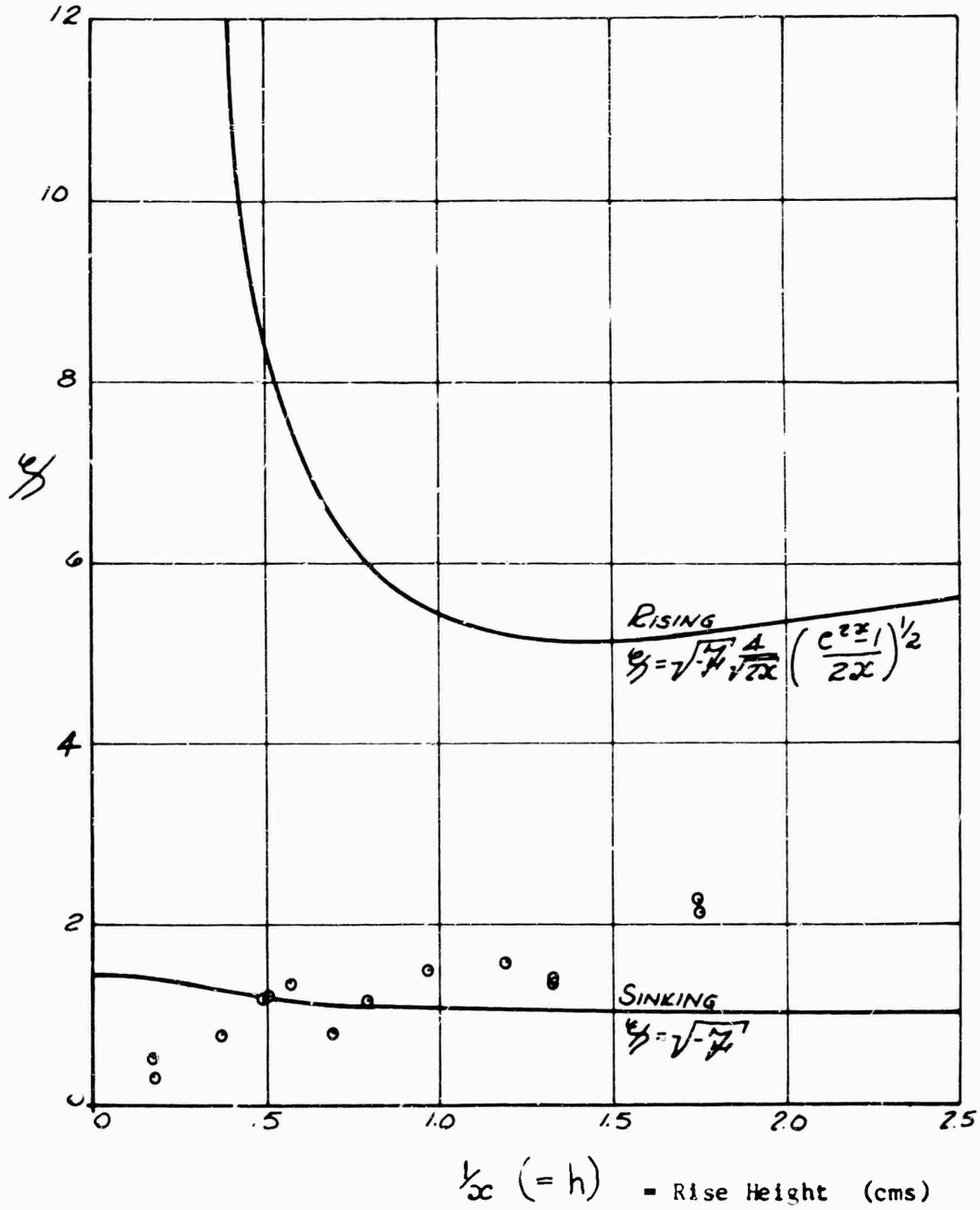

Figure 38. Comparison of the Experimentally Determined Damping Ratio " ζ " With the Constant Mass Flow Theory.

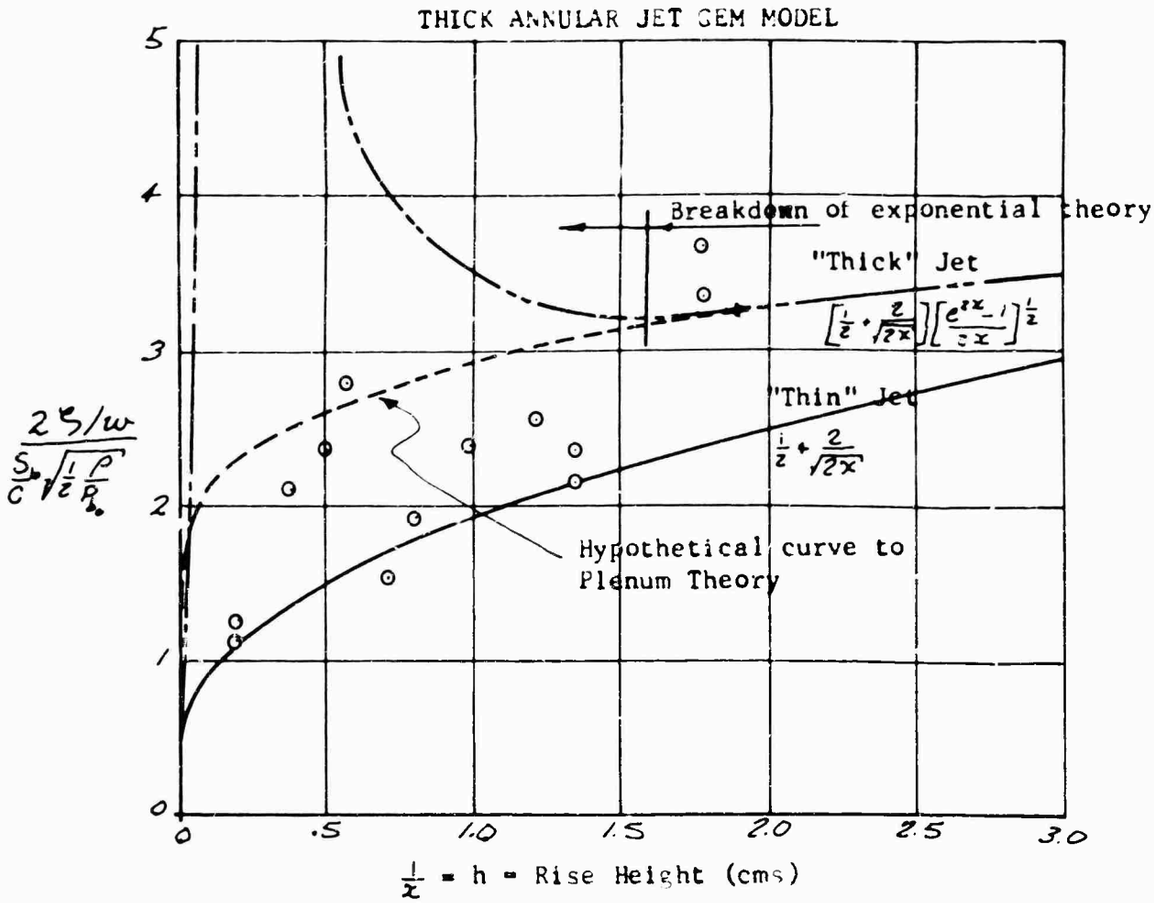

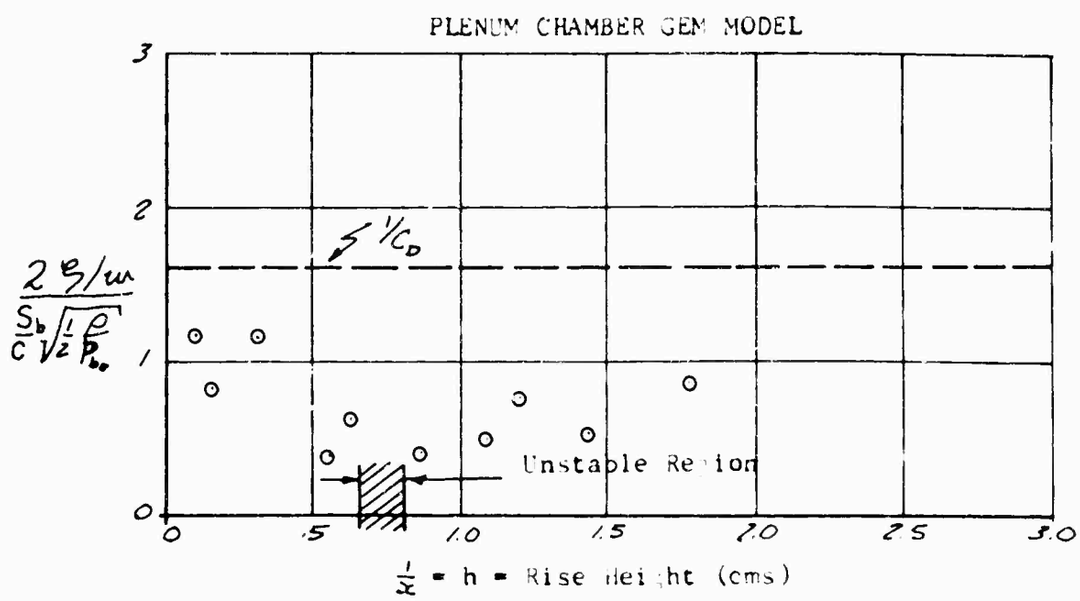

Figure 39. Comparison of Heave Damping Parameter $\frac{2\zeta/\omega}{S_b/C\sqrt{\frac{1}{2}\rho/P_{b_0}}}$ as Determined from Oscillation Tests and Simple Theory.

by taking the reference area to be the same for the plenum and annular jet models.) The mean of the two theoretical values is assumed to apply to the oscillation.

We can also derive the simpler result for a "thin" jet:

$$\frac{2\,\zeta/\omega}{\frac{S_b}{C}\sqrt{\frac{\rho}{2\,P_{bo}}}} = \tfrac{1}{2} + \sqrt{2/x} \quad . \tag{52}$$

Results for the thick annular jet model and for the plenum chamber are plotted in Figure 39 and tabulated in Tables 12 and 13; these show that the "oscillation" results are in surprisingly good agreement with the simple theories, although the scatter is very great and the exponential theory obviously is inapplicable when:

$$h < 1.5 \text{ cms.}$$

A hypothetical curve tending toward the plenum theory result ($C_D = 0.62$) agrees well with the experiment in this region.

The results for the plenum chamber approach the theoretical value $1/C_D$ at very low altitudes, but near the unstable region became very low and even at altitudes well above the region of instability the value of $2\,\zeta/\omega$ is much less than $1/C_D$. It is possible that in this flow regime the actual average value of the base pressure is much less than the total head, whereas the simple theory assumes these are equal. Such a difference could account for this result.

Contract funds did not permit a further examination of this interesting result. However, the trends predicted by theory confirmed that there is fair quantitative agreement and that an empirical curve of $2\,\zeta/\omega$ will give a far better estimate of ζ than any theory available to date.

TABLE 1

VARIATION OF RISE HEIGHT WITH RPM FOR FIXED LIFTS

THICK ANNULAR JET GEM MODEL

Lift (gm)	Rise Height (cm)	RPM 1000	Lift (gm)	Rise Height (cm)	RPM 1000	Lift (gm)	Rise Height (cm)	RPM 1000
342.5	0.09	5.73	255.4	0.32	5.37	209.8	0.12	4.69
	0.09	5.73		0.37	5.40		0.25	4.80
	0.22	5.90		0.48	5.65		0.37	5.06
	0.22	5.96		0.51	5.66		0.50	5.16
	0.35	6.14		0.61	5.80		0.70	5.49
	0.35	6.14		0.61	5.85		1.27	6.54
	0.48	6.41		0.74	6.10		1.43	6.73
	0.48	6.40		0.87	6.35		1.66	7.0
	0.54	6.52		0.81	6.28			
	0.79	7.26		0.91	6.50	177.4	0.93	5.32
	0.86	7.51		1.30	7.15		0.97	5.44
				1.38	7.30		1.13	5.54
304.0	0.04	5.35		1.50	7.50		1.25	5.08
	0.10	5.40					1.25	5.78
	0.25	5.64	210.5	0.68	5.38		1.39	5.96
	0.25	5.60		0.78	5.56		1.51	6.09
	0.37	5.84		0.92	5.80		1.51	6.12
	0.50	6.05		1.04	6.00		1.64	6.25
	0.50	6.04		1.08	6.10		1.77	6.39
	0.63	6.35		1.17	6.17		1.84	6.45
	0.68	6.47		1.30	6.35		2.41	7.15
	0.92	7.20		1.39	6.50		2.52	7.27
	1.14	7.50		1.93	7.30		2.64	7.42
				2.04	7.49			
274.5	0.17	5.36		2.17	7.68	176.7	0.12	4.29
	0.35	5.52					0.25	4.38
	0.50	6.02					0.37	4.56
	0.53	6.04					0.50	4.74
	0.79	6.45					0.63	4.90
	1.14	7.05					0.88	5.37
	1.28	7.36					1.15	5.75
							1.25	6.00

TABLE 2

CONSOLIDATED LIFT RESULTS

THICK ANNULAR JET GEM MODEL

h (cm)	$\frac{Lift}{N^2}$	h (cm)	$\frac{Lift}{N^2}$	h (cm)	$\frac{Lift}{N^2}$
0.04	10.63	0.54	8.07	1.25	5.32
0.09	10.43	0.61	7.58	1.27	4.91
0.09	10.54	0.61	7.45	1.28	5.07
0.10	10.42	0.63	7.55	1.30	4.99
0.12	9.54	0.63	7.36	1.30	5.22
0.12	9.60	0.66	7.27	1.38	4.79
0.22	9.85	0.68	7.27	1.39	4.99
0.22	9.72	0.70	6.97	1.39	5.00
0.2[illegible]	9.56	0.74	6.85	1.43	4.65
0.25	9.70	0.78	6.81	1.50	4.54
0.25	9.12	0.79	6.50	1.51	4.79
0.25	9.20	0.79	6.61	1.51	4.74
0.32	8.85	0.81	6.47	1.64	4.55
0.35	9.10	0.86	6.08	1.66	4.28
0.35	9.10	0.87	6.33	1.77	4.35
0.35	9.00	0.88	6.13	1.84	4.27
0.37	8.76	0.91	6.04	1.93	3.96
0.37	8.92	0.92	6.26	2.04	3.76
0.37	8.02	0.92	5.87	2.17	3.57
0.37	8.48	0.93	6.27	4.21	3.47
0.48	8.34	0.97	6.00	2.52	3.36
0.48	8.37	1.04	5.85	2.64	3.23
0.48	7.99	1.08	5.66		
0.50	8.30	1.13	5.59		
0.50	8.34	1.14	5.41		
0.50	7.58	1.14	5.53		
0.50	7.88	1.15	5.35		
0.50	7.88	1.17	5.53		
0.51	7.95	1.25	4.91		
0.53	7.53	1.25	6.88		

TABLE 3

VARIATIONS OF RISE HEIGHT WITH RPM FOR FIXED LIFTS PLENUM CHAMBER GEM MODEL

Lift (gm)	Rise Height (cm)	RPM / 1000	Lift (gm)	Rise Height (cm)	RPM / 1000	Lift (gm)	Rise Height (cm)	RPM / 1000	Lift (cm)	Rise Height (cm)	RPM / 1000
300.8	0.37	5.750	236.0	0.78	6.03	171.0	0.13	4.34	168.2	0.95	5.24
	0.50	5.900		0.92	6.16		0.25	4.40		1.02	5.28
	0.56	5.920		1.04	6.42		0.38	4.44		1.02	5.34
	0.60	6.060		1.09	6.55		0.50	4.66		1.14	5.65
	0.76	6.460					0.63	4.80		1.27	5.85
	1.02	7.120	216.9	0.13	4.82		0.64	4.85		1.27	5.84
	1.14	7.500		0.25	4.90		0.69	4.90		1.39	6.15
				0.38	5.09		0.70	4.95		1.52	6.44
264.9	0.42	5.510		0.46	5.15		0.71	5.04		1.80	7.06
	0.53	5.640		0.59	5.25		0.78	5.10		1.92	7.27
	0.78	6.300		0.64	5.30		0.83	5.15		2.04	7.62
	0.88	6.440		0.64	5.40		0.90	5.37			
	1.15	7.060		0.65	5.36		0.93	5.42	135.0	1.34	5.35
	1.30	7.400		0.71	5.45		0.94	5.50		1.52	5.73
				0.79	5.70		0.99	5.55		1.52	5.71
235.0	0.13	4.90		0.82	5.70		1.03	5.60		1.66	5.93
	0.25	5.07		0.83	5.80		1.04	5.65		1.67	6.05
	0.38	5.21		0.83	5.75		1.09	5.70		1.79	6.26
	0.50	5.34		0.88	5.82		1.13	5.80		1.88	6.38
	0.56	5.40		0.95	5.93		1.23	6.04		2.20	7.10
	0.60	5.45		0.95	5.89					2.38	7.41
	0.64	5.50		1.08	6.19						
	0.65	5.55		1.08	6.15						
	0.66	5.57		1.21	6.45						
	0.73	5.71		1.22	6.49						
	0.74	5.80									
	0.78	5.90									
	0.83	6.00									

TABLE 4

CONSOLIDATED LIFT RESULTS

PLENUM CHAMBER GEM MODEL

h (cm)	Lift / N^2	h (cm)	Lift / N^2	h (cm)	Lift / N^2
0.13	9.35	0.70	6.98	1.04	5.36
0.13	9.92	0.71	7.31	1.04	5.73
0.13	9.09	0.71	6.74	1.08	5.66
0.25	8.83	0.73	7.30	1.08	5.74
0.25	9.05	0.74	7.08	1.09	5.50
0.25	9.25	0.76	7.19	1.09	5.27
0.37	9.08	0.78	6.57	1.13	5.08
0.38	8.76	0.78	6.68	1.14	5.28
0.38	8.38	0.78	6.85	1.15	5.32
0.38	8.68	0.78	6.50	1.18	5.33
0.42	8.74	0.79	6.68	1.21	5.22
0.46	8.19	0.82	6.68	1.22	5.15
0.50	8.64	0.83	6.45	1.23	4.68
0.50	8.36	0.83	6.56	1.27	4.98
0.50	7.87	0.83	6.62	1.27	4.94
0.53	8.34	0.83	6.45	1.30	4.84
0.56	8.57	0.88	6.40	1.34	4.72
0.56	8.16	0.88	6.42	1.39	4.45
0.59	7.88	0.90	5.93	1.52	4.12
0.60	8.18	0.92	6.22	1.52	4.14
0.60	8.00	0.93	5.83	1.52	4.06
0.63	7.43	0.94	5.65	1.66	3.84
0.64	7.27	0.95	5.13	1.67	3.69
0.64	7.87	0.95	6.17	1.79	3.45
0.64	7.73	0.95	6.25	1.80	3.38
0.64	7.45	0.99	5.55	1.88	3.32
0.65	7.55	1.02	6.04	1.92	3.18
0.65	7.73	1.02	5.91	2.04	2.90
0.66	7.67	1.02	5.93	2.20	2.68
0.69	7.12	1.03	5.46	2.38	2.46

TABLE 5A

PRESSURE COEFFICIENT C_p AND FAN FLOW PARAMETER λ AS A FUNCTION OF DUCT BLOCKAGE

THICK ANNULAR JET MODEL

Blockage	C_p	λ
0	0.0286	0.0836
1	0.0286	0.0642
2B	0.0291	0.0651
2A	0.0361	0.0695
3B	0.0291	0.0630
3A	0.0368	0.0726
3.5	0.0363	0.0658
4B	0.0273	0.0592
4A	0.0377	0.0632
4.5	0.0403	0.0554
5	0.0342	0.0466
6	0.0410	0.0384
8	0.0467	0.0230
Total	0.0500	0.0142

$$C_p = \frac{8.81}{N^2} h_t$$

$$\lambda = \frac{1.61}{N} h_v$$

TABLE 5B

PRESSURE COEFFICIENT C_p AND FAN FLOW PARAMETER AS A FUNCTION OF RISE HEIGHT "h" AS CALCULATED FROM STATIC LIFT RESULTS

Thick Annular Jet Model

h (cms)	C_p	λ
0.18	0.0497	0.0203
0.35	0.0454	0.0364
0.38	0.0434	0.0373
0.50	0.0421	0.0452
0.70	0.0382	0.0528
0.95	0.0341	0.0579
0.97	0.0349	0.0593
1.10	0.0335	0.0608
1.20	0.0330	0.0648
1.33	0.0327	0.0668
1.50	0.0321	0.0665
1.77	0.0316	0.0688

$$C_p = \frac{8.81}{N^2}\left[\frac{L/S}{1-e^{-2/h}}\right]$$

$$\lambda = 0.28h\sqrt{C_p} = 0.0187h\sqrt{\frac{L}{N}}$$

TABLE 6

PRESSURE COEFFICIENT C_p VS. FAN FLOW PARAMETER λ AS CALCULATED FROM STATIC LIFT RESULTS FOR THE PLENUM CHAMBER GEM MODEL

h (cm)	C_p	λ
0.15	0.0478	0.0085
0.25	0.0462	0.0139
0.35	0.0444	0.0192
0.50	0.0416	0.0264
0.60	0.0392	0.0308
0.84	0.0333	0.0396
0.90	0.0317	0.0414
1.00	0.0293	0.0442
1.20	0.0253	0.0494
1.40	0.0222	0.0542
1.55	0.0201	0.0572
1.85	0.0169	0.0615
2.15	0.0144	0.0668

TABLE 7

VARIATION OF LIFT CHANGE $\frac{\Delta L}{L_r}$ WITH THE HEAVE VELOCITY $\frac{\dot{h}}{h_r}$

THICK ANNULAR JET GEM MODEL

h_r (cms)	$\frac{\Delta L}{L_r}$	$\frac{\dot{h}}{h_r}$	h_r (cms)	$\frac{\Delta L}{L_r}$	$\frac{\dot{h}}{h_r}$
0.35	0.097	-34.60	0.95	-0.0623	9.12
	0.205	-52.20		-0.1560	20.85
L	0.129	-34.20	L	-0.0760	9.50
(gms)	0.206	-51.80	(gms)	-0.1480	18.30
279.0	-0.072	25.60	270.0	0.1850	-19.10
	-0.074	28.40		0.1130	-12.20
RPM	-0.116	41.20	RPM	0.1850	-17.40
5500	-0.074	25.50	6720	0.1180	-12.10
	-0.070	26.85			
	-0.116	38.50			

TABLE 8

VARIATION OF LIFT CHANGE $\frac{L}{L_r}$ WITH HEAVE VELOCITY $\frac{\dot{h}}{h_r}$ FOR PLENUM CHAMBER MODEL

	Test Results			Calculated From Lift Results			Test Results			Calculated From Lift Results	
	$\frac{L}{L_r}$	$\frac{\dot{h}}{h_r}$		$\frac{L}{L_r}$	$\frac{\dot{h}}{h_r}$		$\frac{L}{L_r}$	$\frac{\dot{h}}{h_r}$		$\frac{L}{L_r}$	$\frac{\dot{h}}{h_r}$
h_r	-0.0136	22.80	h_r	-0.234	68.10	h_r	-0.1015	15.50	h_r	-0.222	19.60
(cms)	-0.0332	28.30	(cms)	-0.146	47.80	(cms)	-0.0656	8.00	(cms)	-0.161	14.55
0.35	-0.0357	33.35	0.35	-0.105	40.80	0.9	-0.1230	15.50	0.95	-0.095	9.07
	-0.0111	22.30		-0.072	33.30		-0.0821	8.00		-0.064	6.15
L_r	-0.0332	28.30	L_r	-0.057	25.20	L_r	0.1355	-10.46	L_r	-0.031	3.12
(gms)	-0.0413	33.15	(gms)	-0.037	17.00	(gms)	0.245	-15.70	(gms)	0	0
235.2	-0.0493	37.38	228.5	-0.015	8.58	235.3	0.144	-10.55	226.5	0.029	-3.22
	-0.0276	20.80		0	0		0.220	-16.20		0.062	-6.55
RPM	-0.0467	40.50	RPM	0.024	-8.77	RPM			RPM	0.101	-10.00
5060	-0.0825	40.65	5100	0.046	-17.70	6080			6080	0.220	-21.01
	-0.0357	21.00		0.105	-45.20						
	0.215	- 9.35		0.123	-54.99						
	0.0935	-22.30		0.070	-26.84						
	0.1030	-32.10		0.081	-35.95						
	0.1160	-41.40									
	0.1075	-29.52									
	0.1290	-42.50									
	0.1075	-27.95									

TABLE 9

THICK ANNULAR JET MODEL OSCILLATION TESTS

h_r (cms)	L_r (gms)	RPM	ω (RAD/SEC)	ζ	$\frac{\partial L/\partial h}{N^2}$	$\frac{\partial L/\partial \dot{h}}{N}$	$\partial h/\partial \dot{h}$
0.18*	340.5	6000	21.00	0.076	4.22	0.186	0.00728
0.18*	276.1	5400	17.00	0.076	2.76	0.135	0.00900
0.38	257.2	5460	17.95	0.140	3.15	0.270	0.01560
0.50*	340.5	6500	21.00	0.159	3.62	0.356	0.01520
0.57*	276.1	6000	20.30	0.116	3.20	0.221	0.20000
0.70*	304.0	6500	19.70	0.101	2.83	0.190	0.01[illegible]
0.80*	340.5	7230	21.00	0.130	2.95	0.261	0.01240
0.97	175.4	5450	14.00	0.149	1.67	0.178	0.02140
1.20	276.1	7290	17.45	0.159	1.63	0.214	0.01820
1.33	257.2	7240	15.70	0.124	1.38	0.158	0.01580
1.33	208.6	6500	13.10	0.124	1.31	0.163	0.0190[illegible]
1.76	175.4	6500	10.50	0.174	0.905	0.195	0.03300
1.77	208.6	7120	12.10	0.166	0.93	0.177	0.02740

TABLE 10

PLENUM CHAMBER MODEL OSCILLATION TESTS

hr (cms)	Lr (cms)	RPM	ω (RAD/SEC.)	ζ	$\frac{\partial L/\partial h}{N^2}$	$\frac{\partial L/\partial \dot{h}}{N}$	$\partial h/\partial \dot{h}$
0.10	265.3	5400	19.05	0.1022	3.77	0.250	0.01073
0.15	367.0	6400	19.05	0.0628	3.21	0.257	0.00657
0.30	300.8	5950	17.00	0.0550	2.57	0.271	0.01000
0.55	367.0	6950	21.00	0.0721	3.41	0.384	0.00306
0.62	300.8	6400	19.55	0.0545	2.36	0.714	0.00553
0.84	300.0	7000	24.20	0.0455	3.75	0.686	0.00376
0.97	300.0	7300	21.00	0.0580	2.00	0.409	0.00552
1.00	216.9	6500	19.05	0.0434	2.13	0.365	0.00505
1.20	133.9	5400	14.95	0.0467	2.35	0.346	0.00975
1.42	163.3	6400	17.00	0.0521	2.00	0.300	0.00613
1.70	133.9	6400	14.95	0.0715	1.67	0.252	0.00900

TABLE 11

CONSOLIDATED LIFT RESULTS

PLENUM CHAMBER MODEL / THICK ANNULAR JET MODEL

h (cms)	$\frac{\partial L/\partial h}{N^2}$	h (cms)	$\frac{\partial L/\partial h}{N^2}$
0.10	3.15	0.18	5.08
0.15	3.22	0.18	5.08
0.30	3.30	0.38	4.90
0.55	4.45	0.50	5.00
0.62	8.09	0.57	4.70
0.84	7.10	0.70	4.20
0.97	4.05	0.80	3.90
1.08	3.46	0.97	3.60
1.20	3.12	1.20	2.46
1.42	2.49	1.33	2.05
1.78	1.92	1.33	2.05
		1.76	1.51
		1.77	1.51

TABLE 12

THICK ANNULAR JET MODEL - $\dfrac{2\zeta/\omega}{\frac{S_b}{C}\sqrt{\frac{1}{2}\frac{\rho}{P_a}}}$

h_r (cms)	Thin Annular Jet $\dfrac{2\zeta/\omega}{\frac{S_b}{C}\sqrt{\frac{1}{2}\frac{\rho}{P_a}}}$	Thick Annular Jet $\dfrac{2\zeta/\omega}{\frac{S_b}{C}\sqrt{\frac{1}{2}\frac{\rho}{P_a}}}$	Oscillation Tests hr (cm)	$\dfrac{2\zeta/\omega}{\frac{S_b}{C}\sqrt{\frac{1}{2}\frac{\rho}{P_a}}}$
0	0.500	0.50	0.18	1.12
0.2	1.132	53.40	0.18	1.26
0.4	1.392	7.56	0.38	2.11
0.6	1.600	4.54	0.50	2.36
0.8	1.768	3.74	0.57	2.80
1.0	1.920	3.43	0.70	1.52
1.2	2.050	3.30	0.80	1.93
1.4	2.180	3.24	0.97	2.40
1.6	2.228	3.23	1.20	2.55
1.8	1.408	3.25	1.33	2.14
2.0	2.500	3.28	1.33	2.32
3.0	2.956	3.51	1.76	3.69
			1.77	3.35

TABLE 13

PLENUM CHAMBER MODEL

h_r (cms)	$\frac{2\xi/\omega}{\frac{S_b}{c}\sqrt{\frac{1}{2}\frac{\rho}{\rho_0}}}$
0.10	1.173
0.15	0.851
0.30	1.168
0.55	0.396
0.62	0.652
0.84	0.439
0.97	0.645
1.08	0.503
1.20	0.759
1.42	0.526
1.78	0.859

TABLE 14

HEAVE DAMPING PARAMETER $\frac{\partial L/\partial \dot{h}}{N}$ CALCULATED BY VARIOUS METHODS

THICK ANNULAR JET GEM MODEL

Calculated from Lift Results (Feeding)

h (cms)	$\frac{\partial L/\partial \dot{h}}{N}$	$\frac{1}{C_D} \times \frac{\partial L/\partial \dot{h}}{N}$
0.18	0.198	0.319
0.18	0.195	0.316
0.38	0.198	0.319
0.50	0.209	0.339
0.57	0.205	0.332
0.70	0.190	0.308
0.80	0.072	0.278
0.97	0.175	0.264
1.20	0.1[illegible]	0.208
1.33	0.110	0.178
1.33	0.109	0.169
1.76	0.087	0.142
1.77	0.089	0.142

Calculated from feeding and bleeding tests

h (cms)	$\frac{\partial L/\partial \dot{h}}{N}$ (Feeding)	$\frac{1}{C_D} \times \frac{\partial L/\partial \dot{h}}{N}$ (Bleeding)
0.35	0.521	0.392
0.95	0.423	0.322

Calculated from C_p and λ values

h (cms)	$\frac{\partial L/\partial \dot{h}}{N}$ (Feeding)	$\frac{\partial L/\partial \dot{h}}{N}$ (Bleeding)	
0.18	0.194	19.10	Thick Jet Theory
0.35	0.201	15.80	
0.95	0.162	0.79	
0.18	0.405	1.140	Thin Jet Theory
0.35	0.302	0.905	
0.95	0.206	0.501	

TABLE 15

HEAVE DAMPING PARAMETER $\frac{\partial L/\partial \dot{h}}{N}$ CALCULATED BY VARIOUS METHODS

PLENUM CHAMBER GEM MODEL

Calculated from Lift Results		Calculated from Feeding and Bleeding Tests	
h (cms)	$\frac{\partial L/\partial \dot{h}}{N}$	h (cms)	$\frac{\partial L/\partial \dot{h}}{N}$
0.10	0.250	0.35	0.302
0.15	0.257	0.95	0.430
0.30	0.271		
0.55	0.384		
0.62	0.714		
0.84	0.686		
0.97	0.409		
1.08	0.365		
1.20	0.346		
1.42	0.300		
1.78	0.252		

TABLE 16

FREE FLIGHT CIRCULAR FREQUENCY AS A FUNCTION OF RISE HEIGHT

THICK ANNULAR JET GEM MODEL

h (cms)	Measured Value ω	Constant Mass Flow ω_o	Constant Total Head ω_o	Exponential Theory with Fan Characteristics ω_o
0.18	20.9	74.0	1.01	25.3
0.18	16.9	74.0	1.01	25.3
0.38	19.0	50.8	8.8	21.6
0.50	21.0	44.4	12.2	--
0.57	20.3	41.5	13.7	--
0.70	19.7	37.4	15.6	--
0.80	21.1	35.0	16.6	--
0.97	19.6	31.6	17.4	23.4
1.20	17.5	28.6	17.8	21.1
1.33	16.7	27.1	17.8	--
1.33	16.2	27.1	17.8	--
1.76	14.7	23.6	17.2	--
1.77	15.0	23.6	17.2	18.1

TABLE 17

DAMPING RATIO "ζ"

THICK ANNULAR JET GEM MODEL

h (cm)	Calculated from Oscillation Test ζ	Constant Mass Flow (Sinking) ζ	Constant Mass Flow (Rising) ζ
0.18	0.31	1.395	100.0
0.18	0.29	1.395	100.0
0.38	0.79	1.269	14.0
0.50	1.17	1.210	8.35
0.57	1.37	1.65	7.45
0.70	0.80	1.136	6.45
0.80	1.16	1.111	5.97
0.97	1.49	1.078	5.50
1.20	1.59	1.052	5.25
1.33	1.32	1.040	5.15
1.33	1.39	1.040	5.15
1.76	2.30	1.026	5.25
1.77	2.13	1.025	5.25

REFERENCES

1. Walker, Norman K., The Influence of Fan and Ducting on the Stability and Performance of Ground Effect Machines, AIAA Paper presented at the AIAA General Aviation Aircraft Design and Operations Meeting, Wichita, Kansas, May 25-27, 1964.

2. Chaplin, John E., The Development of a Multi Cell Plenum Concept, AIAA Paper 64-1[illegible], Paper presented at AIAA General Aviation Aircraft Design and Operations Meeting, Wichita, Kansas, May 25-27, 1964.

3. Jones, R. Stanton, Some Design Problems of Hovercraft, IAS Paper No. 61-45, Paper presented at the IAS 29th Annual Meeting, New York, N.Y., January 25-29, 1961.

4. Payne, Peter R., Aerodynamic Forces Acting Over the Upper Portions of an ACV in Forward Flight, Walker Associates Technical Memo No. 2, Contract No. Nobs-90127, February 1964.

5. Walker, Norman K. and Neal, Robert J., An Analysis of the Results of Wind Tunnel Tests Made at the University of Wichita on Circular Annular Jet Ground Effect Machine Models, Walker Associates Report No. 5, Contract No. Nobs 3412(00), July 1963.

6. Walker, Norman K., and Neal, Robert J., An Analysis of the Results of Wind Tunnel Tests on a Circular Model Ground Effect Machine, D.T.M.B. Aero Report 954, Walker Associates Report No. 6, Contract No. Nonr-3412(00), June 1963.

7. Walker, Norman K., Some Notes on the Lift and Drag of Ground Effect Machines, Proceedings of the Hydrofoils and Air Cushion Vehicles, Washington, D. C., September 17-1[illegible], 1962.

8. Payne, Peter R., and Barrett, Stanley, The Response of a Linear Damped Dynamic System to Selected Acceleration Inputs, Frost Engineering Paper, 1963.

9. Tulin, M. P., On the Vertical Motions of Edge Jet Vehicles, Symposium on Ground Effect Phenomena, Princeton University, October 1959.

10. Eames, M. C., Fundamentals of the Stability of Peripheral Jet Vehicles, Volumes I, II, and III, Pneudynamics Corporation Report, Bethesda, Maryland, November 1960.

11. Eames, M. C., Basic Principle of the Stability of Peripheral Jet Ground Effect Machines, IAS Paper No. 61-71, New York, New York, 1961.

12. Payne, Peter R., The Theory of Heave Stability of an Annular Jet Gem, Frost Engineering Report No. 142-15, Contract No. DA-44-177-AMC-5(T), September 1963.

13. Nay, H. O., The Hughes Hydrostreak, Hughes Tool Co. presentation to the Tri-service Ground Effect Machine Conference, November 1960.

14. Webster, J. C., and Lin, N. J., Dynamic Heaving Motion of Ground Effect Machines, Hydronautics, Inc. Technical Report 011-3, Contract No. Nonr-3189(00), March 1962.

15. Cross, F. G., Outstanding Problems of Air Cushion Vehicles, Paper presented to Dansk Ingeniorforening, Copenhagen, Denmark, November 24, 1961.

16. Strand, T., A N e on the Vertical Response of a Ground Effect Machine, Unpublished report of the Vehicle Research Corporation, January 1962.

17. Walker, Norman K., Unsolicited Proposal to TRECOM to Investigate Experimentally the Heave Stability and Heave Damping of a Ground Effect Machine, November 1962.

18. ONR, A Study of the Operational Feasibility of the Ground Effect Machine in the Amphibious Support Mission, Office of Naval Research ACR/NAR-26, Appendix I, November 1962.

19. TRECOM, Roll Stability of Ground Effect Machines - Thick Annular Jet and Plenum Types, Walker Associates, Contract No. DA-44-177-AMC-19(T), October 1963.

20. Payne, Peter R., The Applications of Educators and Injections to an Air Cushion Vehicle - Part I - Using Current Diffuser Technology, Walker Associates Report No. 11, Contract No. Nobs 90127, January 1964.

21. Wallis, R. A., Axial Flow Fans, Academic Press, New York, N.Y., 1961.

22. Payne, Peter R., Peripheral Fans for Ground Effect Machines, Paper presented at the AIAA General Aviation Design and Operations Meeting, Wichita, Kansas, May 1964.

23. Payne, Peter R., Helicopter Dynamics and Aerodynamics, Pitman's, London and McMillan, New York, N.Y., 1959.

24. Payne, Peter R., Axial Fan Design Calculations for Search Head Carrier GEM, Frost Engineering Report No. 152-2, Contract No. DA-44-177-AMC-6(T), December 1962.

25. Payne, Peter R., Annular Jet Theory - Part I - Jets With Constant Total Head Distribution, Walker Associates Report No. 17, Contract No. Nobs-90127, May 1964.

26. Payne, Peter R., A Note on the Heave Stability of a Plenum Chamber GEM, Payne Associates Report No. 20-1, March 1964.

27. Walker, Norman K., The Influence of Fan and Ducting Characteristics on the Stability of Ground Effect Machines, AIAA Paper, September 1964.

DISTRIBUTION

US Army Materiel Command	6
US Army Mobility Command	2
US Army Aviation Materiel Command	5
Chief of R&D, D/A	3
US Army Aviation Materiel Laboratories	62
US Army Engineer R&D Laboratories	2
US Army Human Engineering Laboratories	1
Army Research Office-Durham	2
US Army Engineer Waterways Experiment Station	1
US Army Combat Developments Command Transportation Agency	1
US Army War College	1
US Army Command and General Staff College	1
US Army Transportation School	1
US Army Tank-Automotive Center	1
US Army Arctic Test Center	1
TC Liaison Officer, US Army Airborne, Electronics and Special Warfare Board	1
Chief of Naval Operations	1
Bureau of Ships, D/N	1
Bureau of Naval Weapons	2
Bureau of Supplies and Accounts, D/N	1
US Naval Supply R&D Facility	1
David Taylor Model Basin	1
Marine Corps Educational Center	1
Marine Corps Liaison Officer, US Army Transportation School	1
Ames Research Center, NASA	2
Lewis Research Center, NASA	2
NASA Representative, Scientific and Technical Information Facility	2
Defense Documentation Center	20
US Government Printing Office	1

APPENDIX I

DISCUSSION OF FAN AND DUCTING CHARACTERISTICS

FAN CHARACTERISTICS

The delivery of air to the jet nozzles (annular jet) or cushion (plenum) is accomplished by one or more fans, followed by ducts which may include bands and different sections.

If the fan blades have a large pitch angle, then they will be partially stalled at low flow rates. Typical performance characteristics for such a fan are shown in Figure 39.

The fan coefficients in Figure 39 are defined as follows:

$$C_p = \frac{\text{pressure rise above ambient}}{q_t} \tag{53}$$

$$\lambda = \frac{\text{air volume flow rate through fan}}{\text{(fan area)} \times \text{(fan tip speed)}} \tag{54}$$

$$q_t = \tfrac{1}{2}\rho V_t^2$$

In terms of normally measured parameters,

$$C_p = \frac{8\Delta P}{\rho \omega^2 D^2} = \frac{2}{\pi^2}\,\frac{\Delta P}{\rho n^2 D^2} \tag{55}$$

$$\lambda = \frac{8Q}{\pi \omega D^3} = \frac{4}{\pi^2}\,\frac{Q}{n D^3}\,. \tag{56}$$

The pressure rise Δ may be static (Δp, is often used in commercial fan work) or the total pressure ΔP. It may be measured right behind the fan (ΔP_F or Δp_F)or at the end of the ducting to which the fan is connected.

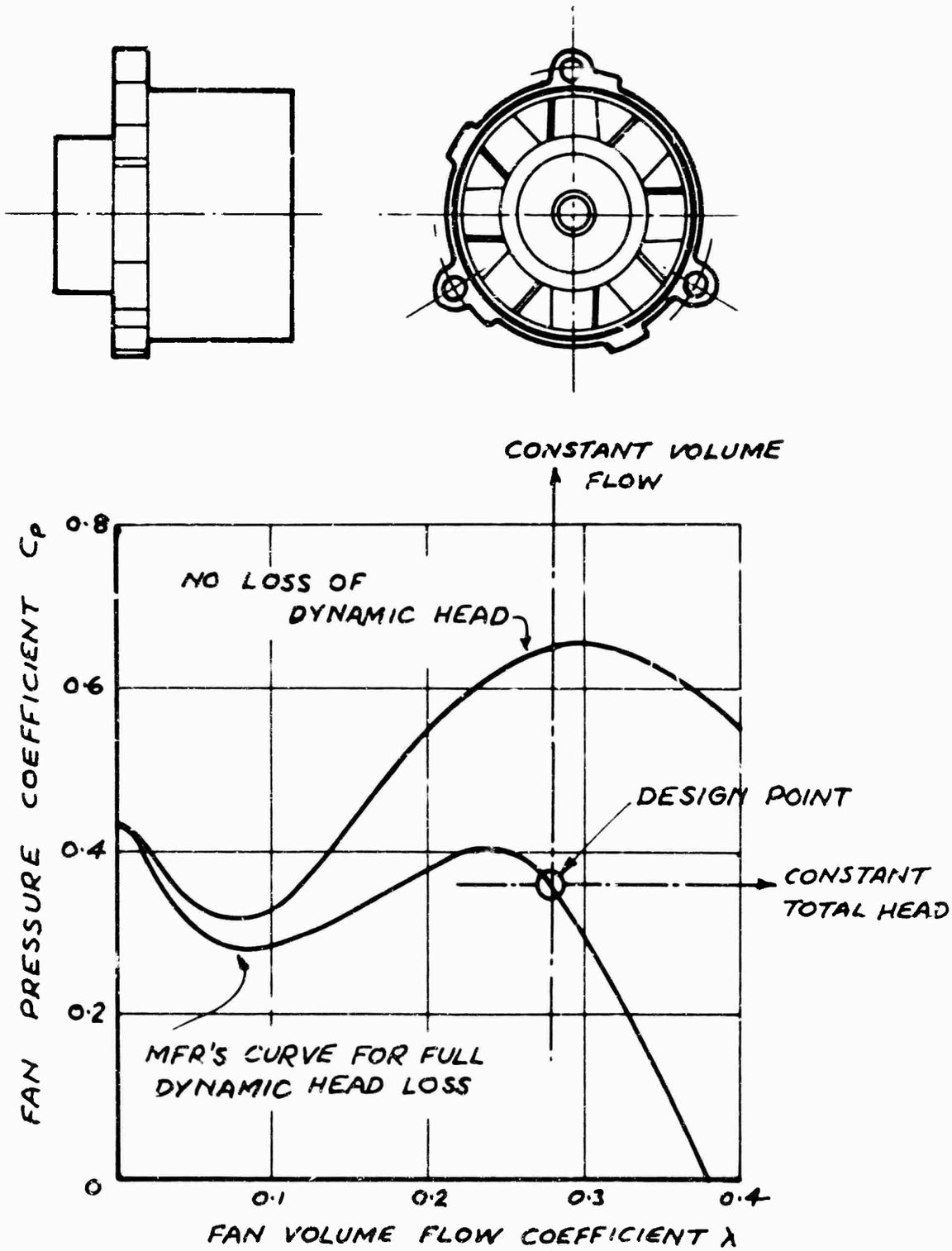

Figure 40. Characteristics of a High-Pitch Axial Fan (Globe Vax-2-MM).

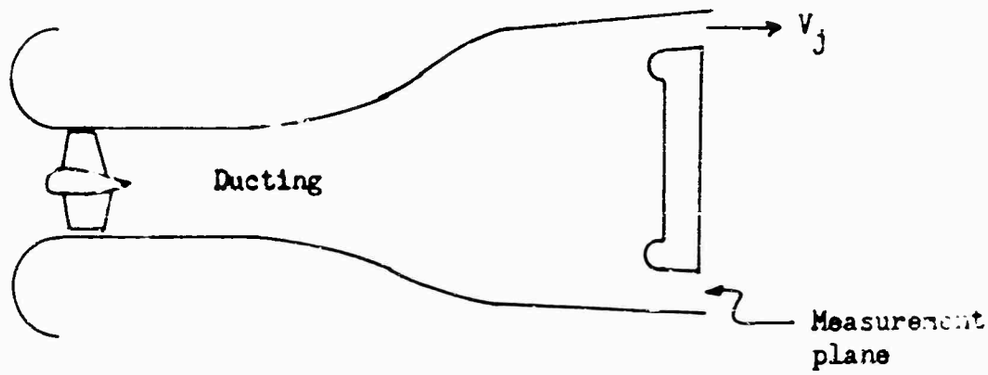

Figure 41. Fan and Ducting Geometry.

In the case of a fan connected to a ducting, it is reasonable to base the duct losses on the velocity, or more precisely, the dynamic head, at the fan station. Thus in Figure 40 the total head measured at the jet exit plane will be

$$\Delta P_j = \Delta P_F - (1 - \eta_D)\, g_F$$

$$= \Delta p_F + \eta_D\, g_F \qquad (57)$$

where $(1 - \eta_D)\, g_F$ is the total duct pressure loss, so that η_D represents the duct efficiency ($\eta_D = 1.0$ for zero losses).

From equation (54)

$$\lambda = \frac{v_F}{V_T} = \sqrt{\frac{g_F}{g_T}}$$

$$\therefore \Delta P_j = \Delta p_F + \eta_D\, g_T\, \lambda^2 \qquad (58)$$

and

$$\left.\begin{aligned} C_{p_j} &= C_{p_F} + \eta_D \lambda^2 \\ &= C_{p_F} - (1 - \eta_D)\, \lambda^2 \end{aligned}\right\} . \qquad (59)$$

These relationships enable the total pressure coefficient to be plotted when only the static coefficient is known (as in Figure 39) and the influence of duct losses to be included in fan characteristics.

The design operating point in Figure 39 corresponds to

$$\frac{\partial C_p}{\partial \lambda} = -\frac{C_p}{\lambda}. \tag{60}$$

This may be shown as follows. The power delivered by a fan is the product of its flow and total pressure rise[20], which can be expressed as

$$\mathcal{P}_F = A_F\, v_F\, \Delta P_F = (A_F\, V_T\, g_T)\,(\lambda C_p).$$

Differentiating with respect to λ,

$$\frac{\partial \mathcal{P}_F}{\partial \lambda} = (A_F\, V_T\, g_T)\,\left(C_p + \lambda \frac{\partial C_p}{\partial \lambda}\right).$$

Equating to zero, we find that the power is at a maximum when the equation is satisfied.

In general, when the pitch angle is large, the fan pressure coefficient must be obtained experimentally, at least so far as performance in the stalled region is concerned. Many methods exist for estimating (and optimizing) fan performance in the unstalled normal operating condition, one of the best summaries being Reference 21. Solutions are obtained by essentially iterative procedures.

CLOSED FORM SOLUTIONS FOR SMALL BLADE ANGLES

Two of the more successful full scale GEMs[2,22] and the model GEM used in the present program have fan blade angles of less than 15° and there is reason to believe that this will become more common in the future. Using extensions of helicopter rotor theory[23] Payne[24] has shown that closed form solutions can be obtained for C_p in terms of λ, and hence the derivative $\partial C_p/\partial\lambda$ can be obtained.

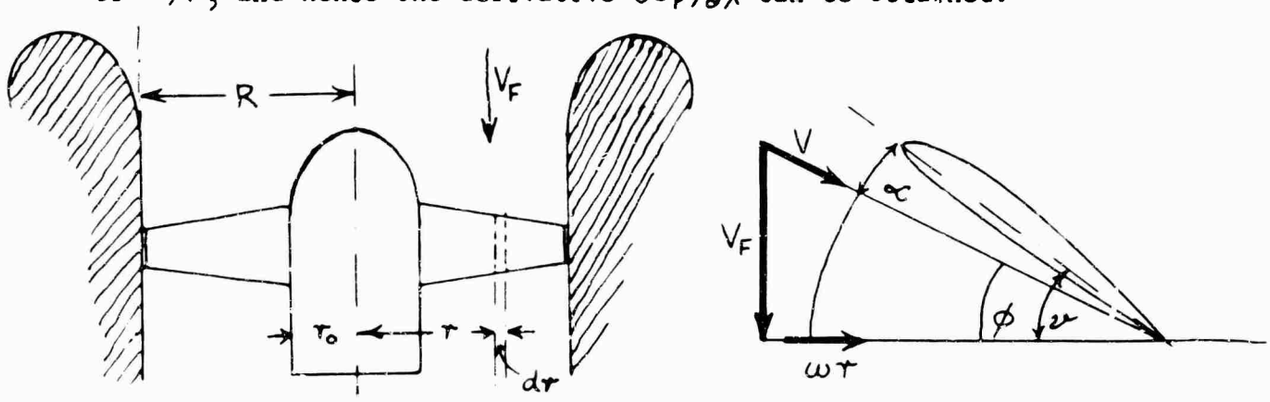

Figure 42. Fan Geometry.

The elemental lift on the blade element dr wide, in Figure 42, is

$$dL = C_L \tfrac{1}{2}\rho v^2 c\, dr \qquad = a(u - \phi)\, \tfrac{1}{2}\rho (v_F^2 + \omega^2 r^2) c\, dr$$

$$= \tfrac{1}{2}\rho V_T^2 Rac\, (\lambda^2 + x^2)(\theta - \phi)\, dx, \qquad (61)$$

where $x = r/R$

$a = \partial C_L / \partial \alpha$ (the lift curve slope)

but $\phi = v_F / \omega r = \lambda / x$

$$\therefore dL = \tfrac{1}{2}\rho V_T^2\, Rac \left[\theta(\lambda^2 + x^2) - \lambda x - \lambda^3/x \right]. \qquad (62)$$

Since $\lambda < 1.0$, λ^3 is negligible. Integrating for N blades we have for the total thrust

$$T = \tfrac{1}{2}\rho V_T^2\, RaN \int_{x_0}^{1.0} (\theta x^2 - \lambda x)\, c\, dx$$

$$= \tfrac{1}{2}\rho V_T^2\, RaNC_o \left[\int_{x_0}^{1.0} \frac{C}{C_o}\, \theta\, x^2\, dx - \lambda \int_{x_0}^{1.0} \frac{C}{C_o}\, x\, dx \right] \qquad (63)$$

where C_o is a reference chord, usually the largest value.

The "twist integrals"

$$k_\eta = 4 \int_{x_0}^{x_1} \frac{C}{C_o}\, \theta\, x^{n-1}\, dx \qquad (64)$$

are tabulated by Payne in Reference 23 for many practical cases. When the platform and blade twist are arbitrary, equation 64 has to be evaluated numerically, of course. For the simple case of uniform blade chord and constant pitch angle,

$$k_1 = 4\theta(1 - x_o)$$

$$k_2 = 2\theta(1 - x_o^2)$$

$$k_3 = 4/3\,\theta(1 - x_o^3). \tag{65}$$

The relationship between thrust and total pressure rise is

$$T = A_F \Delta P$$

$$\therefore \Delta P_F = \frac{\frac{1}{2}\rho V_T^2 \, Ra \, C_D}{\pi R^2}\left[\tfrac{1}{4}k_3 - \tfrac{1}{4}t_2\lambda\right]$$

and $$C_{p_F} = \frac{a\sigma_o}{4}\left[k_3 - t_2\lambda\right], \tag{66}$$

where σ_o = the nominal solidity

$$= \frac{N\,C_D}{\pi R}.$$

The fan derivative is obviously

$$\frac{\partial C_{p_F}}{\partial \lambda} = -\frac{a\sigma_o t_2}{4}. \tag{67}$$

For the constant chord, constant pitch angle case

$$\frac{\partial C_{p_F}}{\partial \lambda} = \frac{a\sigma_o(1 - x_o^2)}{2}$$

$$\cong a\sigma_o / 2. \tag{68}$$

When the duct losses are allowed for by the use of equation 59, we have, for the total pressure coefficient downstream of the ducts

$$C_{p_j} = C_{p_F} - (1 - \eta_D)\lambda^2$$

$$= \frac{a\sigma_o}{4}\left[k_3 - t_2\lambda\right] - (1 - \eta_D)\lambda^2 \tag{69}$$

$$\therefore \frac{\partial C_{p_j}}{\partial \lambda} = -\frac{a\sigma_o t_2}{4} - 2(1 - \eta_D)\lambda \tag{70}$$

$$= -\frac{a\,\sigma_o}{2} - 2(1 - \eta_D)\lambda \tag{71}$$

for the constant chord, constant angle case.

APPENDIX II

THEORETICAL ESTIMATION OF THE HEAVE STABILITY OF A GEM, INCLUDING FAN CHARACTERISTICS

(1) Introduction

This appendix is a concise treatment of the theory developed earlier in Reference 1, emphasizing the points shown to be important by the experimental tests described in the main body of the report and giving more discussion of the physical assumptions underlying various theories.

(2) Equation of Heave Motion

It is assumed that, following Eames and others, the air is incompressible and that the equation of motion is

$$\ddot{h} + 2\zeta\omega_o \dot{h} + \omega_o^2 (h - h_o) = 0, \tag{72}$$

where ζ is the damping ratio

and ω_0 is the undamped circular frequency (corrected for low values of ζ_o).

Note that, also following Eames and Tulin, ζ may be given one value with the GEM sinking and another value with the GEM rising. (Provided that Tulin's stability criteria is met -- as is always the case in practice -- the former implies the jet is "underfed", and the latter that the jet is "overfed".)

Eames, Strand, Cross and Walker all agree that this equation may also be written

$$\ddot{h} + g/W \left(\frac{\partial L}{\partial h}\right) \dot{h} + g/W \frac{\partial L}{\partial h} (h - h_o) = 0, \tag{73}$$

and that the derivative $\partial L/\partial \dot{h}$ may be written

$$\frac{\partial L}{\partial \dot{h}} = \frac{\partial L}{\partial h} \cdot \frac{\partial h}{\partial \dot{h}} . \tag{74}$$

Previous work has concentrated on the prediction of parameters ζ and ω_0, but Walker in Reference 1 suggested that it might be much more convenient to use the results for ω_0 and $2\zeta/\omega_0$, since the latter did not depend on fan characteristics.

It is easy to see, comparing equations, that

$$\omega_0 = \sqrt{g/W \cdot \partial L/\partial h} \tag{75}$$

and

$$\frac{2\zeta}{\omega_0} = \frac{\partial h}{\partial \dot{h}} \tag{76}$$

where ∂h is the effective change in altitude brought about by vertical velocity $\partial \dot{h}$.

(3) Estimation of the Stability Derivative $\frac{\partial L}{\partial h}$ and the Undamped Natural Frequency.

Let us assume that the characteristics of the fan can be completely described by the volume flow, so that the total head in the jet is given by

$$P_t = f(Q). \tag{77}$$

A variation of base pressure will cause a variation in back pressure on the jet and vary both volume flow and P_t. However, this can be calculated by assuming that the volume flow is related to the total head in the jet by a function of the height parameter, h/h_o.

$$Q = S_j V_{e_o} \xi(h/h_o) \tag{78}$$

where

$$V_{e_o} = \left[2P_t/\rho\right]^{\frac{1}{2}} \tag{79}$$

and the base pressure is also related to total head and height by the equation

$$p_o = P_t \chi(h/h_o). \tag{80}$$

Now from (15),

$$Q \propto \xi (P_t)^{\frac{1}{2}} \tag{81}$$

$$Q'/Q = \tfrac{1}{2} P_t'/P_t + \xi'/\xi \tag{82}$$

where $Q' = \partial Q/\partial (h/h_o)$ etc.

and $$\frac{P_t}{Q}\frac{\partial Q}{\partial P_t}\frac{P_t'}{P_t} = \frac{1}{2}\frac{P_t'}{P_t} + \frac{\xi'}{\xi}$$

$$\frac{P_t'}{P_t} = \frac{\xi'}{\xi} \Big/ \left[\frac{P_t}{Q}\frac{\partial Q}{\partial P_t} - \frac{1}{2}\right] = F\left[\xi'/\xi\right]. \tag{83}$$

From (80) $$\frac{P_b'}{P_b} = \frac{P_t'}{P_t} + \frac{\chi'}{\chi}$$

$$\frac{P_b'}{P_b} = \xi'/\xi \,.F + \chi'/\chi = \mathcal{F} \tag{84}$$

and $$\frac{\partial L}{\partial h} = \frac{P_b' S_b}{h_o} = \frac{P_b S_b}{h_o}\mathcal{F} \,. \tag{85}$$

Now the undamped natural frequency is given by

$$\omega_o^2 = g/W \,.\, \partial L/\partial h \tag{86}$$

and $$W = S_b P_{b_o} \,;$$

therefore, $$\omega_o = \left[g/h_c\right]^{\frac{1}{2}}\left[-\mathcal{F}\right]^{\frac{1}{2}}. \tag{87}$$

Note that the stability depends not only on F, the fan characteristics, but also on the characteristics of the annular jet. If χ'/χ is negative, F could take an appreciable positive value before instability occurred.

<u>Application of the Results to the Plenum Chamber</u>

$$Q = C_D\, h\, C\, V_{e_o}, \tag{88}$$

but $$Q = S_j\, V_{e_o}\, \xi(h/h_o). \tag{89}$$

Hence, $$\xi(h/h_o) = C_D\, C\, h\, /\, S_j \tag{90}$$

and $$\xi = C_D\, C\, h_o/\, S_j \tag{91}$$

at $$h = h_o\,, \qquad \xi'/\xi = 1. \tag{92}$$

Similarly, $$P_{b_o} = P_m \tag{93}$$

$$\therefore\ \chi(h/h_o) = 1$$

$$\chi' = 0$$

and $$\psi'/\psi = 0. \tag{94}$$

Hence, for this case $\mathcal{H} = \xi'/\xi \; F + \psi'/\psi$

$$= F. \tag{95}$$

The undamped natural frequency ω_o is then

$$\omega_o = \sqrt{-F}\,\sqrt{g/h_o} \; . \tag{96}$$

Note that since $2\zeta/\omega$ is shown later to be essentially positive, the motion of the plenum chamber is determined by the sign of -F.

If -F is positive, the motion will be a damped oscillation or a subsidence, and if -F becomes negative a divergence will occur. No divergent oscillation is possible, and if such does occur it implies that the physical basis for this theory is not applicable in that region.

Note that the stability is also completely determined by the fan characteristics.

Plenum Chamber - Constant Total Head

For constant total head, $\partial P_t/\partial Q = 0$ and $F = 0$. (97)

There is no variation of lift with altitude, no restoring force due to displacement, and no damping. The craft has "neutral" stability in heave.

Plenum Chamber - Constant Momentum Flux

This is exactly the same for incompressible flow as the assumption of constant mass flow or constant volume flow.

Hence, $$\partial Q/\partial P_t = 0 \quad \text{and} \quad F = -2. \tag{98}$$

Whence, $$\omega_o = \sqrt{2g/h_o} \; . \tag{99}$$

The Annular Jet GEM

Results for the annular jet GEM are most easily appreciated by assuming that some simple theory such as the exponential theory is applicable. This gives results in terms of the nondimentional parameter x, where

$$x = \frac{G}{h\,(1 + \sin\lambda)} \tag{100}$$

and

$$\frac{\partial(\;)}{\partial h/h_o} = -x\,\frac{h_o}{h}\,\frac{\partial(\;)}{\partial x}\,. \tag{101}$$

We are interested in small perturbations around the equilibrium condition, so $h = h_o$

and

$$\frac{\partial(\;)}{\partial h/h_o} = -x\,\frac{\partial(\;)}{\partial x}\,.$$

The exponential theory gives

$$\frac{Q}{S_j V_{e_o}} = \frac{1 - e^{-x}}{x},$$

so

$$\xi'/\xi = 1 - \frac{x}{(e^x - 1)}\,. \tag{102}$$

As $x \longrightarrow 0$, this function tends to $\frac{1}{2}x$, the thin jet theory result and in the limit tends to zero.

For base pressure

$$\frac{P_{b_o}}{P_t} = 1 - e^{-2x}, \tag{103}$$

so

$$\psi'/\psi = \frac{-2x}{e^{2x} - 1}\,. \tag{104}$$

As $x \rightarrow 0$, this parameter tends to $x - 1$ (thin jet theory result) and then to -1. Taking the thin jet results, we find that for constant total head

$$w_o = \sqrt{g/h_o}\,\sqrt{1 - x}\,, \tag{105}$$

and that for constant mass flow

$$\omega_o = \sqrt{g/h_o} \quad . \tag{106}$$

(4) Estimation of the Stability Parameter $2\zeta/\omega$

$$2\zeta/\omega = \partial h/\partial \dot{h} \ , \tag{107}$$

and this is most easily interpreted by considering first the case of the plenum chamber.

Plenum Chamber GEM

Suppose the plenum chamber is hovering at a given altitude h_o, with a base pressure P_{b_o} (total head) and an outflow of Q_o.

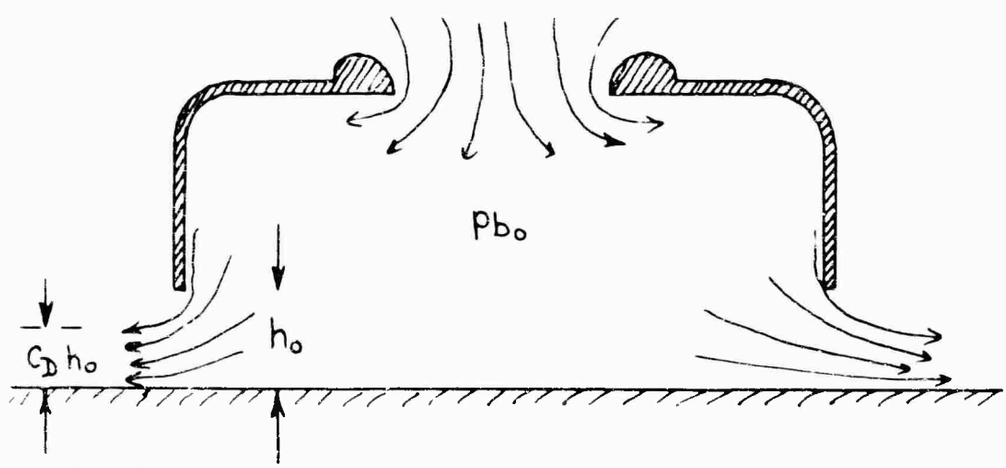

Now the outflow from the cushion will be

$$Q_o = C_D \, h_o \, C \, V_{e_o}$$

where V_{e_o} = velocity of jet exhausting fron base

$$= \sqrt{2 \, P_{b_o} / \rho}$$

and Lift $= S_b \, P_{b_o}$.

Now let the chamber be moving down through t . equilibrium altitude with a velocity $-\dot{h}$.

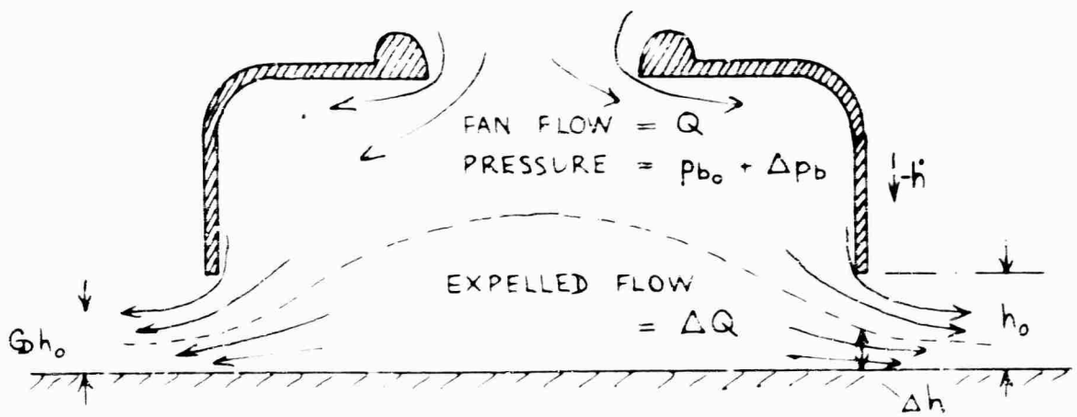

It is clear that if the internal flow conditions are unaltered, then there will be an outflow due to the downward motion equal to

$$\Delta Q = -S_b \dot{h} . \tag{108}$$

Now the outflow from the GEM will follow the same streamlines as before from the exit, and if the downward velocity and resulting changes of base pressure are small, then the total flow will be the same, and the efflux velocity will be substantially the same.

Hence Δh = effective change in air gap at the periphery of the GEM to discharge air from the fan

$$= \delta h / C_D$$

and

$$\Delta Q = -S_b \dot{h}$$

$$= C_D \Delta h C \sqrt{2 P_{b_o} / \rho} \tag{109}$$

or

$$\partial h / \partial \dot{h} = \frac{-S_b}{C_D C} \sqrt{\frac{\rho}{2 P_{b_o}}} . \tag{110}$$

The change in lift under these conditions is, of course,

$$\Delta L = \frac{\partial L}{\partial h} \Delta h \, ,$$

and since there is a reduction in exit area, there will be a change in flow, and hence a change in base pressure, but these changes will be included in the estimates of $\partial L / \partial h$, as previously given.

$$\text{Hence} \quad \frac{2\zeta}{\omega} = -\frac{\partial h}{\partial \dot{h}} = \frac{1}{C_D} \frac{S_b}{C} \sqrt{\frac{\rho}{2 P_{b_o}}} \, . \tag{111}$$

It is easy to see that, for instance, in the case of a constant total head air supply, $\dot{h}$ may be so large that the entire exit area is needed pass the flow due to $\dot{h}$.

Under these circumstances there will be no flow through the fan. There will be no resulting increase in base pressure and no damping force, but the value of $-\partial h/\partial \dot{h}$ will still be given by the above simple formula.

Since the flow pattern is unaltered if the GEM is rising rather than sinking, the same value of $2\zeta/\omega$ will hold for either case.

Annular Jet GEM - Sinking

If an annular jet GEM is sinking and Tulin's stability criterion is satisfied, then air will be forced out of the base beneath the curtain, and the jet will be "underfed".

Here again the velocity of escape of the air, V_e, will be determined substantially by the base pressure, and we may ignore the very small proportional change in V_e from V_{e_o} due to the increase of the base pressure.

Hence we find that the edge of the jet curtain will be lifted an amount δh such that

$$\Delta Q = -\dot{h} S_b = C \, \delta h \, V_{e_o}$$

and hence,

$$\delta h / \dot{h} = -\frac{S_b}{C} V_{e_o} = -\frac{S_b}{C} \sqrt{\frac{\rho}{2 P_{b_o}}} \, . \tag{112}$$

A point which must now be discussed is the relation between δh and Δh, where Δh is the equivalent change in static altitude of the GEM.

Early work on this subject by Cross[15], Strand[16], Walker[17], and Payne[18] assumed that the pressure around the inner edge of the main jet mass be constant. Hence the flow due to sinking must discharge at an excess pressure of P_{b_0} below the jet curtain, and then accelerate to V_{e_0}.

Hence the basic cushion bubble behaves like a piston, as shown below:

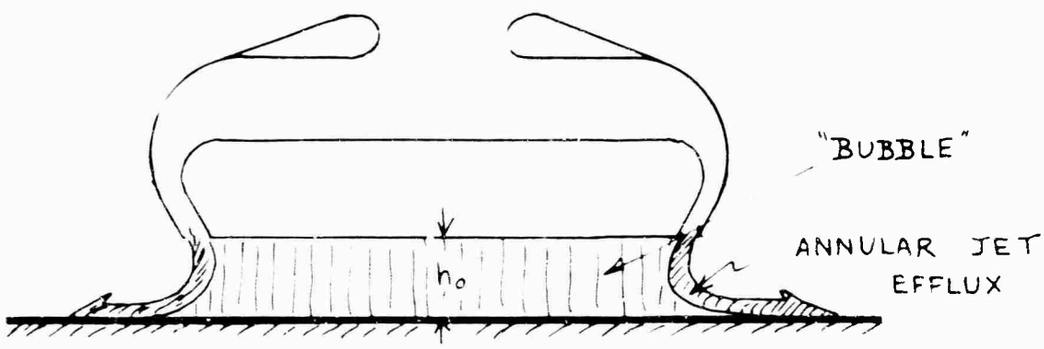

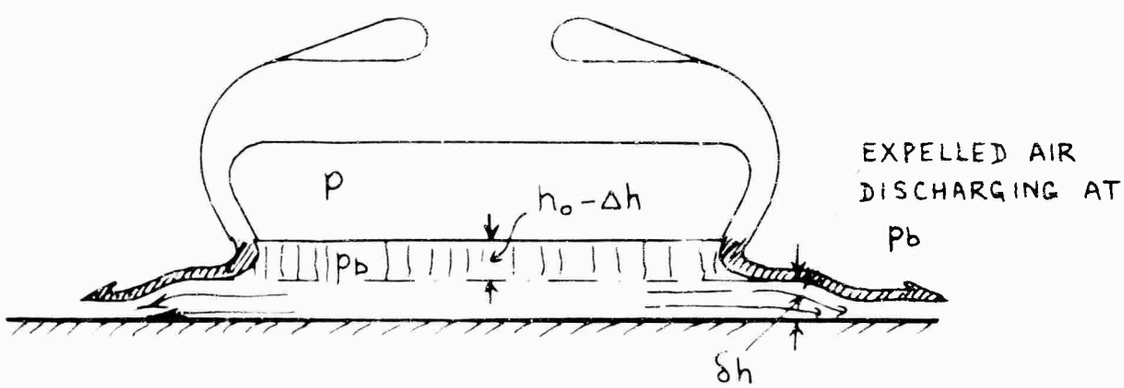

For this case $\Delta h = \delta h$. (113)

However, the picture is unsatisfying, since clearly the expelled air must accelerate to atmospheric pressure.

An alternative is shown below,

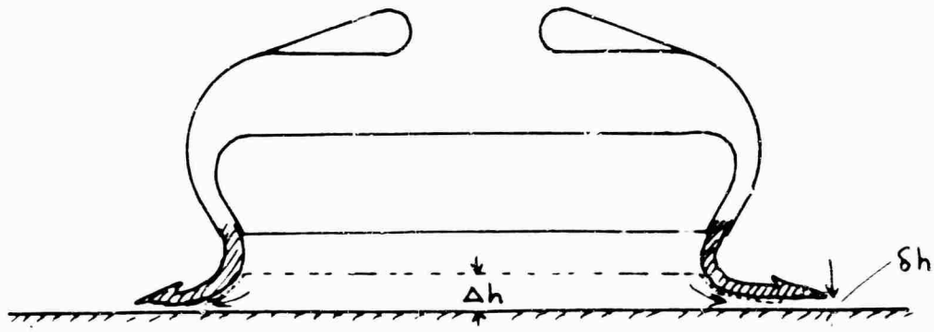

where it is assumed that the line of demarcation between "bubble" and expelled flow is flat to the point of contact with the annular jet, and then the expelled air accelerates to atmospheric pressure.

In the case of a first approximation

$$\Delta h = \delta h / C_D$$ where C_D is a discharge coefficient.

This further assumption presents philosophical difficulties about the variation of base pressure along the inner surface of the jet, but so does the ordinary annular jet theory for the estimation of base pressure, where it is assumed that the static pressure along the inner edge of the jet is constant until ground contact is made, when instantaneously the static pressure and atmospheric falls demanding a sudden decrease in jet thickness. (This point is currently being examined by Payne.)

However, the second result agrees with the Plenum Chamber in the low altitude limit, which is obviously desirable (especially if the discharge coefficient is adjusted for the angle of the outer wall of the jet), and in any case gives better agreement with the experimental results in this report.

Annular Jet GEM - Rising

Suppose the GEM is rising through the equilibrium altitude. The air to feed the cushion must now be derived from the annular jet. Suppose the jet splits to supply air to the cushion at a rate $S_b \dot{h}$.

This airflow, being supplied from the cushion side of the jet, must be at a static pressure of p_{b_o} if the displacements are small.

Walker then assumes that turbulent mixing dissipates the momentum of this section of the jet as below:

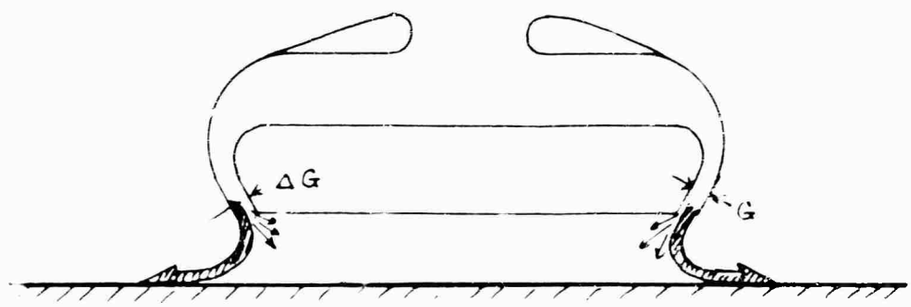

The portion of the jet supplying air to the cushion will have a width of ΔG, and

$$\dot{h}\, S_b = C\, \Delta G \sqrt{\frac{P_t - P_{b_o}}{\frac{1}{2}\rho}} \,. \tag{115}$$

Now the reduced jet width will support a reduced base pressure, equivalent to a gain in altitude of Δh, and we will have

$$\frac{\Delta G}{G} = \frac{\Delta h}{h_o} \,.$$

Hence,

$$\frac{\partial h}{\partial \dot{h}} = \frac{h_o\, \Delta G}{\dot{h}\, G}$$

But

$$\Delta G = \frac{\dot{h}\, S_b}{C} \sqrt{\frac{\frac{1}{2}\rho}{P_{t_o} - P_{b_o}}} \,.$$

Hence,

$$\frac{\partial h}{\partial \dot{h}} = \frac{h_o\, S_b}{C\, G} \sqrt{\frac{\frac{1}{2}\rho}{P_{t_o} - P_{b_o}}} \tag{116}$$

But

$$P_{b_o} = \chi\, P_{t_o}$$

$$\frac{h_o}{G} = \frac{1 + \sin\lambda}{x} \,.$$

$$\therefore \frac{\partial h}{\partial \dot{h}} = \frac{1 + \sin\lambda}{x} \frac{S_b}{C} \sqrt{\frac{\rho}{2 P_{b_o}}} \sqrt{\frac{x}{1 - x}} , \tag{117}$$

and this solution was used to prepare the damping estimates in the proposal.

Payne, however, has pointed out that the numerical result depends on the assumption about the loss of momentum. If the jet does not split where it enters the base, but splits at the ground board, and no momentum is lost, then the net momentum balance is changed and so is the change of base pressure. In particular, if the momentum is all lost at that point then the factor is not $\frac{1 + \sin\lambda}{x}$, but $1/x$. Furthermore, if the jet splits at the ground, but no momentum is lost, then the factor becomes $2/x$.

A similar discussion, with less definite conclusions, was also given in the original papers by Eames.

The three possibilities are shown below:

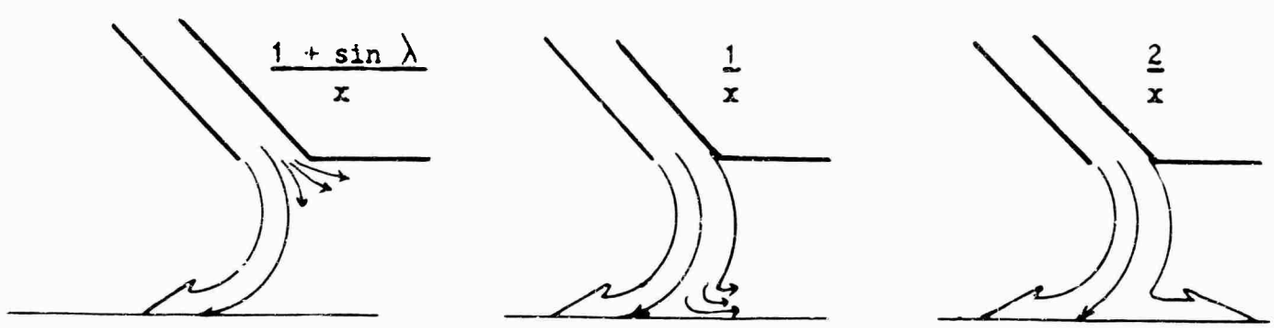

(a) (b) (c)

A very elegant series of experiments by D.L Hughes of the University of Wales were reported by Walker in Ref. 28, in which the streamlines in two-dimensional "overfed" and "underfed" jets of water in water were photographed and analyzed. The following picture from the report shows that assumption c is the most correct.

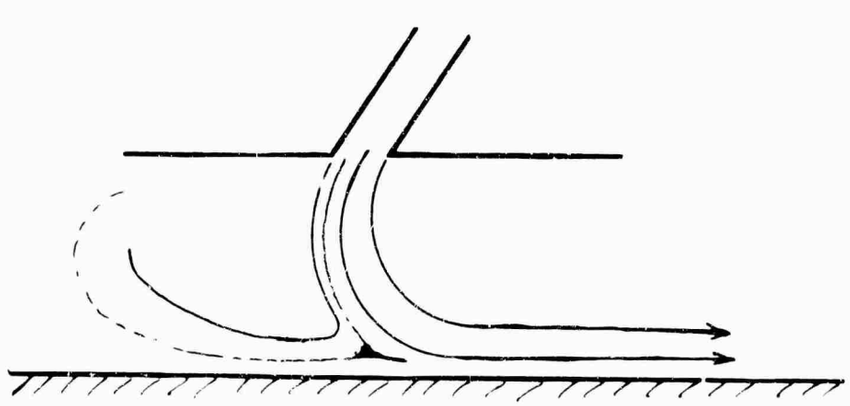

Accordingly, the recommended formula for $2\zeta/w$, GEM rising, is given by:

$$\frac{2\zeta}{w} = \frac{2}{x}\,\frac{S_b}{C}\sqrt{\frac{\rho}{2\,P_{b_o}}}\;\sqrt{\frac{x}{1-x}}\;. \tag{118}$$

For the exponential theory this may be written:

$$\frac{2\zeta}{w} = \frac{S_b}{C}\sqrt{\frac{\rho}{2\,P_{b_o}}}\;\frac{2}{\sqrt{2x}}\;\sqrt{\frac{e^{2x}-1}{2x}}\;, \tag{119}$$

and taking only the first terms of the expansion for e^{2x} this becomes:

$$\frac{2\zeta}{w}\ \text{(thin jet)} = \frac{S_b}{C}\sqrt{\frac{\rho}{2\,P_{b_o}}}\;\frac{2.828}{\sqrt{x}}\;. \tag{120}$$

The experimental results show that the average of the latter formula and the result for GEM sinking ($C_D = 0.62$) is in very fair agreement with the experimental results (the exponential form goes to infinity when $x \cong 1.0$ and is obviously not in agreement with experiment. This is deemed to be a failing of this particular formulation, and does not, we believe, invalidate the physical assumptions causing damping.)

(5) Summarized Results

Plenum Chamber

$$w_o = \sqrt{g/\,W\cdot\partial L/\,\partial h}$$

$$= \sqrt{g/h_o}\,\sqrt{-F} \tag{121}$$

$$= 0 \qquad \text{constant total head}$$

or

$$= \sqrt{2g/h_o} \qquad \text{constant momentum flux}$$

$$\frac{2\zeta}{w_o} = \frac{1}{C_D}\;\frac{S_b}{C}\sqrt{\frac{\rho}{2\,P_{b_o}}}\;. \tag{122}$$

Annular Jet GEM

$$w_o = \sqrt{g/W \cdot \partial L/\partial h}$$

$$= \sqrt{g/h_o}\ \sqrt{-\mathcal{L}} \tag{123}$$

$$= \sqrt{g/h_o}\left[(-F)\left(1 - \frac{x}{e^x - 1}\right)\left(\frac{2x}{e^{2x} - 1}\right)\right] \tag{124}$$

(Exponential Theory)

or

$$\sqrt{g/h_o}\left[(-F)\left(\tfrac{1}{2}x\right) - x + 1\right] \tag{125}$$

(Thin Jet)

$$\frac{2\mathcal{G}}{w} = \frac{S_b}{C}\sqrt{\frac{\rho}{2\,P_{b_o}}}\left[\frac{1}{2\,C_D} + \sqrt{\frac{2}{x}}\right]. \tag{126}$$

UNCLASSIFIED
Security Classification

DOCUMENT CONTROL DATA - R&D

(Security classification of title, body of abstract and indexing annotation must be entered when the overall report is classified)

1 ORIGINATING ACTIVITY *(Corporate author)*
Norman K. Walker Associates, Inc.
7240 Wisconsin Avenue, Bethesda 14, Maryland

2a REPORT SECURITY CLASSIFICATION
UNCLASSIFIED

2b GROUP

3 REPORT TITLE
Heave Stability and Heave Damping of Ground Effect Machines - Thick Annular Jet and Plenum Types

4 DESCRIPTIVE NOTES *(Type of report and inclusive dates)*
Final Report - Part II

5 AUTHOR(S) *(Last name, first name, initial)*
Walker, Norman K.
Shaffer, David A.

6 REPORT DATE
July 1965

7a TOTAL NO OF PAGES
107

7b NO OF REFS
27

8a CONTRACT OR GRANT NO
DA 44-177-AMC-19(T)

b. PROJECT NO
Task 1D021701A04802

c

d

9a ORIGINATOR'S REPORT NUMBER(S)
USAAVLABS Technical Report 65-26

9b OTHER REPORT NO(S) *(Any other numbers that may be assigned this report)*
Report No. 14

10 AVAILABILITY LIMITATION NOTICES
Qualified requesters may obtain copies of this report from DDC.
This report has also been furnished to the Office of Technical Services, Department of Commerce, for sale to the Public.

11 SUPPLEMENTARY NOTES

12 SPONSORING MILITARY ACTIVITY
US Army Aviation Materiel Laboratories
Fort Eustis, Va

13 ABSTRACT

This report describes an experimental investigation of the heave stability and heave damping characteristics in hovering arranged firstly with a thick annular jet and, secondly, as a simple plenum chamber.

The lift, rise height, and power relationship was determined, and the fan characteristics of the thick annular jet were measured. Air was bled from and fed into the air cushion to evaluate the GEM's change in lift. Finally, the machine was allowed to hover at a specific height, and then forced to oscillate. From this, the heave stiffness and damping ratio were determined.

The results were shown that the physical basis of the theory is correct and that good estimates may be made of the heave characteristics and ω_o and $2\zeta/\omega_o$ from which, of course, ζ can be determined.

DD FORM 1 JAN 64 1473

UNCLASSIFIED
Security Classification

14 KEY WORDS	LINK A ROLE	LINK A WT	LINK B ROLE	LINK B WT	LINK C ROLE	LINK C WT
1) Aerodynamics 2) Stability & Control - Ground Effect Machines						

INSTRUCTIONS

1. ORIGINATING ACTIVITY: Enter the name and address of the contractor, subcontractor, grantee, Department of Defense activity or other organization *(corporate author)* issuing the report.

2a. REPORT SECURITY CLASSIFICATION: Enter the overall security classification of the report. Indicate whether "Restricted Data" is included. Marking is to be in accordance with appropriate security regulations.

2b. GROUP: Automatic downgrading is specified in DoD Directive 5200.10 and Armed Forces Industrial Manual. Enter the group number. Also, when applicable, show that optional markings have been used for Group 3 and Group 4 as authorized.

3. REPORT TITLE: Enter the complete report title in all capital letters. Titles in all cases should be unclassified. If a meaningful title cannot be selected without classification, show title classification in all capitals in parenthesis immediately following the title.

4. DESCRIPTIVE NOTES: If appropriate, enter the type of report, e.g., interim, progress, summary, annual, or final. Give the inclusive dates when a specific reporting period is covered.

5. AUTHOR(S): Enter the name(s) of author(s) as shown on or in the report. Enter last name, first name, middle initial. If military, show rank and branch of service. The name of the principal author is an absolute minimum requirement.

6. REPORT DATE: Enter the date of the report as day, month, year; or month, year. If more than one date appears on the report, use date of publication.

7a. TOTAL NUMBER OF PAGES: The total page count should follow normal pagination procedures, i.e., enter the number of pages containing information.

7b. NUMBER OF REFERENCES: Enter the total number of references cited in the report.

8a. CONTRACT OR GRANT NUMBER: If appropriate, enter the applicable number of the contract or grant under which the report was written.

8b, 8c, & 8d. PROJECT NUMBER: Enter the appropriate military department identification, such as project number, subproject number, system numbers, task number, etc.

9a. ORIGINATOR'S REPORT NUMBER(S): Enter the official report number by which the document will be identified and controlled by the originating activity. This number must be unique to this report.

9b. OTHER REPORT NUMBER(S): If the report has been assigned any other report numbers *(either by the originator or by the sponsor)*, also enter this number(s).

10. AVAILABILITY/LIMITATION NOTICES: Enter any limitations on further dissemination of the report, other than those imposed by security classification, using standard statements such as:

(1) "Qualified requesters may obtain copies of this report from DDC."

(2) "Foreign announcement and dissemination of this report by DDC is not authorized."

(3) "U. S. Government agencies may obtain copies of this report directly from DDC. Other qualified DDC users shall request through _____."

(4) "U. S. military agencies may obtain copies of this report directly from DDC. Other qualified users shall request through _____."

(5) "All distribution of this report is controlled. Qualified DDC users shall request through _____."

If the report has been furnished to the Office of Technical Services, Department of Commerce, for sale to the public, indicate this fact and enter the price, if known.

11. SUPPLEMENTARY NOTES: Use for additional explanatory notes.

12. SPONSORING MILITARY ACTIVITY: Enter the name of the departmental project office or laboratory sponsoring *(paying for)* the research and development. Include address.

13. ABSTRACT: Enter an abstract giving a brief and factual summary of the document indicative of the report, even though it may also appear elsewhere in the body of the technical report. If additional space is required, a continuation sheet shall be attached.

It is highly desirable that the abstract of classified reports be unclassified. Each paragraph of the abstract shall end with an indication of the military security classification of the information in the paragraph, represented as *(TS)*, *(S)*, *(C)*, or *(U)*.

There is no limitation on the length of the abstract. However, the suggested length is from 150 to 225 words.

14. KEY WORDS: Key words are technically meaningful terms or short phrases that characterize a report and may be used as index entries for cataloging the report. Key words must be selected so that no security classification is required. Identifiers, such as equipment model designation, trade name, military project code name, geographic location, may be used as key words but will be followed by an indication of technical context. The assignment of links, rules, and weights is optional.

Annular Jet GEM

$$w_o = \sqrt{g/W \cdot \partial L/\partial h}$$

$$= \sqrt{g/h_o}\,\sqrt{-\mathcal{F}} \tag{123}$$

$$= \sqrt{g/h_o}\left[(-F)\left(1 - \frac{x}{e^x - 1}\right)\left(\frac{2x}{e^{2x} - 1}\right)\right] \tag{124}$$

(Exponential Theory)

or

$$\sqrt{g/h_o}\left[(-F)\left(\tfrac{1}{2}x\right) - x + 1\right] \tag{125}$$

(Thin Jet)

$$\frac{2\mathcal{G}}{w} = \frac{S_b}{C}\sqrt{\frac{\rho}{2\,P_{b_o}}}\left[\frac{1}{2\,C_D} + \sqrt{\frac{2}{x}}\right]. \tag{126}$$